PhD degree in Molecular Medicine

European School of Molecular Medicine (SEMM),

University of Milan and University of Naples "Federico II"

Faculty of Medicine

Settore disciplinare: BIO/10

Insights into the mechanism of recruitment of checkpoint proteins Bub1 and BubR1 to kinetochore sites

Veronica Krenn

IFOM-IEO Campus, Milan

Matricola n. R08891

Supervisor: Prof. Dr. Andrea Musacchio

IFOM-IEO Campus, Milan

Anno accademico 2012-2013

Table of Contents

List of abbreviations

SAC, spindle assembly checkpoint; **MCC**, mitotic checkpoint complex; **APC/C**, anaphase-promoting complex/cyclosome; **RZZ**, Rod–Zwilch–Zw10; **MT**, microtubule.

List of publications

The work described in this thesis has been published in the following articles:

Krenn et al, ***Structural analysis reveals features of the spindle checkpoint kinase Bub1-kinetochore subunit Knl1 interaction.*** J Cell Biol. **2012** Feb 20; 196(4):451-67.

Krenn et al, ***MELT motifs of human Knl1 seed the assembly of spindle checkpoint complexes and KI motifs strongly enhance their function.*** Submitted.

List of Figures

Table of Contents

Abstract

Bub1 and BubR1 are essential components of the spindle assembly checkpoint (SAC), a ubiquitous safety mechanism required for accurate segregation of chromosomes during mitosis. Recruitment to mitotic kinetochores, protein assemblies built on the centromeric DNA, might be essential for the functions of Bub1 and BubR1, but the exact recruitment mechanism has been unknown. During my doctoral work, I have tried to investigate this issue at a molecular level. Previously, kinetochore recruitment of Bub1 and BubR1 had been proposed to rely on the interaction of their tetratricopeptide repeats (TPR repeats) with two motifs, named the KI motifs, in the outer kinetochore protein Knl1. In the first part of my doctoral work, I demonstrate that point mutations on the TPR repeats that impair the interaction of Bub1 and BubR1 with Knl1 *in vitro* and *in vivo* have essentially no macroscopic effect on the localization of Bub1 and BubR1 at kinetochores. Indeed, we have been able to define a 62-residue segment of Bub1, comprising a motif that mediates the interaction with another checkpoint protein, Bub3, as the minimal kinetochore-binding domain of Bub1. Subsequent studies in other laboratories have identified multiple Met-Glu-Leu-Thr (MELT) motifs in the kinetochore protein Knl1 as crucial docking sites, when phosphorylated by the Mps1 kinase, for the recruitment of Bub1 and BubR1. In the second part of my work, I therefore began to test the hypothesis that Bub1 recognizes MELT repeats on Knl1, through the minimal kinetochore targeting domain and its partner Bub3. Within the context of this new model, I have re-investigated the question whether the KI1 and KI2 motifs have any role in the interaction of Bub1 and BubR1 with Knl1. I provide evidence that Knl1$^{1\text{-}250}$ (N-terminal 250 residues of Knl1), with a single MELT motif, drive the assembly of complexes that included all SAC proteins and are sufficient to respond robustly to spindle poisons. Interestingly, I have found that the KI motifs, which flank the MELT motif in Knl1$^{1\text{-}250}$, strongly enhance the interaction with SAC components. Conversely, MELT motifs outside of Knl1$^{1\text{-}250}$, which lack flanking KI motifs, establish qualitatively similar sets of interactions, but

less efficiently. Thus, my analyses indicate that MELT motifs act as independent docking sites for Bub1/Bub3 and assembly stations for SAC signaling complexes, and that KI motifs are MELT enhancers. Collectively, my work has contributed to elucidating important aspects of the molecular mechanism of kinetochore recruitment of two fundamental components of the spindle assembly checkpoint.

Introduction

General principles of chromosome segregation

Mitosis is the process responsible for the division of the replicated DNA material, which, together with the division of the cytoplasm during cytokinesis, leads to the generation of two genetically identical daughter cells. During this process, cells are very fragile, as defects occurring in division can result in aneuploidy and genetic instability, culminating eventually either in cell death or in cancer (Gordon et al., 2012). In most cases, cells distribute their chromosomes with great accuracy, orchestrating a large number of proteins to dictate rapid morphological and biochemical changes in a tightly ordered sequence. Since its original discovery (Flemming, 1882), mitosis has been a very active research topic in cell biology that has led to the characterization of the main players and general mechanisms that drive accurate chromosome segregation. However, a detailed picture of the molecular and biophysical principles that contribute to the accuracy is still incomplete.

Cells are driven into mitosis as result of the activity of cyclin-dependent kinases (CDKs), which phosphorylate a number of substrates to dictate changes in nuclear and cytoskeleton architecture. Such changes lead on one hand to the condensation of DNA and the formation of sister chromatids, held together by a molecular glue called cohesin, and on the other hand to the assembly of a bipolar mitotic spindle, a microtubule-based structure (Figure 1). To ensure that each daughter cell inherits an identical copy of the genome, each pair of sister chromatids must attach to microtubules that emanate from opposite ends of the spindle, in a configuration called bi-orientation (Figure 1). Interaction of the chromosomes with microtubules is mediated by the kinetochore, a specialized proteinaceous network that assembles onto chromosomes upon mitotic entry (Santaguida and Musacchio, 2009; Westermann and Schleiffer, 2013). Once all chromosomes have bi-orientated, cohesin is cleaved and sister chromatids are irreversibly separated and pulled apart by microtubule-driven

forces (Figure 1). Sister chromatids that do not bi-orient are at risk of missegregation. Kinetochores are crucial for accuracy as they safeguard against erroneous missegregation events on one hand by correcting erroneous attachments and on the other hand by activating the spindle assembly checkpoint, a cell cycle control mechanism that delays mitotic progression and the irreversible cohesin cleavage until all chromosomes are bi-oriented (Foley and Kapoor, 2013). Thus, kinetochores are crucial signaling hubs that integrate attachment to microtubules and checkpoint signaling to ensure accuracy and timeliness of the chromosome segregation during mitosis.

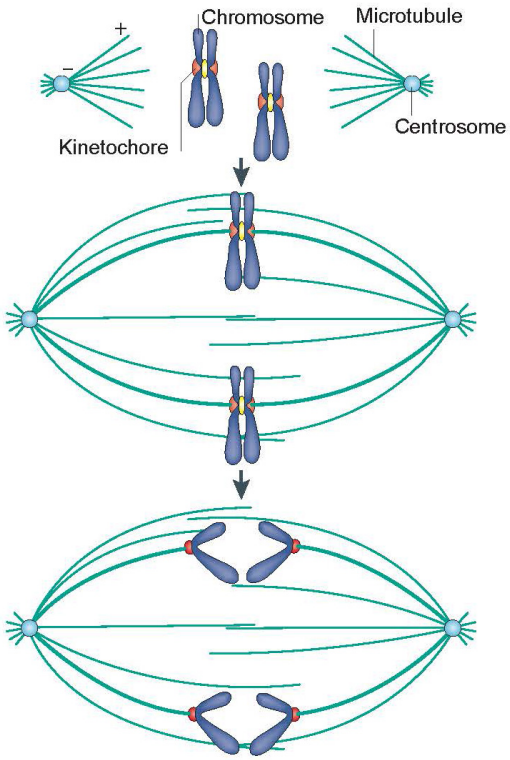

Figure 1 Overview of chromosome segregation

At the start of mitosis, a bipolar microtubule-based spindle assembles (top). Microtubules orientate their plus ends (+) towards the spindle equator and cluster their minus ends (-) at the centrosome, the microtubule nucleation site. Pairs of replicated chromosomes, held together by centromeric cohesin (yellow), attach to the spindle via kinetochores (red) (middle). Accurate chromosome segregation depends on each sister chromatid attaching to microtubules from opposite sites of the spindle (bi-orientation). Once all chromosomes have bi-oriented, cohesin is lost and sister chromatids are segregated to opposite spindle poles (bottom). Adapted from (Foley and Kapoor, 2013).

Kinetochore function and organization

Kinetochores are hierarchical protein assemblies of nearly 100 proteins, organized as multi-layered structures, with an inner kinetochore layer embedded in chromatin and an exposed outer kinetochore layer involved in microtubule binding (Figure 2) (Santaguida and Musacchio, 2009). The core structural components of kinetochores are conserved from yeast to humans (Santaguida and Musacchio, 2009; Westermann and Schleiffer, 2013), suggesting that the building plan of kinetochores is largely conserved in evolution. On the other hand, kinetochores in different organisms display dramatic variations in complexity. The simplest kinetochores are found in *Saccharomyces cerevisiae* (Westermann et al., 2007), where centromeres consist of ~150 base pairs of DNA organized in a specialized centromeric nucleosome containing the histone H3 variant CENP-A (Cse4 in *S. cerevisiae*). These simple centromeres, known as "point" centromeres, assemble kinetochores that bind a single microtubule. Conversely, higher eukaryotes exhibit "regional" centromeres, which extend over very large segments of DNA and display no univocal relationship between DNA sequence and kinetochore assembly. Kinetochores formed on regional centromeres usually bind multiple microtubules, from 3 in *Schizosaccharomyces pombe* to 15-30 in humans (Santaguida and Musacchio, 2009). They appear as trilaminar plates, with electron-opaque inner and outer plates, and a translucent middle layer (Dong et al., 2007), built on compact centromeric heterochromatin containing specialized CENP-A and H3 nucleosomes (Figure 2 A). In vertebrates, a subset of DNA-proximal kinetochore proteins, termed the constitutive associated centromere network (CCAN), sits on the centromeric chromatin throughout the cell cycle to built a platform for outer kinetochore assembly upon mitotic entry (Perpelescu and Fukagawa, 2011). One key outer kinetochore component that is recruited by the CCAN module upon mitotic entry is the KMN network (Knl1/Mis12/Ndc80), a highly conserved protein complex that provides direct interaction with microtubules, thus acting as a linker between the CCAN module and microtubules (Figure 2 A) (Cheeseman et al., 2006;

Cheeseman and Desai, 2008; Cheeseman et al., 2004; DeLuca et al., 2006; Musacchio and Salmon, 2007; Obuse et al., 2004; Welburn and Cheeseman, 2008).

The KMN network is a 10-subunit protein assembly composed of three sub-complexes (Figure 2 A): the Knl1 complex (Knl1-C), the Mis12 complex (Mis12-C, also known as MIND or Mtw1 complex) and the Ndc80 complex (Cheeseman et al., 2004; De Wulf et al., 2003; Desai et al., 2003; Liu et al., 2005; Nekrasov et al., 2003; Obuse et al., 2004; Pinsky et al., 2003; Przewloka et al., 2011; Westermann et al., 2003). Specifically, the Mis12 complex consists of the four subunits Mis12, Nsl1, Dsn1 and Pmf1. The Ndc80 complex is a heterotetramer of Ndc80 (Hec1 in human), Nuf2, Spc24 and Spc25 (Figure 2 A). The Knl1 complex is a

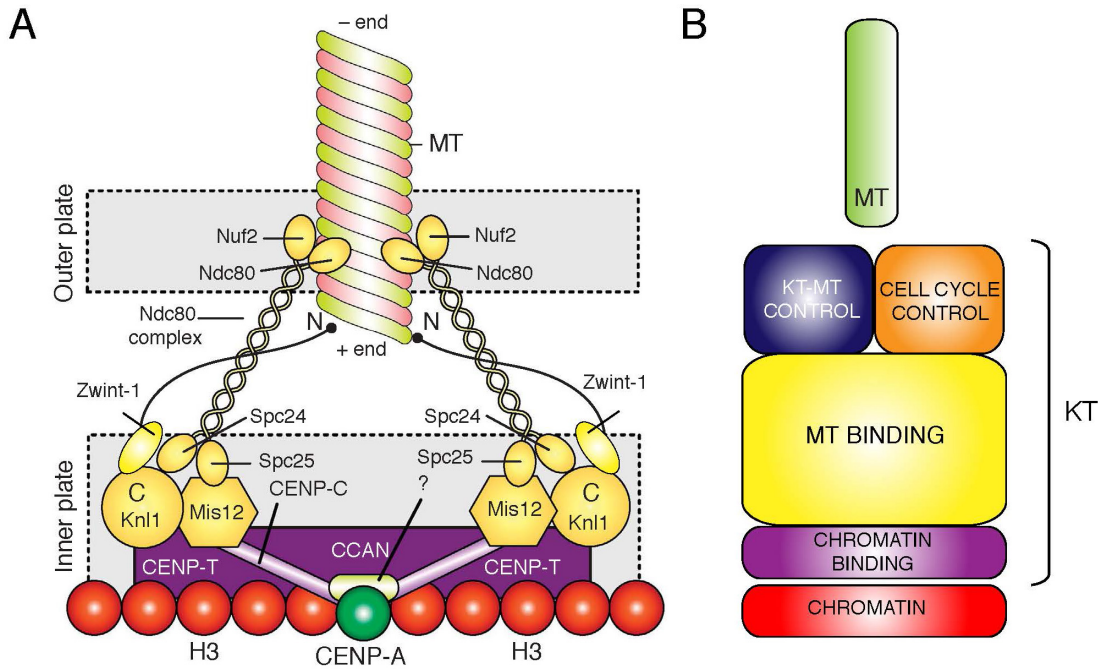

Figure 2 Organization of the human kinetochore

A) Structure and composition of the human kinetochore. The CCAN module (purple) is built on CENP-A and H3 containing nucleosomes. The KMN network (yellow) interacts with CENP-C and CENP-T. The Ndc80 complex is composed of Spc24, Spc25, Nuf2 and Ndc80 (Hec1 in human). The Mis12 complex is composed of Mis12, Nsl1, Dsn1 and Pmf1 (single subunits are not shown). The Knl1 complex is composed of Knl1 and Zwint-1. Microtubule binding is mediated by the Ndc80 and the Knl1 complexes. B) Schematic of the kinetochore functions. Kinetochores perform four different functions, represented as modules: they bind centromeric chromatin (purple), they have microtubule-binding activity (yellow), they regulate kinetochore-microtubule attachments via the error correction machinery (blue) and they control the cell cycle progression (orange) via the spindle assembly checkpoint. N, N-terminus; C, C-terminus; MT, microtubules; KT, kinetochore. Adapted from (Santaguida and Musacchio, 2009).

heterodimer of kinetochore-null-1 (Knl1, also known as Spc105, Spc7, CASC5, AF15q14 and Blinkin), the largest subunit of the KMN network, and Zw10-interactor 1 (Zwint-1) (Hornung et al., 2011; Kiyomitsu et al., 2010; Maskell et al., 2010; Petrovic et al., 2010).

Several studies based on knock-out and RNAi experiments for individual kinetochore components, and on ectopic localization of kinetochore proteins to centrosomes or to a non-centromeric locus have been used to map the assembly pathways and the localization-hierarchy of KMN components in several organisms (Cheeseman et al., 2004; Gascoigne et al., 2011; Hori et al., 2013; Liu et al., 2006; Przewloka et al., 2011; Takeuchi and Fukagawa, 2012). Overall, these studies have elucidated a conserved pathway for kinetochore assembly (despite the presence of some species-specific differences), now strongly corroborated by physical interactions characterized by direct biochemical experiments (Takeuchi and Fukagawa, 2012). The Mis12 complex is recruited to kinetochores via direct association with the CCAN protein CENP-C (Figure 2 A) (Przewloka et al., 2011; Screpanti et al., 2011), which acts as a linker connecting outer kinetochore components to centromeric DNA (Gascoigne et al., 2011; Perpelescu and Fukagawa, 2011). The Mis12 complex is as an intra-complex scaffold that recruits Knl1- and Ndc80- complexes to position them in a way that favors microtubule binding (Cheeseman et al., 2004). Very recently, it has been shown that, in addition to the Mis12-dependent recruitment, the Ndc80 complex can be recruited also via a distinct pathway, through an interaction with the CCAN protein CENP-T (Bock et al., 2012; Carroll et al., 2010; Gascoigne et al., 2011; Hori et al., 2008; Hori et al., 2013; Nishino et al., 2013). Collectively, according to the current model, the kinetochore assembly of KMN components relies on both CENP-C and CENP-T pathways.

The functions of the KMN network

In human cells, the interactions of kinetochores with microtubules arise concomitantly with the formation of the spindle. Thus, at the beginning of mitosis, all chromosomes lack spindle

attachments. End-on attachments are not immediately achieved, rather, the majority of kinetochores form transient, unstable lateral attachments to the sides of the microtubule filaments, rather than at the microtubule plus end (Cai et al., 2009; Magidson et al., 2011). These lateral interactions are eventually replaced by stable end-on attachments. A large body of work [reviewed in (Kline-Smith et al., 2005)], including the reconstitution of the recombinant KMN network from different organisms, has collectively established that the KMN network, in eukaryotic chromosomes, constitutes the core-microtubule binding site responsible for end-on attachments. Specifically, this function relies on the ability of the Ndc80 complex and Knl1 to directly interact with the plus-end of microtubule polymers (Figure 2 A).

While the Spc24-Spc25 globular heads of the Ndc80 complex are essential for kinetochore targeting, as they directly bind to the Mis12 complex and CENP-T (Bock et al., 2012; Nishino et al., 2013; Petrovic et al., 2010), the globular heads of Ndc80-Nuf2, which fold into a calponin homology domain and are located at the N-terminal end (Ciferri et al., 2005; Ciferri et al., 2008; Wang et al., 2008; Wei et al., 2005), interact with the plus end of microtubule polymers for the formation of load-bearing kinetochore-microtubule attachments (Figure 2 A) (Cheeseman et al., 2006; Ciferri et al., 2008; DeLuca et al., 2006; Wei et al., 2007). According to recent high-resolution images (Alushin et al., 2010), the Ndc80 complex binds to microtubules at least in two ways: first, via an electrostatic interaction between the basic amino-terminal tail of the Ndc80 protein and the acidic C-terminal tails of tubulin subunits (so called E-hooks), and by recognizing both α-tubulin and β-tubulin at the inter- and intra-tubulin interfaces (Alushin et al., 2010; Ciferri et al., 2008; Wei et al., 2007). Due to these features, the Ndc80 complex has been proposed to bind in a cooperative fashion and oligomerize along the microtubule lattice, with a preferential binding to straight microtubules versus curled tubulin at the depolymerizing tips of the microtubules.

The Knl1 complex has also been implicated in microtubule binding in several organisms (Cheeseman et al., 2006; Espeut et al., 2012; Kerres et al., 2007; Pagliuca et al., 2009; Welburn

et al., 2010). Human Knl1 is the largest subunit of the KMN network with its 2316 residues. Like the Ndc80 complex, kinetochore embedding and microtubule binding functions are located distally from each other, at the C- and N-terminus respectively (Figure 2 A). At its C-terminus, a region of approximately 450 residues (also called Mis12-binding domain) mediates the interaction with Zwint-1 and Mis12 and is sufficient for incorporation into the kinetochore (Kiyomitsu et al., 2011; Kiyomitsu et al., 2007; Pagliuca et al., 2009; Petrovic et al., 2010). At the extreme N-terminal end, Knl1 harbors a conserved microtubule-binding domain, a short positive patch that synergistically enhances KMN network association with microtubules *in vitro* (Cheeseman et al., 2006; Espeut et al., 2012; Pagliuca et al., 2009; Welburn et al., 2010). However, the function of this microtubule-binding activity has been questioned recently by the finding that in *C. elegans* Knl1 mutants in the microtubule-binding domain do not exhibit defects in the formation of load-bearing attachments (Espeut et al., 2012). As high-resolution structures of Knl1 and reconstitution experiments with large protein segments encompassing the microtubule-binding domain are lacking, the mechanism and the function of the microtubule-binding domain of Knl1 remain elusive.

In addition to its role in microtubule-binding, the KMN network is crucial for the activity of two control mechanisms that ensure accurate chromosome segregation (Figure 2 B): one control mechanism, generally referred to as 'error correction', that regulates kinetochore-microtubule attachments and one, named the 'spindle assembly checkpoint', that coordinates the state of attachment with mitotic progression. These two mechanisms will be described separately in the next sections.

Regulation of kinetochore-microtubule attachments

Microtubule binding needs to be sufficiently dynamic to allow the correction of erroneous attachments of kinetochores and the stabilization of proper bi-oriented kinetochore-microtubule attachments. The latter are high affinity interactions that need to be maintained as

microtubules grow and shrink, so that chromosome movement can be powered through depolymerization of microtubule during anaphase. These attachments are stabilized by the activity of microtubule-binding complexes such as Dam1 complex in fungi and Spindle- and Kinetochore-Associated (SKA) complex in mammals (Cheeseman and Desai, 2008). As Ndc80 complex is the major component of the microtubule-binding site it is not surprising that these microtubule-binding complexes work mainly by regulating the binding of the Ndc80 complex to microtubules. For example, the SKA complex binds processively to dynamic microtubules and contributes to retaining the Ndc80 complex at depolymerizing microtubule tips, possibly enhancing the overall processivity of microtubule binding (Asbury et al., 2006; Chan et al., 2012; Grishchuk et al., 2008; Jeyaprakash et al., 2012; Miranda et al., 2005; Schmidt et al., 2012; Welburn et al., 2009; Westermann et al., 2005; Westermann et al., 2006). Additionally, it has been recently proposed that targeting of proteins to the Ndc80 complex may be another mechanism of regulating the kinetochore- microtubules interactions. For example, such proteins include CDT1 in human cells (Varma et al., 2012) and the regulator of microtubule polymerization Dis1 in fission yeast (Hsu and Toda, 2011). They associate with the Ndc80 loop, a short region that interrupts the coiled-coil domain of the Ndc80 subunit but the contribution of these proteins to kinetochore- microtubule binding remains to be clarified.

The dynamics of kinetochore- microtubule interactions are regulated mainly through reversible phosphorylation events at the kinetochore, via the activity of several kinetochore-localized kinases and phosphatases of the 'error correction' machinery. Among these, of crucial importance are Aurora B kinase and PP2A phosphatase, with its regulatory subunit B56 subunit (Foley and Kapoor, 2013). The role of Aurora B in destabilizing and eliminating erroneous kinetochore-microtubule interactions is in part achieved through the phosphorylation of KMN components, which in turn reduces the microtubule binding affinity (Welburn et al., 2010). In particular, Aurora B phosphorylates multiple sites on the positively charged N-terminal tail of Ndc80 (Alushin et al., 2010; Ciferri et al., 2008; Tooley et al., 2011),

therefore decreasing the microtubule-binding affinity *in vitro* and weakening microtubule-induced clustering of Ndc80 complexes (Alushin et al., 2010; Cheeseman et al., 2006; Ciferri et al., 2008; DeLuca et al., 2006). Aurora B also phosphorylates Knl1, the Dsn1 subunit of the Mis12 and CENP-U (member of the CCAN) (Hua et al., 2011; Welburn et al., 2010), but the effects of these phosphorylation events on microtubule binding are poorly understood. Additionally, Aurora B phosphorylation negatively regulates the association of SKA complex with Ndc80 complex and microtubules to prevent precocious stabilization of erroneous attachments (Chan et al., 2012; Jeyaprakash et al., 2012; Schmidt et al., 2012).

How Aurora B activity is maximized when erroneous attachments are present is still a controversial issue. According to current models (Figure 3), this can be achieved by differential access to kinetochore substrates according to the status of attachment. In the presence of erroneous attachments and low inter-kinetochore tension, Aurora B, enriched at the centromeric region, is located close to its substrates, leading to their phosphorylation (Liu et al., 2010). When bi-orientation is achieved, the resulting high tension increases the distance of Aurora B from its substrates. However, as the accessibility of Aurora B to kinetochore substrates appears to be highest in prometaphase [e.g. in nocodazole, (Liu et al., 2010)], it is therefore unclear how stable attachments can be at all formed at the start of mitosis.

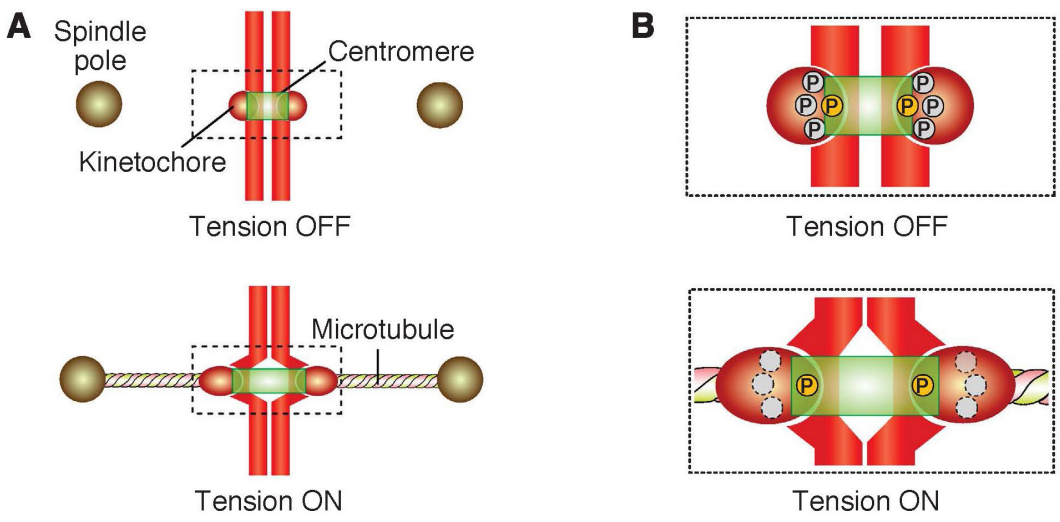

Figure 3 Phosphorylation status of the kinetochore in response to tension

A) Schematic of the geometry of the centromere–kinetochore interface in the absence (OFF) and presence of

tension (ON). B) Magnification of the centromere–kinetochore interface showing the change in the phosphorylation status of kinetochore substrates in response to tension. In the absence of tension, kinetochores are close to the centromere (green), where high kinase activity is present. In this configuration, substrates that are either proximal or distal to the centromere are phosphorylated. Conversely, in the presence of tension, the distance of kinetochores from the centromere increases and therefore distal substrates are not phosphorylated, while phosphorylation of close substrates persists (the yellow circle marked by 'P' indicates constitutive phosphorylation). From (Santaguida and Musacchio, 2009).

Aurora B phosphorylation is counteracted by the activity of kinetochore-bound phosphatases, such as protein phosphatase 2 A (PP2A) and, to a minor extent, protein phosphatase 1 (PP1) (Foley and Kapoor, 2013). PP2A is associated with the B56 regulators that target the holoenzyme to kinetochores during mitosis, via a direct association with the checkpoint component BubR1 (Suijkerbuijk et al., 2012b; Xu et al., 2013). PP2A-B56 promotes dephosphorylation of kinetochore substrates at unattached kinetochores to facilitate kinetochore-microtubule attachment and to ensure that phosphorylation remains low on bi-oriented chromosomes. However, little is known about the PP2A-specific substrates and how PP2A activity is regulated at the kinetochore.

The regulation of kinetochore–microtubule attachments depends on additional proteins, including Polo-like kinase 1 (Plk1) and checkpoint proteins, such as Mps1, Bub1 and BubR1 (Foley and Kapoor, 2013). It is likely that they regulate kinetochore-microtubule attachments indirectly, possibly by influencing Aurora B and PP2A-B56 recruitment. In fact, Aurora B targeting to centromeres depends on Bub1-mediated phosphorylation of histone H2A and on Mps1 activity (van der Waal et al., 2012; Yamagishi et al., 2010), whereas recruitment of PP2A-B56 to the kinetochore depends on Plk1-mediated phosphorylation of BubR1 (Suijkerbuijk et al., 2012b; Xu et al., 2013). The identification of the substrates of Aurora B, PP2A-B56 and their kinetochore regulators, and of their docking sites at the kinetochore, will be instrumental to understand how microtubule- dependent rearrangements in the centromere and kinetochore are integrated with phospho-signaling networks to stabilize proper kinetochore-microtubule interactions.

Molecular basis of the spindle assembly checkpoint

The spindle assembly checkpoint (SAC), or mitotic checkpoint, herewith abbreviated as SAC or simply 'checkpoint', is a safety mechanism, conserved in all eukaryotes, that coordinates mitotic timing with chromosome–spindle interactions during mitosis, restricting mitotic exit to cells that have bi-oriented all their chromosomes (Foley and Kapoor, 2013; Lara-Gonzalez et al., 2012; Musacchio and Salmon, 2007). In contrast with what the name 'spindle assembly checkpoint' suggests, the SAC does not monitor spindle assembly per se but rather the status of kinetochore–microtubule attachment.

Cells in which the checkpoint is altered or artificially inactivated undergo precocious mitotic exit in the presence of unattached or incorrectly attached chromosomes and are therefore prone to missegregation events. These errors may lead to the development of aneuploidies (aberrations in chromosome numbers) and eventually genetic instability, common hallmarks of cancer cells (Kolodner et al., 2011; Weaver and Cleveland, 2006).

The SAC delays precocious chromosome segregation through the inactivation of Cdc20, a cofactor of the E3 ubiquitin ligase known as the APC/C (anaphase-promoting complex; also known as the cyclosome) (Figure 4). The APC/C^{Cdc20} triggers both sister chromatid segregation and exit from mitosis via the ubiquitylation and subsequent proteasome-dependent destruction of Cyclin B (the master kinase of mitotic progression) and Securin (an inhibitor of the enzyme separase, which proteolytically cleaves cohesin complexes). Together with the APC/C subunit APC10, the Cdc20 co-activator forms a site that recognizes destruction box (D-box) motifs present in both Cyclin B and Securin. The SAC catalyzes the formation of a Cdc20 inhibitory complex, referred to as the mitotic checkpoint complex (MCC). As a result of its ability to inhibit APC/C activity, the SAC stabilizes Securin and Cyclin B, blocking the mitotic progression at the metaphase/anaphase transition (Figure 4).

The SAC includes the Ser/Thr kinases Aurora B (Ipl1 in *S. cerevisiae*), monopolar spindle protein 1 (Mps1) and budding uninhibited by benomyl 1 (Bub1), as well as the non-kinase

components mitotic arrest deficient 1 (Mad1), Mad2, Bub3, Bub1-Related 1 (BubR1; the human ortholog of yeast Mad3) (Musacchio and Salmon, 2007). Beside the 'core' SAC components, additional proteins that regulate SAC activity in higher eukaryotes include Rod-Zw10-Zwilch (RZZ) complex, p31^{comet}, several protein kinases including mitogen-activated protein kinase (MAPK), Cdk1-Cyclin B, Nek2, Haspin and polo-like kinase-1 (Plk1), the microtubule motors centromere protein (CENP)-E (also known as Kinesin-7) and Dynein, and dynein-associated proteins (Musacchio and Salmon, 2007).

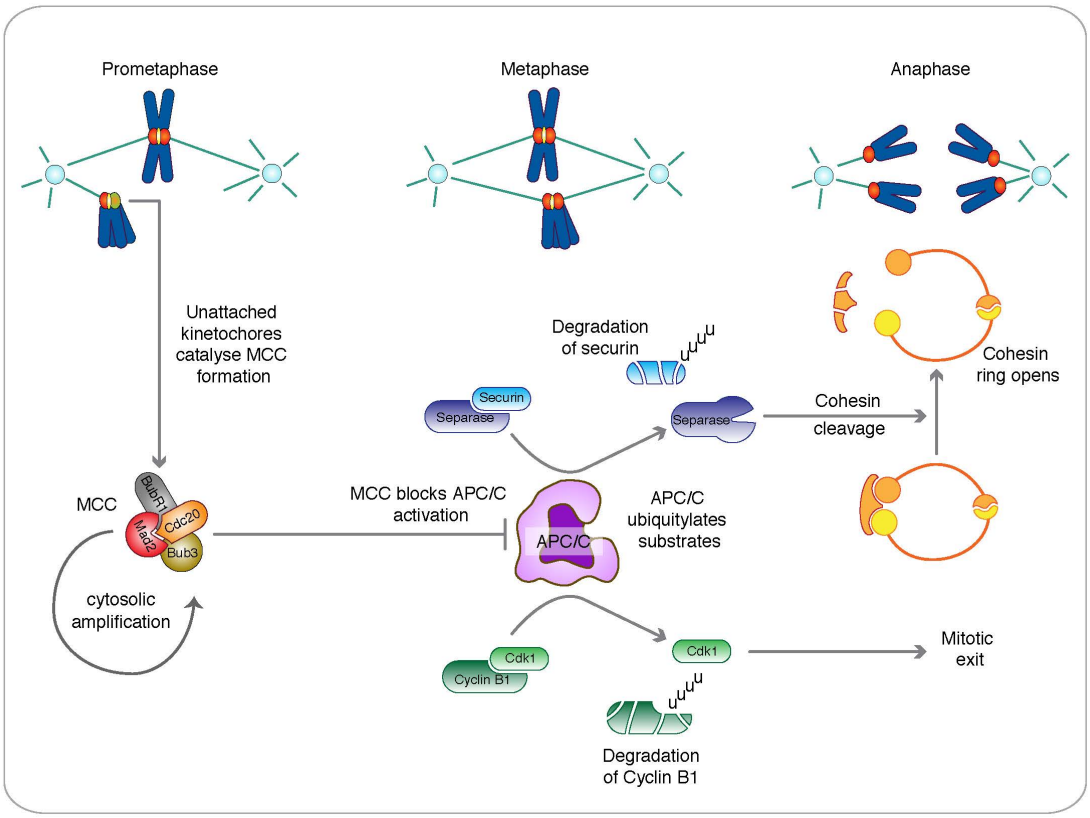

Figure 4 Molecular basis of the spindle assembly checkpoint

At mitotic entry, sister chromatids are held together by cohesin (yellow). During the early stages of mitosis (prometaphase), unattached kinetochores (green) catalyze the formation of the mitotic checkpoint complex (MCC) composed of BubR1, Bub3, Mad2 and Cdc20, leading to inhibition of the APC/C. Once all the chromosomes are attached to the spindle (attached kinetochore are colored in red) and aligned at the spindle equator (metaphase), generation of the MCC ceases, allowing Cdc20 to activate the APC/C, leading to the ubiquitylation and degradation of Securin and Cyclin B1. Degradation of Securin liberates Separase, a protease that in turn cleaves the Scc1 subunit of the cohesin ring structure; this opens the ring, allowing sister chromatids to separate (anaphase). Meanwhile, degradation of Cyclin B1 inactivates Cdk1, leading to mitotic exit. U, ubiquitin. Adapted from (Lara-Gonzalez et al., 2012).

All SAC components contribute, via direct and indirect mechanisms, to the formation of the MCC and therefore to APC/C inhibition. The MCC is a heterotetramer composed of Cdc20, Mad2, BubR1 and Bub3 (Figure 4) (Sudakin et al., 2001), where Mad2 and BubR1 bind to two distinct binding sites on Cdc20 (Hardwick et al., 2000; Hwang et al., 1998) and, together, have a synergistic effect on APC/C inhibition (Davenport et al., 2006; Fang, 2002; Han et al., 2013; Izawa and Pines, 2012; Morrow et al., 2005; Tang et al., 2001; Wu et al., 2000). However, BubR1 bound to Cdc20 is currently considered the bona fide APC/C inhibitor as it blocks substrate binding to the APC/C^{Cdc20} (Lara-Gonzalez 2012).

Several biochemical and structural studies have significantly contributed to the understanding of the protein-protein interactions involved in MCC assembly (Chao et al., 2012; De Antoni et al., 2005; Luo et al., 2000; Luo et al., 2002; Luo et al., 2004; Mapelli et al., 2007). The MCC is assembled from two sub-complexes, the Mad2:Cdc20 and the BubR1:Bub3 complexes. It is well established that binding of Mad2 to Cdc20 is necessary for binding of BubR1 to Cdc20 and that BubR1 uses a K-E-N sequence for Cdc20 binding (Davenport et al., 2006; Musacchio and Salmon, 2007). Mad2 bound to Cdc20 interacts with BubR1 and exposes Cdc20 for efficient BubR1 binding, as suggested by the recent crystal structure of the S. *pombe* MCC complex (Chao et al., 2012).

How Mad2:Cdc20 and BubR1:Bub3 can come in closer contact and therefore how MCC is formed remain controversial. Unattached kinetochores have a central role in MCC formation and Cdc20 inhibition, as conditions that affect the structural integrity of kinetochores generally inhibit SAC activity (Musacchio and Salmon, 2007). With the possible exception of Aurora B, all SAC components, including Mps1, Bub1, BubR1, Bub3, Mad1 and Mad2, are recruited to unattached kinetochores (Fava et al., 2011; Kiyomitsu et al., 2011; Kiyomitsu et al., 2007; Liu et al., 2006; London et al., 2012; Martin-Lluesma et al., 2002; McAinsh et al., 2006; Miller et al., 2008; Nijenhuis et al., 2013; Pagliuca et al., 2009; Schittenhelm et al., 2009; Shepperd et al., 2012; Yamagishi et al., 2012). As BubR1-Bub3 appear to bind to each other constitutively throughout the cell cycle (Chen, 2002; Taylor et al., 1998), kinetochores are

crucial for catalyzing the formation of Mad2:Cdc20 (De Antoni et al., 2005; Kulukian et al., 2009) and, by forcing high local concentrations, for promoting the interaction of Mad2:Cdc20 with BubR1:Bub3 complexes (Figure 4) (Foley and Kapoor, 2013; Lara-Gonzalez et al., 2012). The current model for the kinetochore-catalyzed formation of Mad2–Cdc20 complexes is the 'Mad2 template' model (De Antoni et al., 2005). Mad2 exists in two conformations: a 'closed' conformer that is competent to bind Cdc20 and Mad1 (which is the kinetochore receptor for closed Mad2), and an 'open' conformer that does not associates with these binding partners. According to the model, a heterodimer of closed Mad2 bound to kinetochore-localized Mad1 catalyzes the conversion of cytosolic Mad2 from an open to a closed state and hence the ability of Mad2 to bind Cdc20. Beside this mechanism, little is known about the molecular nature of other interactions taking place at the kinetochore, specifically, how the Mad2:Cdc20 and BubR1:Bub3 intersect at the kinetochore to promote efficient MCC formation.

As a single unattached kinetochore is sufficient to inhibit APC/C^{Cdc20} activity (Rieder et al., 1995), it has been proposed that, once MCC is generated at the kinetochore, the number of MCC molecules is amplified via a cytosolic (kinetochore-independent) mechanism (De Antoni et al., 2005) (Figure 4). It has been suggested that this amplification step relies on the ability of cytosolic Cdc20:C-Mad2 complexes to promote the conversion of O-Mad2 into Cdc20:C-Mad2 via Mad2 dimerization (Simonetta et al., 2009). However, the discovery that the dimerization interface of C-Mad2 is implicated in the binding of other proteins, such as $p31^{comet}$ (limitedly to metazoans) (Mapelli et al., 2006; Teichner et al., 2011; Varetti et al., 2011; Yang et al., 2007) and BubR1/Mad3 (Chao et al., 2012; Tipton et al., 2011), suggests that Mad2 dimerization might not be crucial for the cytosolic amplification of MCC. Recently, it has been proposed that Mad2 released from the final inhibitory BubR1-Cdc20 complex can act catalytically to facilitate the loading of additional BubR1 molecules into inhibitory complexes with Cdc20 (Han et al., 2013), thereby increasing the number of APC/C^{Cdc20} molecules inhibited by BubR1. This would explain how kinetochore-derived Mad2-Cdc20 complexes amplify the number of MCC complexes in the cytosol.

Kinetochore recruitment of SAC components

Despite the crucial importance of kinetochore in the generation of the SAC signal and amplification of the rate of MCC formation, the early events that prime kinetochore proteins to unattached kinetochores are still poorly understood. Studies of the localization dependency of checkpoint proteins over many years have demonstrated that all SAC components, with the possible exception of Aurora B, dock on the KMN network when recruited to kinetochores (Fava et al., 2011; Kiyomitsu et al., 2011; Kiyomitsu et al., 2007; Liu et al., 2006; London et al., 2012; Martin-Lluesma et al., 2002; McAinsh et al., 2006; Miller et al., 2008; Nijenhuis et al., 2013; Pagliuca et al., 2009; Schittenhelm et al., 2009; Shepperd et al., 2012; Yamagishi et al., 2012). In particular, the Ndc80 and Knl1 complexes have emerged as crucial receptors for the checkpoint proteins but the direct interactions defining the association of checkpoint proteins with KMN components are not known.

Targeting of checkpoint proteins to the KMN network follows a non-hierarchical structure that relies upon inter-dependent pathways (Figure 5). Chemical inhibition of Aurora B and Mps1 kinases has revealed that these proteins use their activity to control the kinetochore recruitment of Bub1, BubR1, Bub3, Mad1, Mad2, and additional SAC regulators, such as CENP-E, RZZ and Dynein (Ditchfield et al., 2003; Emanuele et al., 2008; Kasuboski et al., 2011; Santaguida et al., 2010; Saurin et al., 2011; Vigneron et al., 2004), placing these kinases at the top of the recruitment pathway. Additionally, they control SAC signaling at downstream levels, likely regulating MCC formation and the MCC-APC/C interaction (Funabiki and Wynne, 2013; Lara-Gonzalez et al., 2012), indicating that their activities are required for both kinetochore-dependent and independent mechanisms of MCC assembly.

How Aurora B and Mps1 are initially recruited to kinetochores is poorly understood. Aurora B, a subunit of the chromosomal passenger complex (CPC), which contains Incenp, Survivin, and Borealin (Carmena et al., 2012) is localized to the inner centromere (Figure 5) from prophase to metaphase where it recognizes two histone marks, phopsho-Thr3 of H3 and

phospho-Thr120 of H2A, substrates of Haspin and Bub1 kinases respectively (Kelly et al., 2010; Wang et al., 2010; Yamagishi et al., 2010). Whether a kinetochore-associated pool of Aurora B exists, in addition to the centromeric one, is unclear. Mps1, whose structural organization is very similar to Bub1 and BubR1, is recruited to kinetochores by a still unclear mechanism dependent on the Ndc80 complex (Figure 5) (Abrieu et al., 2001; Martin-Lluesma et al., 2002; Nijenhuis et al., 2013; Stucke et al., 2004; Stucke et al., 2002).

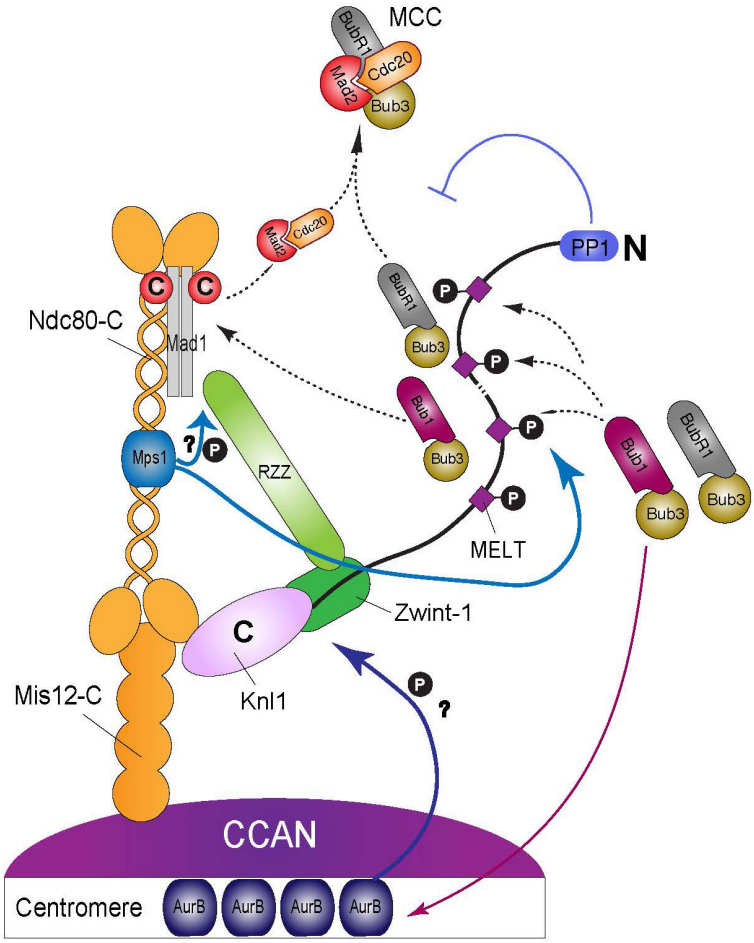

Figure 5 Model for kinetochore recruitment of SAC components

Kinetochore recruitment of SAC components relies on two branches of the KMN network, the Ndc80 complex (Ndc80-C) and the Knl1 complex. Aurora B (AurB), enriched at the centromeric region, and Mps1, recruited to the Ndc80 complex, phosphorylate several sites on the KMN network to promote recruitment of downstream components. Mps1 phosphorylates some yet unidentified substrates to recruit Mad1/Mad2 (C, C-Mad2 in red) and RZZ to the Ndc80 complex and MELT sites to dock Bub1/Bub3 to Knl1. Bub1/Bub3 recruits, in turn, BubR1/Bub3 to Knl1 and positions it close to the Mad1/Mad2 complex, so that Mad2:Cdc20 and BubR1:Bub3 complexes can be incorporated into MCC. Additionally, Bub1 phosphorylates H2A to promote the enrichment of Aurora B at the centromere. Mad1/Mad2 on the Ndc80 complex is further stabilized by the Knl1 branch: by RZZ, which contacts Zwint-1, and Bub1, bound to MELT repeats. PP1, recruited to the N-terminus of Knl1, is

positioned very close to the site where MCC is formed to promote efficient silencing of the SAC at the kinetochore. Mis12-C, Mis12 complex; C, C-terminus.

How Aurora B and Mps1 kinases promote the recruitment of downstream SAC component has not been clarified yet. As the kinase activity of both kinases is required for this role, it is plausible that they phosphorylate one or multiple KMN proteins to generate docking sites for SAC components. Consistent with this model, it has been shown very recently that Mps1 phosphorylates Knl1 on multiple sites to dock Bub1/Bub3 complexes in different species (Figure 5) (London et al., 2012; Shepperd et al., 2012; Yamagishi et al., 2012). Importantly, as Bub1/Bub3 are required for the recruitment of BubR1/Bub3 and Mad1/Mad2, this might explain how Mps1 controls the recruitment of Mad1/Mad2 to kinetochores. However, kinetochore-bound Bub1/Bub3 is not sufficient to recruit Mad1 and Mad2 in the absence of Mps1 activity (Ito et al., 2012; Yamagishi et al., 2012), indicating that Mps1 may control Mad1 and Mad2 recruitment via additional mechanisms, other than Knl1 phosphorylation. Indeed, Mad1 recruitment relies on multiple low affinity binding sites on the KMN network, provided by proteins such as Bub1, RZZ and the Ndc80 complex (Bharadwaj et al., 2004; Brady and Hardwick, 2000; Kim et al., 2012; Klebig et al., 2009; Kops et al., 2005; Martin-Lluesma et al., 2002).

Collectively, kinetochore recruitment of SAC components relies on various yet uncharacterized contributions from Mps1 and Aurora B activities on the two branches of the KMN network, the Ndc80 complex and the Knl1 complex (Figure 5). Specifically, Mps1, Mad1/Mad2 and RZZ might be recruited to the Ndc80 complex while Bub1, BubR1 and Bub3 to Knl1. Mad1/Mad2 and RZZ recruitment might be stabilized by additional association with Knl1-bound Bub1 and Zwint-1 respectively.

The silencing of the SAC

Timeliness of mitotic division relies on the SAC inactivation at each kinetochore. SAC extinction is achieved essentially via two mechanisms: the removal of SAC proteins from kinetochores and the disassembly of MCC from the APC/C.

Protein removal from the kinetochore is a crucial step in SAC extinction, as constitutive targeting of Mad1 to the kinetochore is sufficient to sustain Mad2-dependent signaling even after bi-orientation has been achieved (Maldonado and Kapoor, 2011). Once cohesin is lost, chromosomes cannot re-establish cohesin and are irreversibly committed to anaphase. Therefore, SAC removal must be timely controlled and coupled with bi-orientation. Indeed, SAC signaling is influenced by binding of microtubules at the kinetochore. For example, SAC proteins become enriched at unattached kinetochores and are subsequently depleted upon microtubule attachment. However how this coupling is achieved is poorly understood. As the KMN network is the crucial microtubule-binding site and SAC recruiting platform at the kinetochore, the current view is that coupling might be achieved through the ability of the KMN network to tune SAC recruitment and signaling according to changes in the microtubule-binding status. However, the molecular mechanisms responsible for this coupling remain unclear. As anticipated before, the KMN component Knl1 harbors, at its extreme N-terminus, a short stretch of basic amino acids that has been found to interact with microtubules (Espeut et al., 2012). It has been recently proposed that, at least in *C. elegans*, this microtubule- binding domain senses the presence of microtubules attached to the kinetochore, potentially via the closely associated Ndc80 complex, and relays their presence to shut off the checkpoint signal at the kinetochore (Espeut et al., 2012). For example, since Knl1 has been proposed to recruit Bub1/Bub3 and BubR1/Bub3, which generate in turn the MCC together with Mad1/Mad2 and Cdc20, microtubule binding sensed by Knl1 may affect the formation of the MCC. How exactly this may occur and whether this mechanism is

conserved is unknown. Moreover, how microtubule- dependent extinction pathways at the kinetochore are relayed to MCC disassembly in the cytoplasm remains unclear.

Dissociation of SAC components from bi-oriented kinetochores is achieved mainly via the 'stripping' of the SAC proteins and changes in the phosphorylation state of the kinetochore. For example, Mad1 and Mad2 are physically removed ('stripped') away from their kinetochore site towards microtubule minus ends, through the microtubule-dependent action of cytoplasmic dynein (Funabiki and Wynne, 2013; Gassmann et al., 2010; Howell et al., 2001; Kasuboski et al., 2011). As the dynein-dependent pathway does not seem to be conserved in yeast, it is plausible that additional dynein-independent pathways exist, possibly even in those organisms where dynein is present (Funabiki and Wynne, 2013).

As phosphorylation is important in SAC activation, it is expected that phosphatase activity plays a crucial part in SAC extinction. Indeed, SAC silencing has been recently shown to require the kinetochore recruitment of the protein phosphatase 1 PP1 (γ isoform, herewith called simply PP1) (Liu 2010, Rosenberg 2011, Meadows 2012). Disruption of the kinetochore recruitment of PP1 compromises the SAC in different species, and leads to lethality in budding yeast as a result of the inability to silence the SAC. However, in vertebrates the impact of PP1 on SAC silencing remains to be established. PP1 (Glc7 and Dis2 in budding and fission yeasts respectively) localizes at kinetochores via a highly conserved PP1-docking site present on the KMN component Knl1 (Figure 5 and 6). In human Knl1, the docking site is bipartite, as it includes the [S/G]ILK and RVxF motifs (Liu et al., 2010), two motifs that are commonly found in PP1-interacting proteins (Hendrickx et al., 2009). However, PP1 binding to Knl1 seems to be entirely dependent on the RVxF motif (Liu et al., 2010). It is likely that PP1 might be recruited to kinetochores via interactions with additional PP1-binding proteins, such as Fin1 in budding yeast (Akiyoshi et al., 2009), kinesin-8 (Klp5 and Klp6) in fission yeast (Meadows et al., 2011) and CENP-E in human cells (Kim et al., 2010). However, a yeast study

has indicated that the amount of PP1 recruited at the kinetochore must be finely tuned for proper phospho-regulation (Rosenberg et al., 2011).

A series of experiments supports the idea that kinetochore-bound PP1 acts to oppose the function of Aurora B (Francisco et al., 1994; Hsu et al., 2000; Liu et al., 2010; Pinsky et al., 2006; Pinsky et al., 2009; Rosenberg et al., 2011; Vanoosthuyse and Hardwick, 2009), and possibly Mps1 (London et al., 2012), by dephosphorylating their kinetochore substrates. How the balance of kinase and phosphatase activity contributes to SAC signaling is poorly understood. Moreover, little is known about PP1 specificity and regulation at the kinetochore. In contrast with Ser/Thr kinases, many of which (including SAC kinases) recognize substrates based on consensus sequences, PP1 and other phosphatases do not exhibit substrate selectivity *in vitro* (Boens et al., 2013). Phosphatases exist as holoenzymes, whose activity and specificity are influenced by regulatory subunits. PP1 activity seems to be controlled by Sds22, a regulator that binds PP1 though its leucine-rich repeats (Ceulemans et al., 2002; Heroes et al., 2013; Lesage et al., 2007; Stone et al., 1993) and acts as inhibitor for specific substrates but not others (Posch et al., 2010). How PP1 achieves substrate specificity at the kinetochore remains unclear.

Little is known on the PP1 substrates important for SAC silencing at the kinetochore. An attractive candidate is Knl1, as it is phosphorylated by Mps1 to recruit Bub1/Bub3 complexes (Figure 5). However, it is unlikely that Bub1 dissociation from the kinetochore triggers SAC silencing since Bub1 remains on bi-oriented kinetochores (Howell et al., 2004; Shah et al., 2004), albeit at reduced levels compared to unattached kinetochores. Other candidates include Ndc80, BubR1 (Mad3), which is phosphorylated by Ipl1 (Aurora B) (King et al., 2007) and Zwint-1 (Kasuboski et al., 2011).

To ensure timely dephosphorylation of kinetochore substrates upon bi-orientation, PP1 activity must be finely tuned and coupled with microtubule attachment. Indeed, PP1 levels are low in prometaphase and increased on bi-oriented chromosomes at the metaphase plate (Liu et al., 2010). Interestingly, PP1 localization at the kinetochore is negatively regulated by

Aurora B to ensure low phosphatase activity at unattached kinetochores (Liu et al., 2010). This is achieved through the Aurora B phosphorylation of the RVSF motif of Knl1. Other kinetochore-bound kinases or structural arrangements of the microtubule-binding site might timely regulate PP1 activity.

Finally, extinction of SAC signaling at the kinetochore must also be integrated with dissociation of Cdc20 from its inhibitors Mad2, BubR1 and Bub3 to activate the APC/C^{Cdc20}. The mechanisms that promote APC/C de-inhibition include 1) the APC/C-dependent auto-ubiquitylation of Cdc20; 2) the disassembly of the MCC promoted, in metazoans, by $p31^{comet}$, a binding partner of closed Mad2 and 3) the APC/C-dependent ubiquitylation and degradation of BubR1 (Choi et al., 2009; Foley and Kapoor, 2013). It remains to be tested if and how these mechanisms are controlled by microtubule attachment.

The functions of Bub1 and BubR1

Bub1 was originally characterized as a conserved component of the SAC (Hoyt, 2001; Musacchio and Salmon, 2007; Taylor and McKeon, 1997). More recently, Bub1 was also shown to play a role in chromosome alignment (Johnson et al., 2004; Meraldi and Sorger, 2005; Taylor and McKeon, 1997; Windecker et al., 2009). Precisely how Bub1 performs these functions at the molecular level is unclear (Bolanos-Garcia and Blundell, 2011; Elowe, 2011).

Like its orthologs, human Bub1 contains an N-terminal tetratricopeptide repeats (TPR) domain, a Bub3-binding domain and a C-terminal kinase domain (Figure 6). More recently, two conserved motifs of unknown functions, named conserved domain I and II (CDI and CDII), have been identified (Klebig et al., 2009). Bub1 forms a constitutive 1:1 complex with the checkpoint protein Bub3 throughout the cell cycle (Hardwick et al., 2000; Larsen et al., 2007; Roberts et al., 1994; Taylor et al., 1998). Bub3 folds as a 7-bladed β-propeller (Larsen and Harrison, 2004), a structural domain often used for protein-protein interactions (Neer et al., 1994). The interaction of Bub1 with Bub3 is mediated by its Bub3-binding domain, which

is defined as the segment necessary and sufficient for the interaction with Bub3 *in vitro* (Larsen et al., 2007).

The Bub3-binding domain undergoes a transition from an unfolded conformation to a well defined and ordered structure upon binding to the top surface of the β-propeller of Bub3 (Larsen et al., 2007). The Bub3-binding motif is also often referred to as GLEBS motif, for Gle2-binding site (Wang et al., 2001). Here, however we prefer to use the name Bub3-binding

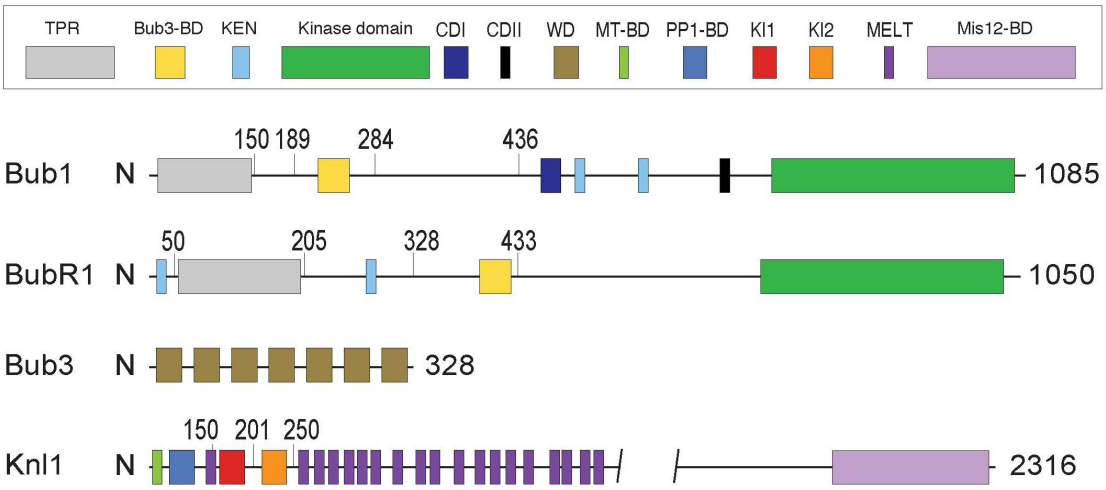

Figure 6 Domain composition of Bubs and Knl1

Schematic view of the domain composition of human Bub1, BubR1, Bub3 and Knl1. Numbers refer to protein residues. TPR, tetratricopeptide repeats; Bub3-BD, Bub3-binding domain, also known as GLEBS; KEN, Lysine (K)- Glutamin acid (E)-Asparagin (N) box; CDI, conserved domain I; CDII, conserved domain II; MT-BD, microtubule-binding domain; PP1-BD, protein phosphatase 1 binding domain; WD, WD40, Tryptophan-aspartic acid (W-D) repeats; KI1, Lysine- Isoleucine (K-I) motif 1, Bub1-binding domain 1; KI2, Lysine-Isoleucine (K-I) motif 1 Bub1-binding domain 2; MELT, Methionine (M)- Glutamic acid (E)- Leucine (L)-Threonine (T) repeats; Mis12-BD, Mis12-binding domain; N, N-terminus.

domain because there is no evidence that Bub1 and BubR1 interact with the Gle2 protein (also known as Rae1).

Bub1 localization at kinetochores might be important or even essential for its functions. Bub1 localizes at kinetochores during very early mitotic stages, where it promotes kinetochore recruitment of other checkpoint proteins, such as Mad1, Mad2, BubR1 and Bub3. Such recruitment is in turn believed to be important for the activity of these proteins and downstream signaling events (Boyarchuk et al., 2007; Chen, 2002; Johnson et al., 2004; Klebig

et al., 2009; Meraldi and Sorger, 2005; Rischitor et al., 2007; Sharp-Baker and Chen, 2001; Storchova et al., 2011; Vigneron et al., 2004). As Bub1 displays slow exchange dynamics at kinetochores (Howell et al., 2004; Shah et al., 2004) and contains a TPR domain, a fold that is used as interaction module (D'Andrea and Regan, 2003; Zeytuni and Zarivach, 2012), it has been proposed that Bub1 acts as a scaffold at the kinetochore to promote SAC recruitment of downstream components, in particular Mad1 and BubR1 (Brady and Hardwick, 2000; Rischitor et al., 2007). It is likely that Bub1 recruits Mad1 and BubR1 via direct protein-protein interactions. Consistently, yeast-two hybrid assays have shown a physical but weak interaction between human Bub1 and BubR1 (D'Arcy et al., 2010; Kiyomitsu et al., 2007). However, direct biochemical evidences defining the physical interactions between Bub1-Mad1 and Bub1-BubR1 are still missing.

Bub1 is a Ser/Thr kinase, with an N-terminal extension that wraps around the N-lobe of its kinase domain and regulates the kinase activity (Kang et al., 2008). It phosphorylates Cdc20, the target of the checkpoint, on several sites, to inhibit the catalytic activity of APC/C (Kang et al., 2008; Tang et al., 2004). However, whether the phosphorylation of Cdc20 contributes to SAC signaling is controversial, as Bub1 kinase activity is not directly required for SAC activation in yeast (Fernius and Hardwick, 2007; Kawashima et al., 2010), *Xenopus* egg extracts (Sharp-Baker and Chen, 2001) and mammalian cells (Klebig et al., 2009; Perera et al., 2007; Ricke et al., 2012). Nevertheless, Bub1 kinase activity may contribute to SAC signaling through the phosphorylation of Thr120 of histone 2A (H2A), which promotes the recruitment of Aurora B to the centromere (Figure 5) (Fernius and Hardwick, 2007; Kawashima et al., 2010; Perera et al., 2007; Wang et al., 2011; Yamagishi et al., 2010).

BubR1 (Mad3 in yeast), whose overall domain organization is very similar to that of Bub1 (Figure 6), is also implicated both in checkpoint signaling and chromosome alignment (Chan et al., 1999; Elowe et al., 2010; Harris et al., 2005; Johnson et al., 2004; Lampson and Kapoor, 2005; Li and Murray, 1991; Taylor et al., 1998). Like Bub1, BubR1 forms a stoichiometric complex with Bub3 via a binding mechanism very similar to Bub1 (Larsen et al., 2007).

However, unlike Bub1, the main function of BubR1 is to be incorporated, together with Bub3, Mad2 and Cdc20, in the checkpoint effector MCC (Musacchio and Salmon, 2007). The presence of Bub3 in the MCC might not be crucial for the inhibition of the APC/C, as fission yeast BubR1 does not contain the Bub3-binding domain and does not interact with Bub3. BubR1 contains two KEN boxes that have been implicated in Cdc20 binding and APC/C inhibition (Figure 6). Recent structural analysis of fission yeast MCC has revealed that BubR1/Mad3 uses its N-terminal KEN box, that precedes the TPR domain (and is absent in Bub1), to establish direct interactions with both Mad2 and Cdc20 (Chao et al., 2012), and the second KEN box to block substrate binding to the APC/C (Lara-Gonzalez et al., 2011). Additionally, the TPR domains of BubR1 also directly interact with Cdc20, consistent with the observation that mutating the TPR or the KEN boxes of BubR1 disrupts its ability to bind Cdc20 and impairs SAC signaling (Burton and Solomon, 2007; Davenport et al., 2006; Kiyomitsu et al., 2007; Lara-Gonzalez et al., 2011).

Like Bub1, BubR1 has a C-terminal kinase domain. However, while some organisms appear to have lost the kinase domain, yielding Mad3-like proteins, others, like the human BubR1, have accumulated mutations in several motifs critical for kinase activity. Therefore, human BubR1 has been recently proposed to be a pseudokinase, with its kinase domain active as protein stabilizer rather than an active enzyme (Suijkerbuijk et al., 2012a). Overall, the SAC function of BubR1 is therefore in MCC formation and relies on the N-terminal region preceding the kinase domain, which is sufficient for SAC function in cells and APC/C inhibition *in vitro* (Han et al., 2013; Lara-Gonzalez et al., 2011; Malureanu et al., 2009).

Overall, despite a large degree of sequence and structural similarity, Bub1 and BubR1 perform distinct and non-redundant functions in SAC signaling, assisted in their roles by Bub3.

Kinetochore recruitment of Bub1 and BubR1

Like all SAC components, Bub1 and BubR1 are recruited to unattached kinetochores (Musacchio and Salmon, 2007). Understanding exactly how Bub1 binds the kinetochore is of crucial importance, as Bub1 is a scaffold that recruits BubR1, Bub3, Mad1 and Mad2, thereby promoting the formation of MCC complexes at the kinetochore (Boyarchuk et al., 2007; Chen, 2002; Johnson et al., 2004; Klebig et al., 2009; Meraldi and Sorger, 2005; Rischitor et al., 2007; Sharp-Baker and Chen, 2001; Storchova et al., 2011; Vigneron et al., 2004). It is plausible that kinetochore recruitment of Bub1 and BubR1 is strongly intertwined with their activation and functions there. For instance, kinetochore localization of Bub1 and BubR1 might be important for their phosphorylation, which in turn contributes to the functions of these kinases (Elowe et al., 2010; Yamaguchi et al., 2003). The structural and sequence similarity of Bub1 and BubR1 together with the data gathered so far, support the idea that the mechanisms controlling Bub1 and BubR1 kinetochore recruitment might be similar. However, one important difference is that BubR1 recruitment requires Bub1 whereas the opposite is not true (Boyarchuk et al., 2007; Chen, 2002; Johnson et al., 2004; Klebig et al., 2009; Meraldi and Sorger, 2005; Rischitor et al., 2007; Sharp-Baker and Chen, 2001; Storchova et al., 2011; Vigneron et al., 2004). The molecular details of such mechanisms, however, are currently missing.

A pioneering finding was the discovery that 300 residues in the N-terminal region of murine Bub1 are sufficient for kinetochore localization (Taylor et al., 1998; Taylor and McKeon, 1997), leading to the identification of a N-terminal kinetochore-localization domain that includes the TPR and the Bub3-binding domain (Figure 6). Further deletion mapping of Bub1 demonstrated that the TPR region is dispensable for kinetochore localization, and that a segment containing the Bub3-binding domain might be sufficient for kinetochore localization (Taylor et al., 1998). Consistently, mutations in the Bub3-binding domain prevent kinetochore localization of Bub1 (Klebig et al., 2009) and BubR1 (Elowe et al., 2010; Lara-Gonzalez et al.,

2011), and impair BubR1's function in checkpoint and chromosome congression (Elowe et al., 2010; Lara-Gonzalez et al., 2011; Malureanu et al., 2009).

As the only known function of the Bub3-binding domain is binding to Bub3, these studies argue that the interaction of Bub1 and BubR1 with Bub3 might be necessary and sufficient for their kinetochore localization. In line with this, Bub3 is required for recruitment of Bub1 and BubR1 in yeast (Gillett et al., 2004; Vanoosthuyse et al., 2004; Windecker et al., 2009). Partially contradicting this idea, however, in human cells depletion of Bub3 does not affect Bub1 localization, although it might affect the localization of BubR1 (Logarinho et al., 2008; Meraldi et al., 2004). Conversely, depletion of Bub1 or BubR1 was found to reduce kinetochore recruitment of Bub3 in *Xenopus* egg extracts (Chen, 2004; Sharp-Baker and Chen, 2001), suggesting that these proteins are not simply recruited by Bub3 but rather co-recruited with Bub3.

In line with idea that the KMN is a crucial platform for checkpoint assembly, dependency studies in different organisms have unveiled that Bub1 and BubR1 recruitment is dependent on the KMN component Knl1 (Kiyomitsu et al., 2007; Pagliuca et al., 2009). More recently, insight into the mechanism of kinetochore recruitment of Bub1 and BubR1 developed around the discovery that their TPR domains interact with the outer kinetochore protein Knl1 in yeast two-hybrid interaction studies (Kiyomitsu et al., 2011; Kiyomitsu et al., 2007; Schittenhelm et al., 2009) and *in vitro* (Bolanos-Garcia et al., 2011; Krenn et al., 2012). This was a crucial finding that has provided evidence, for the first time, for direct interactions between Bub1 and BubR1, and in general SAC proteins, with a kinetochore component. Specifically, the TPR domains of Bub1 and BubR1 interact with two distinct but related 12-residue motifs in the N-terminal region of human Knl1, the KI-motifs (from the first two residues of their consensus sequence, KI(D/N)XXXF(L/I)XXLK, where X are non-conserved residues) (Bolanos-Garcia et al., 2011; Kiyomitsu et al., 2011; Krenn et al., 2012) (Figure 6 and 7). The two consecutive motifs are herewith indicated as KI1 and KI2. A TPR domain consists of multiple repeats of 34 amino acids sharing a degenerate consensus

sequence defined by a pattern of small and large hydrophobic residues. A canonical repeat adopts a basic helix-turn-helix fold and adjacent repeats form antiparallel α-helices due to their parallel packing, yielding an overall super-helical structure with a concave and convex curved surfaces. There are three repeats in the TPR domain of Bub1 and BubR1 that fold in a very similar TPR arrangement (Figure 7), consistent with the fact that Bub1 and BubR1 are closely related. As they share high structural similarity with the TPR domains of protein phosphatase 5, it has been proposed that Bub1 and BubR1 may interact with Knl1 in a mode similar to that observed in complexes formed between the TPR of PP5 and its ligands (Scheufler et al., 2000), via a "cradle" on the concave face of the TPR unit (Bolanos-Garcia

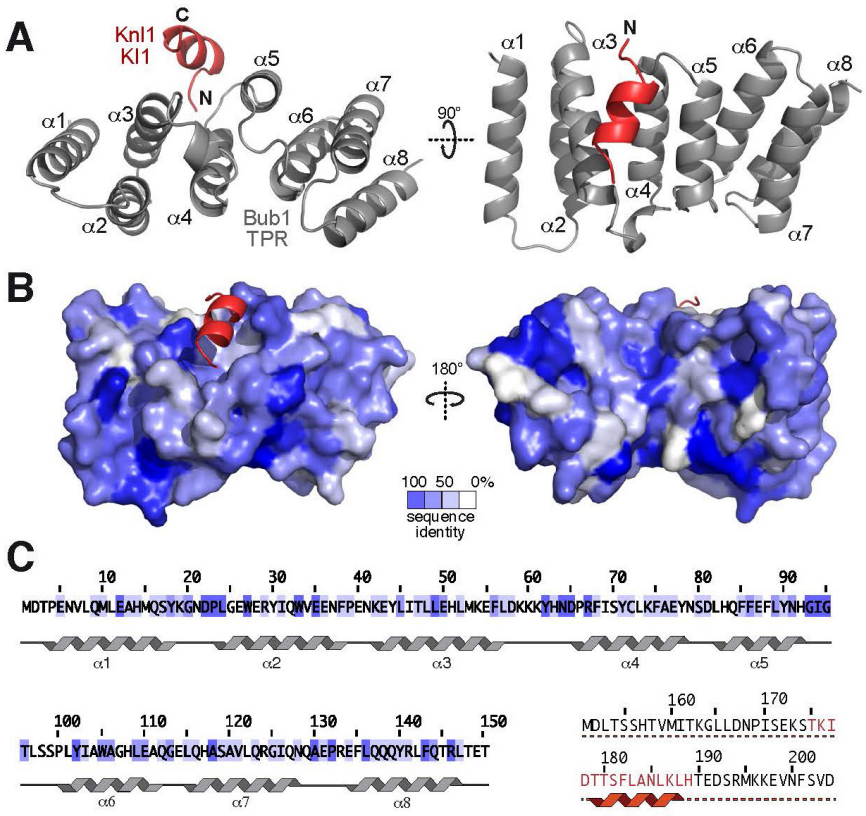

Figure 7 Crystal structure of the TPR domain of Bub1 in complex with KI1 of Knl1

A) Side and top view of a cartoon representation of Bub1 TPR domain (residues 1–150, in gray) and Knl1 peptide (residues 150-200, in red). B) Surface representation of the complex, oriented so as to show the convex (left) and concave (right) side. Sequence conservation (limited to Bub1 orthologues) was mapped onto the Bub1 structure using ConSurf. C) Sequence of the Bub1 (gray) and Knl1 (red) fragments used for crystallization. Secondary structure elements are mapped onto the sequence. C, C terminus; N, N terminus. From (Krenn et al., 2012).

and Blundell, 2011; D'Arcy et al., 2010; Kiyomitsu et al., 2011). Unexpectedly, the structures of Bub1:KI1 and BubR1:KI2 reveal that the KI fragment binds to a moderately conserved ridge on the convex surface of the TPR of both Bub1 and BubR1 (Figure 7) (Bolanos-Garcia et al., 2011; Krenn et al., 2012), revealing a common mode of interaction but different from that observed in the structurally similar TPR-peptide complexes (D'Andrea and Regan, 2003; Grove et al., 2008; Zeytuni and Zarivach, 2012). Furthermore, KI1 and KI2 adopt a similar helical conformation in both complexes, indicating that there are extensive structural similarities between these two interactions (Kiyomitsu et al., 2011; Kiyomitsu et al., 2007) (Bolanos-Garcia et al., 2011; Krenn et al., 2012).

The potential importance of the interaction of the Bub1 TPR repeats with the KI motif of Knl1 is highlighted by the observation that a point mutant in the TPR repeats prevents kinetochore recruitment of Bub1 (Kiyomitsu et al., 2007). Moreover, a deletion mutant lacking the TPRs of Bub1 failed to localize to kinetochores, reinvigorating the previously dismissed idea that this region of Bub1 participates in kinetochore recruitment (Klebig et al., 2009). However, the fact that so far KI1 and KI2 have only been identified in vertebrate Knl1 orthologs (Bolanos-Garcia and Blundell, 2011; Bolanos-Garcia et al., 2011; Kiyomitsu et al., 2011; Vleugel et al., 2012) has questioned the significance of this interaction. Collectively, both the N-terminal TPR repeats and the Bub3-binding domain, which bind respectively to Knl1 and Bub3, are thought to contribute to kinetochore recruitment of Bub1 and BubR1, but there is no unifying view of the relative importance of their contributions.

Only more recently (after two years from the beginning of my project), it was shown in different organisms that crucial for kinetochore recruitment of Bub1, BubR1 and Bub3 is their binding to the phosphorylated version of motifs that contain the consensus sequence [M/I/L/V]-[E/D]-[M/I/L/V]-T, where Thr in position 4 is the target of the SAC kinase Mps1 (London et al., 2012; Shepperd et al., 2012; Yamagishi et al., 2012) (Figure 5 and 6). Such motifs, conserved in all eukaryotes, are now generally referred to as MELT (single letter amino acid code for the sequence Met-Glu-Leu-Thr), even if MELT is only a simplified

consensus for a more complex sequence feature resulting from repeat expansions (Cheeseman et al., 2004; Desai et al., 2003; Schittenhelm et al., 2009). Preventing the phosphorylation of MELT motifs by mutating the crucial Thr at position 4 in most or all MELT repeats resulted in a checkpoint defect both in *S. cerevisiae* and *S. pombe* (London et al., 2012; Shepperd et al., 2012; Yamagishi et al., 2012). The importance of this finding is that it provides an explanation for the mechanism through which Mps1 controls recruitment of Bub1 and consequently BubR1. However, the universality of this model is unclear as there are conflicting reports regarding whether Mps1 is required for Bub1 recruitment in human cells (Hewitt et al., 2010; Maciejowski et al., 2010; Santaguida et al., 2010; Sliedrecht et al., 2010; Tighe et al., 2008).

Collectively, we set out to clarify the mechanism of Bub1 and BubR1 recruitment by dissecting the contributions of the TPR and the Bub3-binding domains. In the light of the new model based on MELT repeats, I started to investigate the relationships of the TPR domain and of the Bub3-binding domain and the KI- and MELT- mediated pathways of recruitment of Bub1, BubR1 and Bub3 (altogether often referred to as Bubs) to Knl1.

Results

1. The kinetochore-binding domain of Bub1and BubR1

1.1 Role of the TPR domain of Bub1 and BubR1 in kinetochore recruitment

We asked which region of Bub1 could be responsible for kinetochore targeting. To address this question, we designed several deletion constructs based on the presence of conserved motifs (Figure 8 A). The kinase domain, the KEN boxes and the conserved domain I (CDI) were progressively removed from the C-terminus up to a minimal construct (Bub1$^{1-284}$) containing the TPR and Bub3-binding domain (Figure 8 A). We then expressed these constructs as GFP-tagged versions in HeLa cells and assessed their ability to target kinetochores in mitotic cells. Immunofluorescence analysis showed that all constructs were able to bind kinetochores efficiently (Figure 8). Importantly, kinetochore localization of the shortest construct (Bub1$^{1-284}$) was indistinguishable from the one of the full-length construct (Figure 8 B), suggesting that residues from 285 to 1085 do not substantially contribute to the

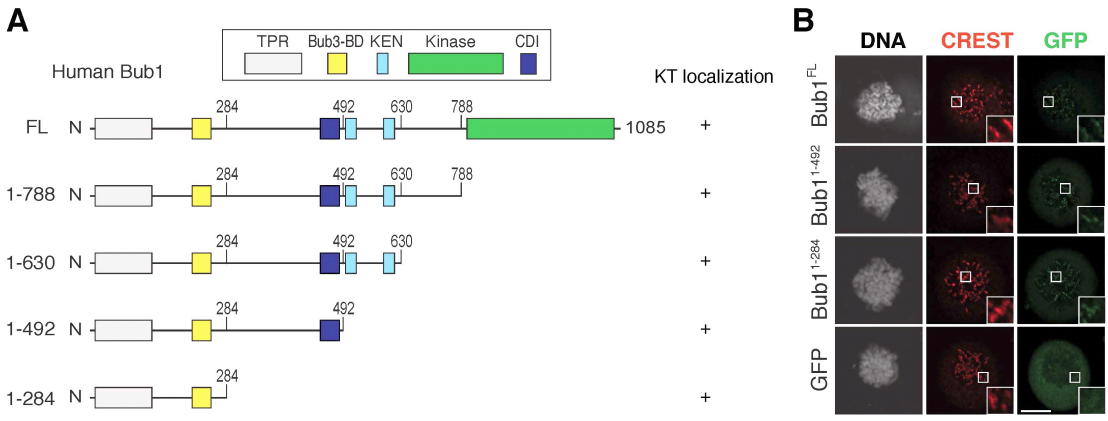

Figure 8 Bub1 fragments capable of targeting kinetochores

A) Domain composition of human Bub1. Relevant domain boundaries are indicated with residue number. Bub3-BD is the Bub3 binding domain, CDI is the conserved domain I. B) Representative images of HeLa cells expressing GFP as control or the N-terminally GFP-tagged Bub1 constructs used in A, after treatment with nocodazole for 6 hours. CREST was used to visualize centromeres. Insets show a higher magnification of kinetochore regions (boxes). KT, kinetochore; FL, full-length. Scale bar, 5 μm.

kinetochore binding affinity of Bub1. These data are consistent with previous observations pointing to a role for both the TPR and Bub3-binding domain in the mechanism of Bub1 recruitment to kinetochores (Kiyomitsu et al., 2007; Klebig et al., 2009; Taylor et al., 1998).

As the TPR domain had been previously proposed to mediate an interaction with Knl1 (Kiyomitsu et al., 2011; Kiyomitsu et al., 2007), we assessed the contributions of the TPR domain to the recruitment of Bub1. We tested if the TPR domain (included in two constructs encompassing residues 1-150 or residues 1-190, see Figure 9 A for domain boundaries) was sufficient for kinetochore binding in HeLa cells. Expression of the GFP fusion of wild type,

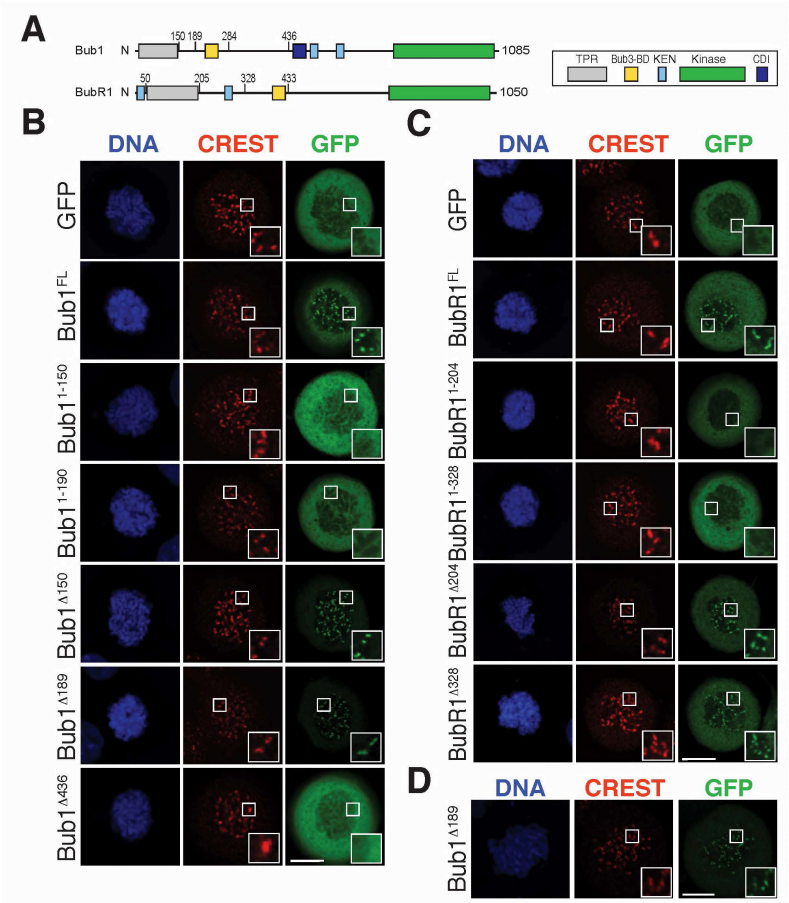

Figure 9 The role of TPR repeats in kinetochore recruitment

A) Domain composition of human Bub1 and BubR1. Relevant domain boundaries are indicated with residue number. Bub3-BD is the Bub3 binding domain, CDI is the conserved domain I. B-C) Representative images of HeLa cells expressing GFP or the N-terminally GFP-tagged Bub1 (B) or BubR1 (C) constructs, after treatment with nocodazole for 6 hours. CREST was used to visualize centromeres. Insets show a higher magnification of kinetochore regions (boxes). D) Immunofluorescence image of HeLa cells expressing C-terminally GFP-fused Bub1 (Bub1$^{\Delta189}$-GFP) treated as in B. The inset shows a higher magnification of kinetochore regions. FL, full-length. Scale bars, 5 μm.

full-length Bub1 ($Bub1^{FL}$) resulted in bright kinetochore staining (Figure 9 B). On the other hand, GFP fusions of $Bub1^{1-150}$ or $Bub1^{1-190}$ failed to localize to kinetochores (Figure 9 B). These results suggest that the TPR region of Bub1 is not sufficient for kinetochore localization. We next tested if this region is necessary for kinetochore binding. Bub1 mutants lacking either 150 or 189 residues from their N-terminus ($Bub1^{\Delta150}$ or $Bub1^{\Delta189}$) localized normally to kinetochores (Figure 9 B). It is unlikely that these results were an artifact from fusing GFP at the N-terminus of the Bub1 deletion constructs, because a C-terminal fusion of $Bub1^{\Delta189}$ also localized normally to kinetochores (Figure 9 D). When we created a longer deletion by removing the first 436 residues of Bub1, the resulting Bub1 construct ($Bub1^{\Delta436}$) failed to localize to kinetochores (Figure 9 B). These results indicate that residues 190-436, from which the TPR repeats of Bub1 are excluded, might be necessary for kinetochore recruitment of Bub1.

Given the similar domain composition of Bub1 and BubR1, we asked if the TPR domain of BubR1 was important for kinetochore recruitment. Two constructs of BubR1 including the TPR region, encompassing residues 1-205 and 1-328 (equivalent to Bub1 1-150 and 1-190), were expressed in HeLa cells and found to be unable to reach kinetochores (Figure 9 C). Analogously to the results obtained with Bub1 deletion mutants, deletion of the TPR domain of BubR1 ($BubR1^{\Delta205}$ or $BubR1^{\Delta328}$) did not evidently affect kinetochore recruitment (Figure 9 C). Overall these results indicate that the TPR region of Bub1 and BubR1 is neither sufficient, nor strictly necessary, for kinetochore recruitment.

1.2 The TPR domains of Bub1 and BubR1 bind Knl1 directly

The TPR regions of Bub1 and BubR1 had been suggested to promote the recruitment of Bub1 and BubR1 to kinetochores via their interaction with the kinetochore protein Knl1 (D'Arcy et al., 2010; Kiyomitsu et al., 2011; Kiyomitsu et al., 2007; Klebig et al., 2009). Our results in Figure 9, however, indicated that the TPR region of Bub1 and BubR1 is neither sufficient nor necessary for kinetochore recruitment. To reconcile these contradictory

observations, we hypothesized a more complex recruitment model. We speculated that an intra-molecular interaction involving the N-terminal TPR motif might be masking a high-affinity, secondary kinetochore-binding domain in Bub1 and BubR1. This secondary site would provide the bulk of the kinetochore-binding affinity but should only become exposed after the initial binding of the TPR motifs to Knl1. In such a model, deletion of the TPR region is predicted not only to remove the Knl1-binding site, but also to relieve an intra-molecular inhibitory function, with the consequent constitutive exposure of the high-affinity binding site even in the absence of Knl1 binding. This would explain why the Bub1 and BubR1 constructs lacking the TPR domain are able to target kinetochores. An implication of the model is that impairment of the interaction of Bub1 with Knl1 (without disrupting the hypothetical intra-molecular switch via deletion of the TPR domain) would prevent kinetochore binding as a consequence of constitutive inhibition of Bub1. Testing this model required the generation of mutants of Bub1 and BubR1 specifically impaired in the TPR:Knl1 interaction. To obtain such separation of function mutants, we resorted to the structural and biochemical characterization of the interaction of the TPRs of Bub1 and BubR1 with Knl1 carried out previously in our laboratory [and currently published in (Krenn et al., 2012)]. *In vitro* work done by Xiaozheng Li and Annemarie Wehenkel formally demonstrated that the interaction of Bub1 and BubR1 with Knl1 is direct and involves a moderately conserved ridge on the convex surface of Bub1 TPR domain and a short Knl1 fragment encompassing the previously identified KI motifs (Figure 7) (Kiyomitsu et al., 2011). Specifically, the TPR motifs of Bub1 and BubR1 bind to the KI1- and KI2-motif, respectively. Moreover, the structure of Bub1 TPR in complex with KI1 motif revealed that several Knl1 residues, including Ile177, Thr179, and Phe182, point towards the Bub1 surface (Figure 10 C) (Krenn et al., 2012). On the other hand, Bub1 contributes the side chains of Phe75, Asn79, Gln84, Phe85 and Phe88, thus participating from the bottom to the creation of the Knl1-binding ridge (Figure 10 C). Importantly, whereas mutation of Gln85 to Ala mutant had mild or no effects on binding, individual mutations of Bub1 residues Phe75, Asn79 and Phe85 to alanine led to complete

disruption of the Bub1:KI1 complex *in vitro*, confirming the role of the convex surface of Bub1 in Knl1 binding *in vitro* (Krenn et al., 2012). The effect of the Phe88 to alanine mutation could not be examined, as the resulting protein was insoluble when expressed in *E. coli*.

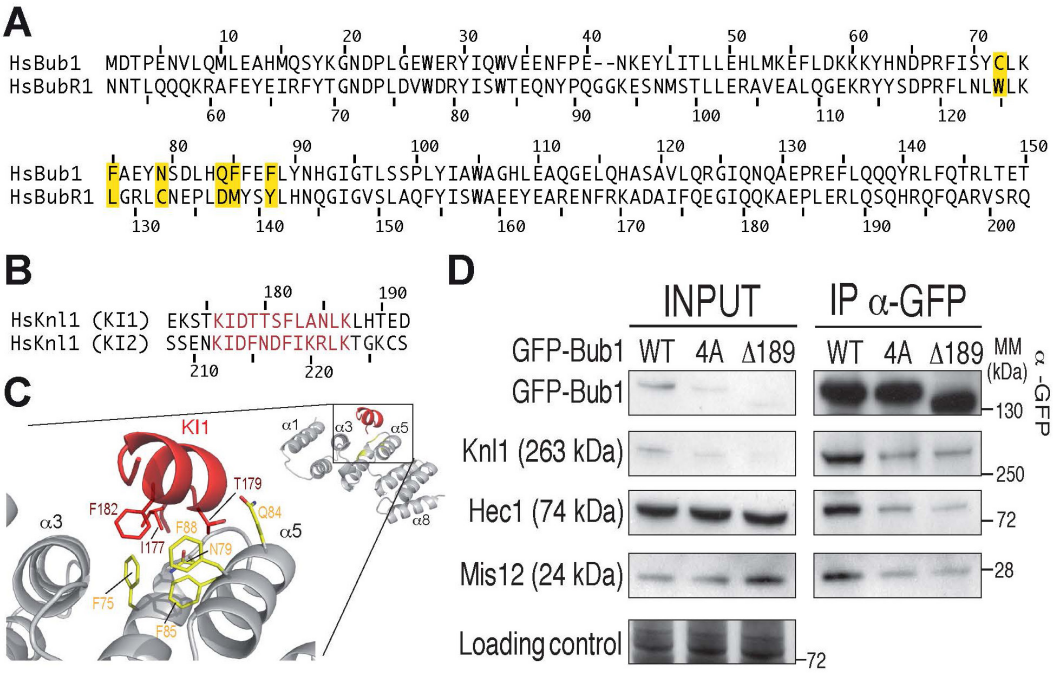

Figure 10 Interaction of the TPR domain of Bub1 with KI1 of Knl1

A) Sequence alignment of the human Bub1 and BubR1 TPR domains. Residues highlighted in yellow occupy similar positions at the Knl1- binding interface and were mutated as discussed in the main text. B) Alignment of the KI motifs of human Knl1. Residues highlighted in red define the conserved binding motifs KI1 and KI2. C) Close-up of the interaction of the Knl1–Bub1 interface (red and gray, respectively). Residues highlighted in yellow define the KI-binding pocket of Bub1 and were mutated as discussed in the main text. D) Immunoprecipitation (IP) from mitotic lysates of inducible cell lines expressing N-terminally GFP-tagged Bub1^{WT}, Bub1^{4A} and Bub1$^{\Delta 189}$. Bub1^{4A} contains the F75A, N79A, Q84A and F85A mutations. Co-immunoprecipitating proteins were analyzed by SDS-PAGE and subsequent Western blotting. Ponceau staining is used as a loading control. WT, wild type; MM, molecular mass.

In our attempt to generate mutants impaired specifically in Knl1 binding, we tested the effects of Bub1 mutations on its ability to bind to Knl1 *in vivo*. We therefore generated inducible Flp-In T-Rex HeLa stable cell lines (See Material and Methods for details) expressing GFP-tagged versions of Bub1 wild type and a mutant carrying, on its TPR, the four alanine mutations characterized *in vitro* (Bub1^{4A}) (Figure 10 C). We next evaluated the interaction of these

constructs with endogenous Knl1, Hec1, and Mis12 by GFP immunoprecipitation (IP) from mitotic lysates followed by western blotting. The Bub1^{4A} mutant was severely impaired in its ability to interact with Knl1, and only modest residual binding was retained (Figure 10 D). Because Knl1 interacts directly with other components of the KMN network, including subunits of the Mis12 and Ndc80 complexes (Cheeseman et al., 2006; Petrovic et al., 2010), the levels of Mis12 and Ndc80 in the Bub1^{4A} IPs were also reduced. Analogous results were obtained with the Bub1$^{\Delta 189}$ deletion mutant (Figure 10 D). These results strongly support the view, based on the crystal structure, that the convex surface of the Bub1 TPR region contributes to Knl1 binding in cells.

The sequences of the TPR region of Bub1 and BubR1 are closely related (Figure 10 A). Similarly, the sequences of the previously identified KI-motifs of Knl1 are also closely related (Figure 10 B). The recent crystal structure of the complex of human BubR1 TPR region bound to the KI2 motif (Bolanos-Garcia et al., 2011) has revealed extensive structural similarities between the BubR1 TPR: KI2 complex and the Bub1 TPR:KI1 interactions. Residues Trp125, Leu128, Cys132, Asp137 and Met138 of BubR1 occupy positions that are equivalent to those identified at the Bub1-Knl1 interface (Figure 10 A). Consistently, individual mutations of Trp125, Leu128, Cys132 or Asp137 to alanine were sufficient to disrupt the interaction of BubR1 TPR with Knl1 *in vitro*, whereas the effect of mutating Met138 was milder (Krenn et al., 2012). Overall, these results reveal that Bub1 and BubR1 interact with Knl1 using analogous surfaces on the TPR and that Bub1 and BubR1 mutants carrying substitutions in their KI-binding pocket are impaired in Knl1 binding. Such mutants can be therefore used as separation of function mutants to verify our hypothesis of the intra-molecular switch.

1.3 Role of Knl1 binding in the kinetochore recruitment of Bub1 and BubR1

As explained in the previous paragraph, the generation of separation of function mutants of Bub1 and BubR1 defective in Knl1 binding would enable us to probe the role of Knl1 binding

in kinetochore recruitment of these proteins in the context of the full-length protein, i.e. without resorting to deletion mutants that might disrupt hypothetical intra-molecular regulatory steps. We therefore tested the ability of GFP fusions of Bub1 or BubR1 mutants carrying single alanine substitutions on their KI1- or KI2 binding sites to decorate kinetochores in mitotic cells (Figure 11). None of the single alanine mutations in the KI-binding interface of Bub1 and BubR1 affected significantly the localization to kinetochores. However, we considered that a single mutation in the TPR, despite being sufficient to disrupt the binding of TPR with KI *in vitro* (as explained in paragraph 1.2), might not be sufficient to visibly affect the robust kinetochore recruitment of GFP-Bub1 and BubR1 in cells.

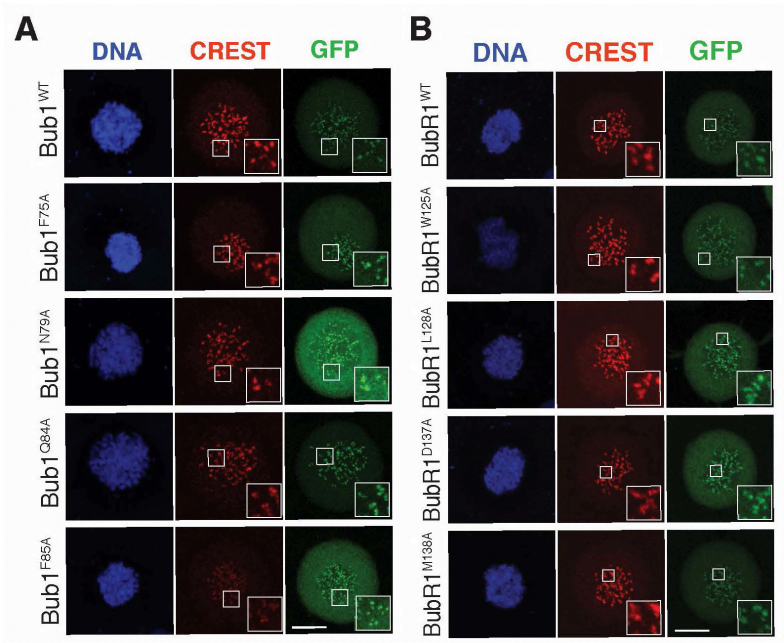

Figure 11 Single mutations at the KI-binding interface of the TPR do not affect recruitment

Representative images of HeLa cells expressing GFP and N-terminally GFP-tagged wild type (WT) Bub1 (A) or BubR1 (B) or their alanine mutants. Cells were treated with nocodazole for 6 hours. CREST was used to visualize centromeres. Insets show a higher magnification of kinetochore regions (boxes). Scale bars, 5 μm.

To overcome this problem and to exclude any possible effect from endogenous Bub1, we expressed a mutant of Bub1 carrying multiple alanine substitutions on its KI1-binding site ($Bub1^{4A}$) in HeLa cells in which we had previously depleted Bub1 by RNA interference. Bub1 depletion was efficient as judged by Western blotting (Figure 12). Multiple mutations in the

KI-binding interface of Bub1 and BubR1 did not affect significantly the recruitment to kinetochores, as GFP-Bub1^{4A} behavior was indistinguishable from GFP-Bub1^{WT} and Bub1$^{\Delta189}$ (Figure 12 C).

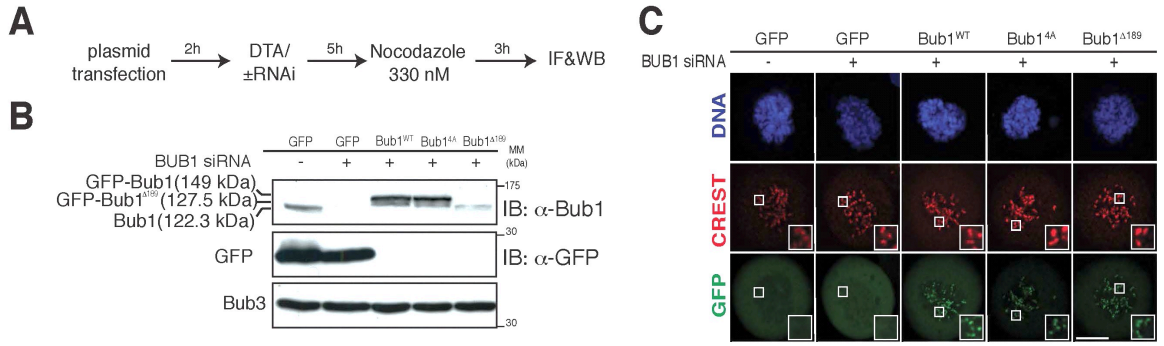

Figure 12 Multiple mutations at the KI-binding interface of the TPR do not affect Bub1 recruitment in the absence of endogenous Bub1

A) Protocol used in B and C. In brief, HeLa cells were transfected with plasmids carrying GFP or GFP-Bub1 constructs. All Bub1 constructs were mutated to be resistant to RNAi-based depletion. Cells were then depleted of endogenous Bub1 by RNAi followed by double thymidine arrest (DTA). 5 h after release from the arrest, cells were treated with nocodazole and then processed for Western blotting (WB) or immunofluorescence (IF). B) Western blot of extracts from cells treated as in A. Bub3 was used as a loading control. Note that anti-Bub1 antibody recognized both endogenous and RNAi-resistant GFP-Bub1 proteins. C) Immunofluorescence images of mitotic HeLa cells treated as described in A. CREST was used to visualize centromeres. Insets show a higher magnification of kinetochore regions (boxes). MM, molecular mass; IB, immunoblot. Scale bar, 5 μm.

These experiments were performed in conditions of high over-expression of GFP-Bub1 constructs. To exclude that differences in the levels of expression might conceal any detectable change in kinetochore recruitment, we resorted to stable inducible cell lines where ectopic expression of GFP-Bub1 and BubR1 constructs, induced by the presence of doxycycline, could reach levels that are close to the endogenous levels of Bub1 and BubR1. We therefore generated stable cell lines expressing GFP fusions of Bub1 or BubR1 mutants carrying multiple alanine substitutions on their KI1- or KI2 binding sites, respectively (described in the legend of Figure 13 and abbreviated as Bub1^{3A}, Bub1^{4A}, BubR1^{4A} and BubR1^{4A*}) and evaluated their ability to localize to kinetochores. Addition of doxycycline for 24 hours led to the expression of all proteins, at comparable levels that equaled or slightly exceeded the levels of endogenous Bub1 or BubR1 (Figure 13 A and B). Under these conditions, as for the case of the N-terminal deletion mutants, kinetochore recruitment of

Bub1^{3A} or Bub1^{4A} was not affected; recruitment of the two variants of BubR1^{4A} was increased relative to the wild-type control (Figure 7 B-D).

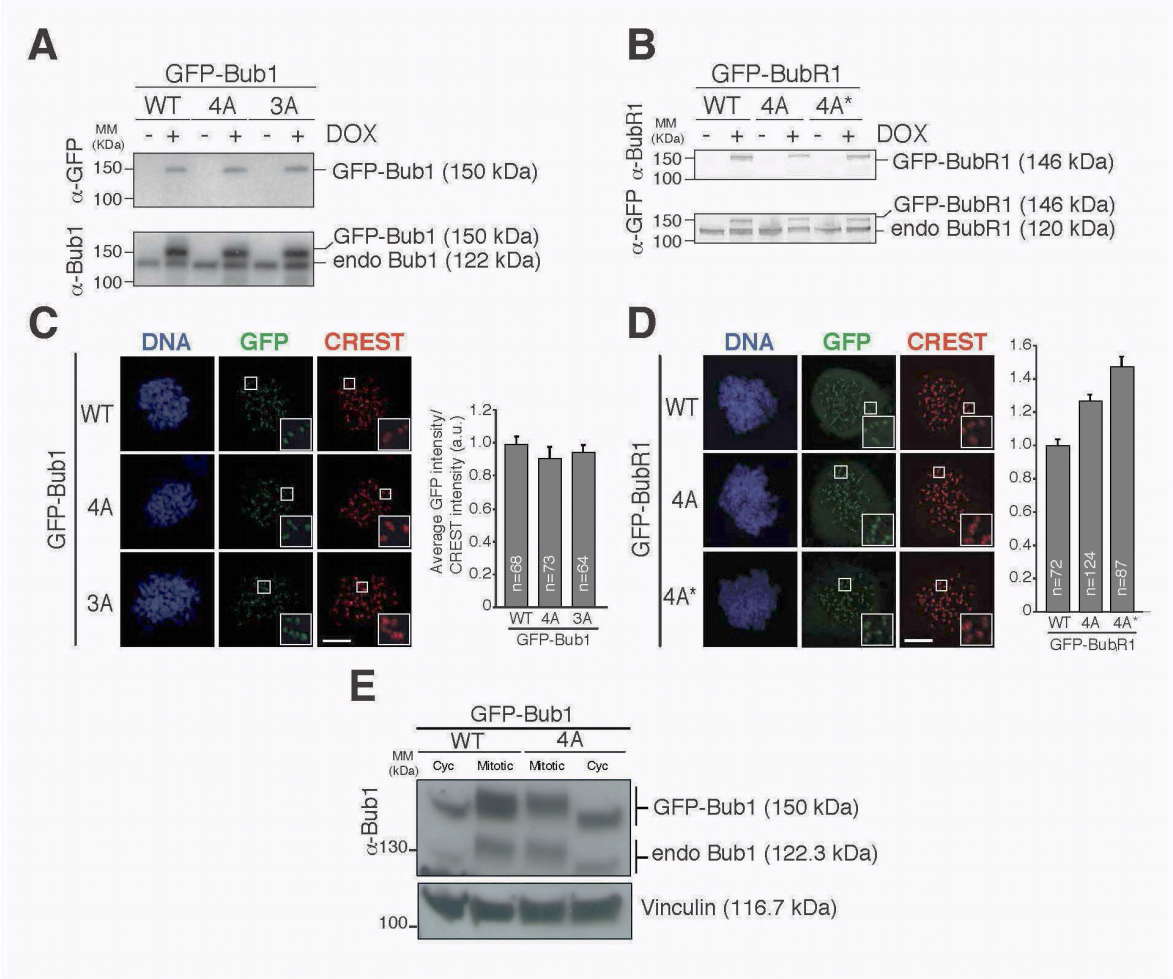

Figure 13 Multiple mutations at the KI-binding interface of the TPR do not affect recruitment

A-B) Western blots of extracts from Flp-In T-REx cell lines expressing GFP-tagged Bub1 (A) and BubR1 (B) wild type (WT) or their mutants, in the absence (-) or presence (+) of doxycycline (DOX). Bub1(4A) and Bub1(3A) contain the F75A, N79A, Q84A and F85A mutations, and N79A, F85A and F88A, respectively. BubR1(4A) and BubR1(4A*) contain the W125A, L128A, C132A, and D137A and W125A, L128A, C132A, and M138A mutations, respectively. C-D) Immunofluorescence of Flp-In T-REx cell lines expressing Bub1 (C) and BubR1 (D) constructs, after treatment with nocodazole for 6 hours. CREST was used to visualize centromeres. Insets show a higher magnification of kinetochore regions (boxes). On the right, graphs showing the mean GFP intensity of kinetochores. The values for the wild-type constructs are set to 1. n indicates the numbers of measured kinetochores. Error bars indicate SEM. E) Western blot of extracts from cycling (cyc) or nocodazole-treated (mitotic) Flp-In T-REx cell lines expressing GFP-tagged Bub1 wild type (WT) or 4A mutant. Vinculin is used as a loading control. MM, molecular mass; endo, endogenous; a.u. arbitrary unit. Scale bars, 5 μm.

With the goal of identifying subtle differences in the dynamics of kinetochore residence of Bub1 or its mutants, we also performed Fluorescence Recovery After Photobleaching (FRAP)

experiments on kinetochore structures. These experiments, however, failed to reveal significant differences in recovery rates between Bub1^{WT} and the Bub1^{4A} mutant (data not shown). We also used an indirect assay to assess efficient recruitment to kinetochores. It has been proposed that Bub1 is hyper-phosphorylated in mitosis in a kinetochore-dependent manner (Chen, 2004). Therefore, we considered that the analysis of the mobility shift of phosphorylated Bub1 in SDS-PAGE could be used as a read out for kinetochore recruitment. We therefore assessed the mobility shifts of the GFP-tagged versions of Bub1 wild type or 4A mutant in mitotic cells compared to a cycling population. As expected, GFP-Bub1 wild type is hyper-phosphorylated in mitotic cells compared to cycling cells (Figure 13 E). GFP-Bub1^{4A} seemed to be phosphorylated in mitosis as efficiently as the wild type counterpart (Figure 13 E). Overall, these results converge to the idea that Bub1 mutants in the KI-binding interface do not display significant difference in their recruitment to kinetochores compared to the wild type protein. In conclusion, these observations confute the hypothesis that the interaction of the TPR regions of Bub1 and BubR1 with the KI motifs of Knl1 regulates intra- or inter-molecularly the degree of exposure of a kinetochore-binding region located elsewhere in the sequence of Bub1 or BubR1. On the contrary, these data solidly suggest that the TPR regions of Bub1 and BubR1 play a marginal role in kinetochore recruitment of Bub1 and BubR1.

1.4 Identification of the minimal kinetochore-binding domain of Bub1

Having excluded any contribution from the TPR domain in the recruitment mechanism, we next tried to identify the minimal kinetochore-binding domain of Bub1. Our results in Figure 8 and Figure 9A indicate that residues 190-436, from which the TPR of Bub1 is excluded, might be necessary for kinetochore recruitment of Bub1. To test if this region is sufficient for kinetochore recruitment, we generated a construct encompassing Bub1 residues 190-447. In agreement with this region of Bub1 being sufficient for kinetochore localization, GFP-Bub1$^{190-447}$ localized at the kinetochore (Figure 14 B). As shown before (Figure 8 and Figure 9), while Bub1$^{1-150}$ failed to localize at kinetochores, inclusion of a C-terminal segment that

contained the Bub3-binding domain of Bub1 (Bub1$^{1-284}$) led to robust kinetochore recruitment (Figure 14 A). These results indicate that, in agreement with a previous report (Taylor et al., 1998), a segment comprised between residues 190 and 284 of human Bub1, which includes the Bub3-binding domain (Figure 6), is sufficient for kinetochore recruitment.

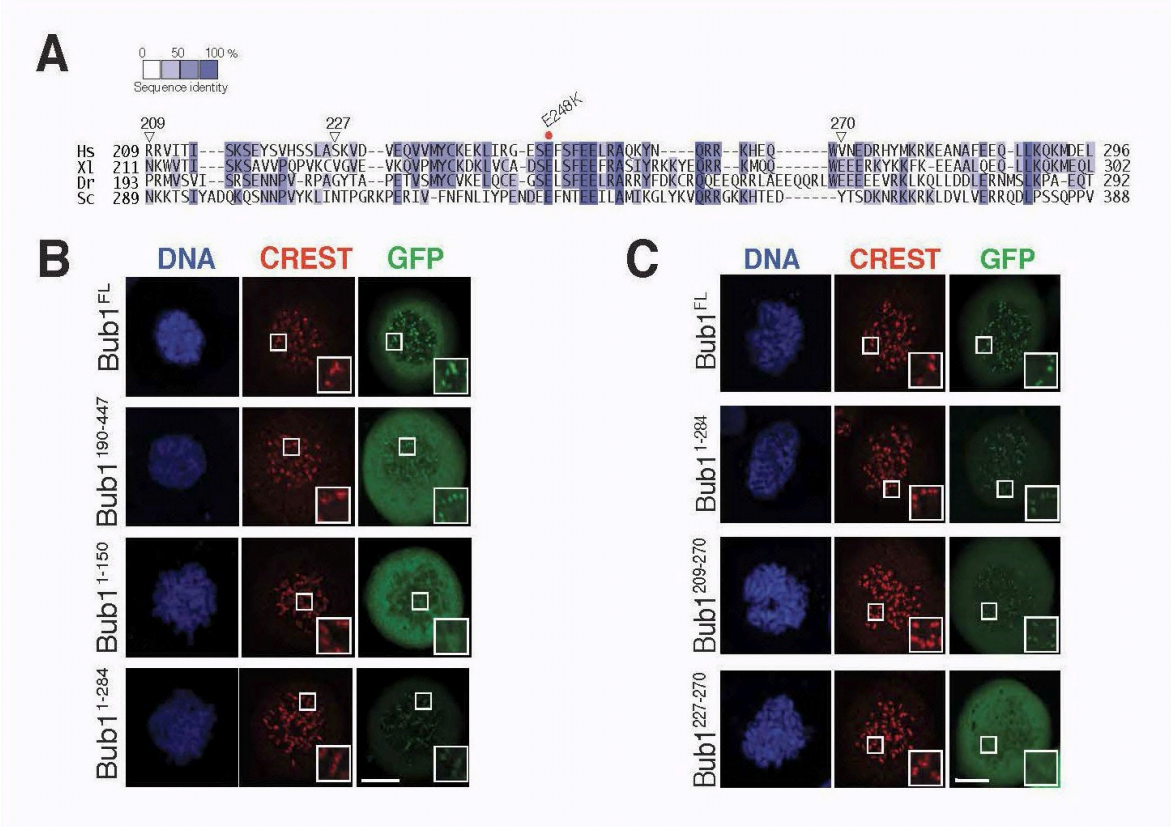

Figure 14 Residues 209-270 of Bub1 are sufficient for kinetochore recruitment

A) Sequence alignment of the Bub3-binding domain of Bub1 from different species (Hs, Homo sapiens; Xl, Xenopus laevis; Dr, Danio rerio; Sc, S. cerevisiae). B-C) Representative images of mitotic HeLa cells expressing the indicated GFP-Bub1 constructs, treated with nocodazole. CREST was used to visualize centromeres. Insets show a higher magnification of kinetochore regions (boxes). FL, full-length. Scale bars, 5 μm.

Next, we refined our analysis by expressing additional constructs. The boundaries of the Bub3-binding domain have been so far defined by the residues of the Bub3-binding domain of *S.cerevisiae* Bub1 (scBub1$^{315-356}$) previously co-crystallized with Bub3 (Larsen et al., 2007). According to the alignment of the Bub3-binding sequences from different species (Figure 14 A), scBub1$^{315-356}$ corresponds to the sequence 227-270 of human Bub1. Interestingly, we observed that this region is surrounded by moderately conserved residues both at the N- and C-terminal boundaries (Figure 14 A). We therefore tested the localization of Bub1$^{227-270}$

segment and longer constructs such as Bub1$^{209-270}$, which includes the N-terminal extension, and Bub1$^{209-314}$, which encompasses both N- and C-terminal extensions (Figure 15 A and C). Surprisingly, Bub1$^{227-270}$ was unable to reach kinetochores. On the other hand, Bub1$^{209-270}$ and Bub1$^{209-314}$ localized robustly to kinetochores (Figure 15 C and data not shown). These results suggest that efficient kinetochore recruitment requires the Bub3-binding domain and, at least, a short N-terminal extension.

As the localization of Bub1 is dependent on Bub3 (Logarinho et al., 2008; Meraldi et al., 2004; Sharp-Baker and Chen, 2001; Taylor et al., 1998; Vigneron et al., 2004) and the only known function of the Bub3-binding domain is to interact with Bub3, we surmised that the identified minimal kinetochore-binding domain of Bub1 may localize to kinetochores via its robust interaction with Bub3. To formally test this concept, we mutated Glu248 of Bub1, a residue previously shown to be essential for the interaction of Bub1 with Bub3 (Larsen et al., 2007), into lysine (E248K, also referred to as EK) in all three Bub1 constructs and expressed them in HeLa cells. As expected, the E248K mutation abolished kinetochore recruitment of Bub1$^{209-270}$ and Bub1$^{209-314}$ (Figure 15 A and not shown), demonstrating that binding to Bub3 is essential for the kinetochore localization of these segments. Moreover, E248K mutation did not have additional effects on kinetochore localization in the context of Bub1$^{227-270}$ (Figure 15 A).

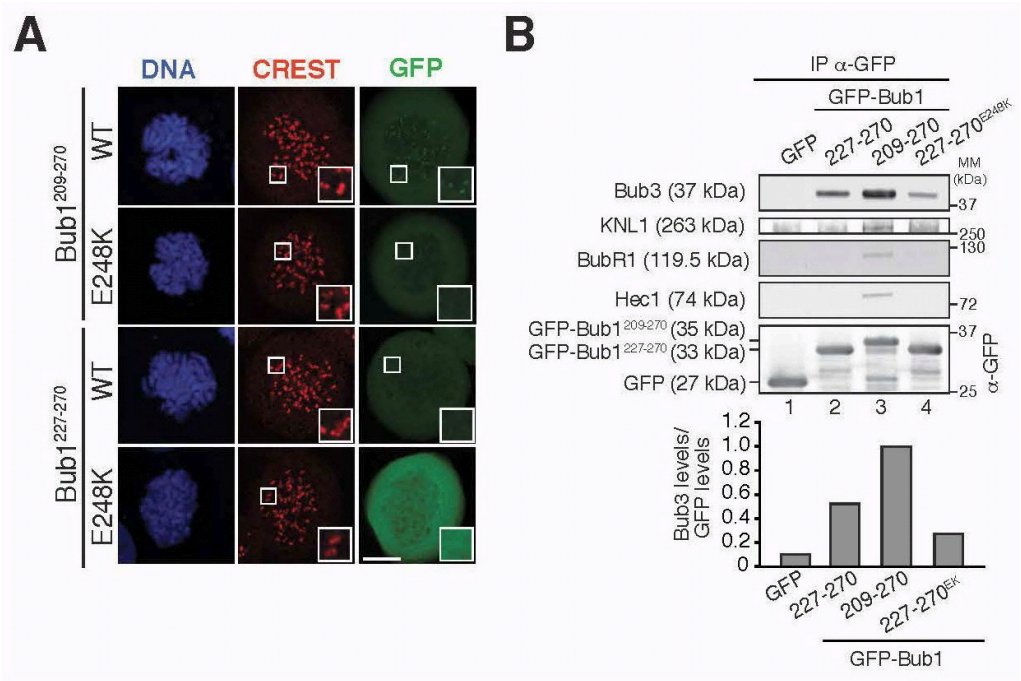

Figure 15 Kinetochore recruitment of the Bub3-binding domain requires the interaction with Bub3
A) Images of mitotic HeLa cells expressing the indicated GFP-Bub1 constructs, after treatment with nocodazole. CREST was used to visualize centromeres. Insets show a higher magnification of kinetochore regions (boxes). B) Immunoprecipitation (IP) of GFP-tagged Bub1 proteins. HeLa cells were transfected with the corresponding plasmids and treated with 330 nM nocodazole for 16 h. On the top, co-precipitating proteins were analyzed by SDS-PAGE and Western blotting. On the bottom, a graph showing the quantification of Bub3 levels from the top panel, normalized to the corresponding GFP levels. The value of $Bub1^{209–270}$ is set to 1. The quantification data shown are from a single representative experiment out of two repeats. WT, wild type; MM, molecular mass. Scale bar, 5 μm.

To assess if the N-terminal extension of the $Bub1^{209-270}$ construct is important for the interaction with Bub3, we expressed GFP fusions of $Bub1^{209-270}$, $Bub1^{227-270}$ and $Bub1^{227-270-EK}$ in HeLa cells and quantified the abundance of Bub3 in the resulting anti-GFP immunoprecipitates (Figure 15 B). In agreement with the idea that the binding to Bub3 is essential for the interaction of Bub1 with kinetochores, we observed an excellent correlation between the ability of the different constructs to bind to Bub3 and their interaction with kinetochores (Figure 15). This result supports the idea that binding to Bub3 is essential for the interaction of Bub1 with kinetochores. This idea was further emphasized by robust co-precipitation of at least two kinetochore subunits, Knl1 and Hec1, with $Bub1^{209-270}$, a construct that binds Bub3 with high affinity (Figure 15 B). Similarly, the interaction of Bub1 with BubR1 appeared to correlate with the ability of Bub1 to bind to Bub3. Conversely, $Bub1^{227-270}$ and $Bub1^{227-270\ EK}$, which bind poorly to Bub3, did not interact robustly with kinetochores or BubR1 (Figure 15 B). Overall, these results indicate that the Bub3-binding domain together with a short N-terminal extension is sufficient for kinetochore recruitment of Bub1. Moreover, the regions surrounding the Bub3-binding domain of Bub1 may promote efficient recruitment to kinetochores by strengthening the interaction of Bub1 with Bub3.

In conclusion, our data strongly suggest that Bub1 and BubR1 recruitment is not based on interactions mediated by the TPR but, on the contrary, at least in the case of Bub1, it relies on the ability of its Bub3-binding domain and surrounding regions to bind kinetochores.

2. Alternative roles of TPR region of Bub1

2.1 Role of the TPR domain of Bub1 in the kinetochore recruitment of BubR1

Consistent with the idea that Bub1 is a scaffold at the kinetochore, it has been proposed that Bub1 may interact directly with BubR1 to recruit BubR1/Bub3 complexes to kinetochores (Brady and Hardwick, 2000; D'Arcy et al., 2010; Kiyomitsu et al., 2007; Rischitor et al., 2007). As TPR repeats are protein-protein interaction modules (D'Andrea and Regan, 2003; Zeytuni and Zarivach, 2012), the TPR domain of Bub1 is likely to mediate the interaction with BubR1, as suggested previously (Kiyomitsu et al., 2007). To investigate the role of the TPR domain of Bub1 in the interaction with BubR1, we used GFP-tagged Bub1 constructs carrying deletion of the TPR domain or mutations at the KI-binding interface, already described in the previous section. First, we evaluated the role of the KI1-binding pocket of Bub1 on the interaction with BubR1 in immunoprecipitation experiments. As expected, BubR1 and Bub3 co-precipitated with GFP-Bub1 from mitotic lysates (Figure 16 A), while neither of them was detected in GFP IP used as negative control. The amounts of BubR1 and Bub3 co-immunoprecipitating with $Bub1^{4A}$ (mutated in the KI-binding pocket of the TPR) were indistinguishable from those of the wild type protein (Figure 16 A), indicating that the KI-binding surface of Bub1 is not required for the interaction of Bub1 with BubR1. However, the results from such an experiment may reflect interactions that can occur away from kinetochores. Therefore, we analyzed the kinetochore localization of BubR1 as a read out of its interaction with Bub1 occurring specifically at kinetochore sites. To avoid any interference from the endogenous Bub1, we carried out the analysis in cells in which Bub1 had been depleted by RNAi. In agreement with previous work (Boyarchuk et al., 2007; Johnson et al., 2004; Klebig et al., 2009; Meraldi and Sorger, 2005; Rischitor et al., 2007; Sharp-Baker and Chen, 2001; Vigneron et al., 2004), BubR1 localization was greatly reduced in Bub1-depleted HeLa cells (Figure 16 B and C). Expression of full-length and wild type GFP-Bub1 ($Bub1^{WT}$)

restored BubR1 staining to levels similar to non-depleted cells. We next asked whether the TPR domain was required for the rescue of BubR1 kinetochore levels.

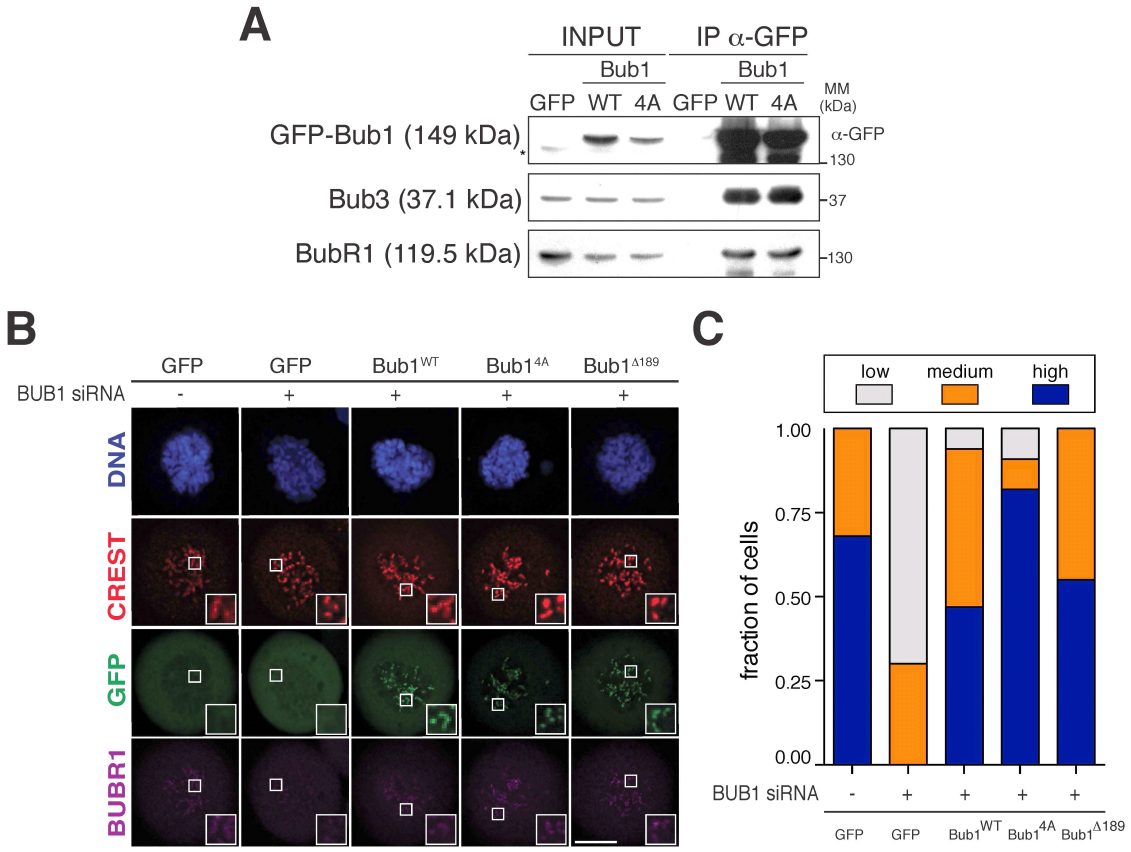

Figure 16 TPR is not required for BubR1 localization and interaction at the kinetochore

A) Immunoprecipitation (IP) from mitotic lysates from stable inducible cell lines expressing GFP or GFP-tagged wild type Bub1 (Bub1^{WT}) or the 4A mutant (Bub1^{4A}). Co-immunoprecipitating proteins were analyzed by SDS-PAGE and Western blotting. The asterisk indicates an unspecific band. B) Immunofluorescence images of mitotic HeLa cells depleted of Bub1 as described in Figure 12. CREST was used to visualize centromeres. Insets show a higher magnification of kinetochore regions (boxes). C) Graph showing the fraction of cells in which the intensity of BubR1 kinetochore signals was low, medium or high in HeLa cells from the experiment shown in B. MM, molecular mass. Scale bar, 5 µm.

Expression of GFP-Bub1$^{\Delta189}$ and Bub1^{4A} rescued BubR1 kinetochore localization to levels that equaled or even exceeded those of the full-length construct, respectively (Figure 16 A and B). The reason of the different degree of the rescue by Bub1$^{\Delta189}$ and Bub1^{4A} is unclear. For unknown reasons, most of cells transfected with Bub1^{4A} construct displayed moderate levels of Bub1 compared to the wild type ones and Bub1$^{\Delta189}$. Previously, we observed that high overexpression of Bub1 slightly reduced BubR1 localization to kinetochores, possibly by

limiting the amount of Bub3 available for BubR1 binding. We therefore suspect that low levels of expression may account for the better rescue of the Bub1^{4A} over the wild type counterpart.

Overall, these results clearly prove that the TPR domain of Bub1 is not involved in the recruitment of BubR1 to kinetochores.

2.2 Role of TPR domain of Bub1 in the regulation of the kinase activity

We demonstrated in sections 1 and 2.1 that the TPR domain of Bub1 is not involved in kinetochore recruitment of Bub1 and BubR1. To investigate alternative functions of the TPR region, we asked if it influenced the catalytic activity of Bub1. For this aim, we set up a kinase assay to measure the activity of different forms of Bub1 kinase against the recombinant histone 2A (H2A), a known Bub1 substrate (Kawashima et al., 2010) already available in the

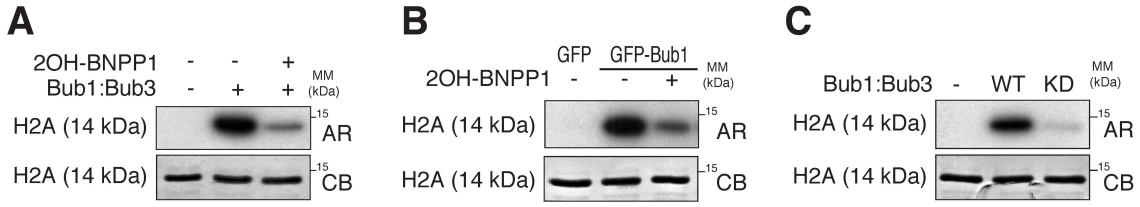

Figure 17 Establishment of an in vitro kinase assay for Bub1

A) In vitro kinase activity toward histone 2A (H2A) of recombinant Bub1:Bub3 in the absence (-) or presence (+) of 2OH-BNPP1 inhibitor. B) In vitro kinase activity toward histone 2A (H2A) of GFP and GFP-fused Bub1 immunopurified from cycling Flp-In T-REx cells, in the absence (-) or presence (+) of 2OH-BNPP1 inhibitor. C) In vitro kinase activity toward H2A of recombinant wild type (WT) and kinase-dead (KD) Bub1:Bub3 kinases. The KD mutant carries the K821R mutation. MM, molecular mass; AR, autoradiography; CB, Coomassie brilliant blue.

laboratory. For this purpose, recombinant full-length human Bub1 kinase, in complex with full-length Bub3, was expressed and purified from insect cells (see Material and Methods for details) and used as kinase in *in vitro* kinase reactions. As already shown before (Santaguida et al., 2010), the purified Bub1:Bub3 complex was active, as it phosphorylated H2A in our assay (Figure 17 A). Moreover, its activity was inhibited by the presence of 5 μM 2OH-BNPP1, a

small-molecule inhibitor of Bub1 (Kang et al., 2008) (Figure 17 A). As additional control for the specificity of the kinase reactions, we tested the effects of mutations in the active site of the recombinant Bub1:Bub3 kinase (Figure 17 C). Mutation of Lys821, which is involved in the stabilization of the ATP molecule (Kang et al., 2008; Tang et al., 2004), into arginine (K821R) strongly reduced Bub1 activity (Figure 17 C). We will therefore refer to this mutant as kinase-dead (KD) Bub1. Altogether, these results attest the specificity of the kinase assay.

Testing the influence of the TPR on the catalytic activity of Bub1 required the expression and purification of Bub1 TPR mutants. Previous work illustrated that a tagged version of Bub1 can be efficiently isolated via immunoprecipitation from human cell lysates in an active form to be used in *in vitro* reactions (Kang et al., 2008). We therefore resorted to the stable doxycycline-inducible cell lines we already generated as a source for several mutants of Bub1 kinase. We partially purified wild type GFP-Bub1 from cycling stable doxycycline-inducible HeLa cells via GFP immunoprecipitation and tested it in kinase assays with histone 2A (H2A)

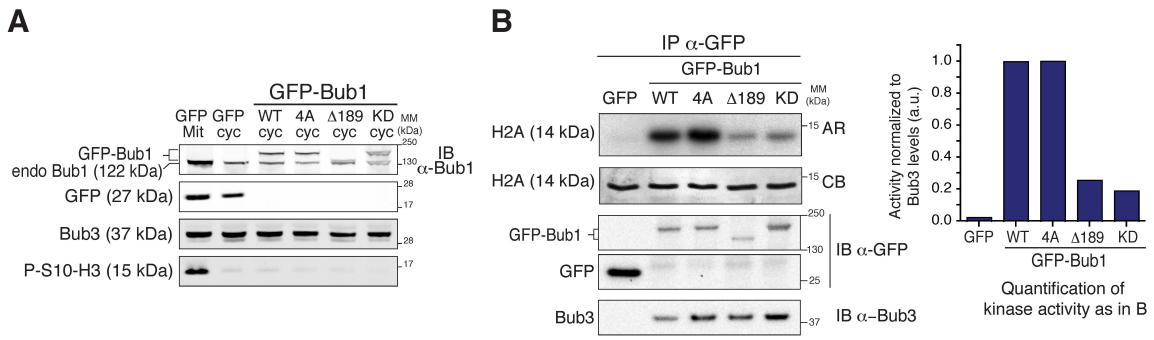

Figure 18 TPR is required for regulation of Bub1 kinase activity

A) Western blot showing the levels of the mitotic marker phosphorylated Ser10 of H3 (P-S10-H3) in extracts from Flp-In T-REx cells expressing GFP-tagged versions of Bub1 used for the assay in B. In the first lane from the left, extracts from cells expressing GFP and treated with 330 nM nocodazole for 16 h were used as a positive control for the phosphorylation of Ser10 of H3. Bub3 was used as a loading control. Note that Bub1 antibody recognizes all Bub1 versions. B) In vitro kinase activity of anti-GFP immunoprecipitates of GFP and the indicated GFP-fused Bub1 proteins from cycling Flp-In T-REx cells. Kinase activity was tested on histone 2A (H2A) as a substrate. The quantification data shown are from a single representative experiment out of two repeats. endo, endogenous; cyc, cycling; Mit, nocodazole-treated cells; IB, immunoblot; WT, wild type; KD, kinase dead; MM, molecular mass; AR, autoradiography; CB, Coomassie brilliant blue; IP, immunoprecipitation; a.u., arbitrary unit.

as a substrate. H2A was efficiently phosphorylated in GFP-Bub1 reactions whereas no phosphorylation could be detected when similar amounts of GFP, instead of GFP-Bub1, were incorporated in the reactions (Figure 18 B). To assess the specificity of Bub1 activity in our immunoprecipitates, we then added 5 μM 2OH-BNPP1 inhibitor to the kinase assay reaction with immunoprecipitated wild type GFP-Bub1, and found levels of inhibition comparable to those observed with the recombinant kinase (Figure 18 B). Next, we tested the effect of TPR mutations on Bub1 kinase activity. Equivalent amounts of GFP-Bub1 or its variants, including Bub1^{4A}, Bub1$^{\Delta 189}$ and the kinase dead mutant (Bub1^{KD}) expressed from the corresponding cycling stable cell lines (Figure 18 A), were immunoprecipitated via GFP and tested against H2A kinase activity. Deletion of the TPR region decreased the kinase activity of Bub1 to levels comparable to those of the kinase-dead mutant (Figure 18 B), indicating that the TPR domain may be required for full kinase activity. On the other hand, the catalytic activity of Bub1^{4A} was unaffected in this assay, suggesting that the ability of the TPR domain to bind Knl1 might not be essential for Bub1 kinase activity, and that the determinants required for activity map elsewhere in the TPR region. Similar results were obtained when using Histone 3 (H3) as a substrate (not shown).

Moreover, we tested the activity of recombinant Bub1:Bub3 in the presence of Knl1$^{150\text{-}200}$, a fragment that includes the KI1 and is expected to bind to the TPR of recombinant Bub1:Bub3. In agreement with the idea that the interaction with Knl1 does not modulate the catalytic activity of the Bub1:Bub3 complex, the H3 kinase activity of recombinant Bub1:Bub3 was unaffected by the addition of Knl1$^{150\text{-}200}$ segment (Figure 19 A).

In our attempt to understand how the kinase activity of Bub1 is regulated, we also tested whether other regions of Knl1 may influence the kinase activity of Bub1. It has been recently shown that the Bub3-binding domain of Bub1 in complex with Bub3 interacts with phosphorylated MELT repeats of Knl1 (Primorac et al., 2013). The kinase responsible for such phosphorylation is Mps1 kinase (London et al., 2012; Shepperd et al., 2012; Yamagishi et al., 2012). We therefore wanted to test whether the interaction of Bub1:Bub3 with a

phosphorylated MELT repeat may influence Bub1 activity. For this purpose, we tested the activity of the recombinant Bub1:Bub3 complex in the presence of unphosphorylated or phosphorylated Knl1$^{138-225}$, a recombinant fragment containing a MELT repeat and KI motifs (Figure 19 B). The activity of Bub1 on H2A was not affected by the presence of Knl1$^{138-225}$, nor even when this was phosphorylated by Mps1. Consistent with Bub1 activity being unaffected, the same level of Bub1 auto-phosphorylation could be detected in all conditions (Figure 19 B). Overall, these results unveil that the TPR of Bub1 might regulate the kinase activity in a way that does not involve the KI-binding pocket. Moreover, these results argue against the idea that Knl1 binding regulates the activity of Bub1.

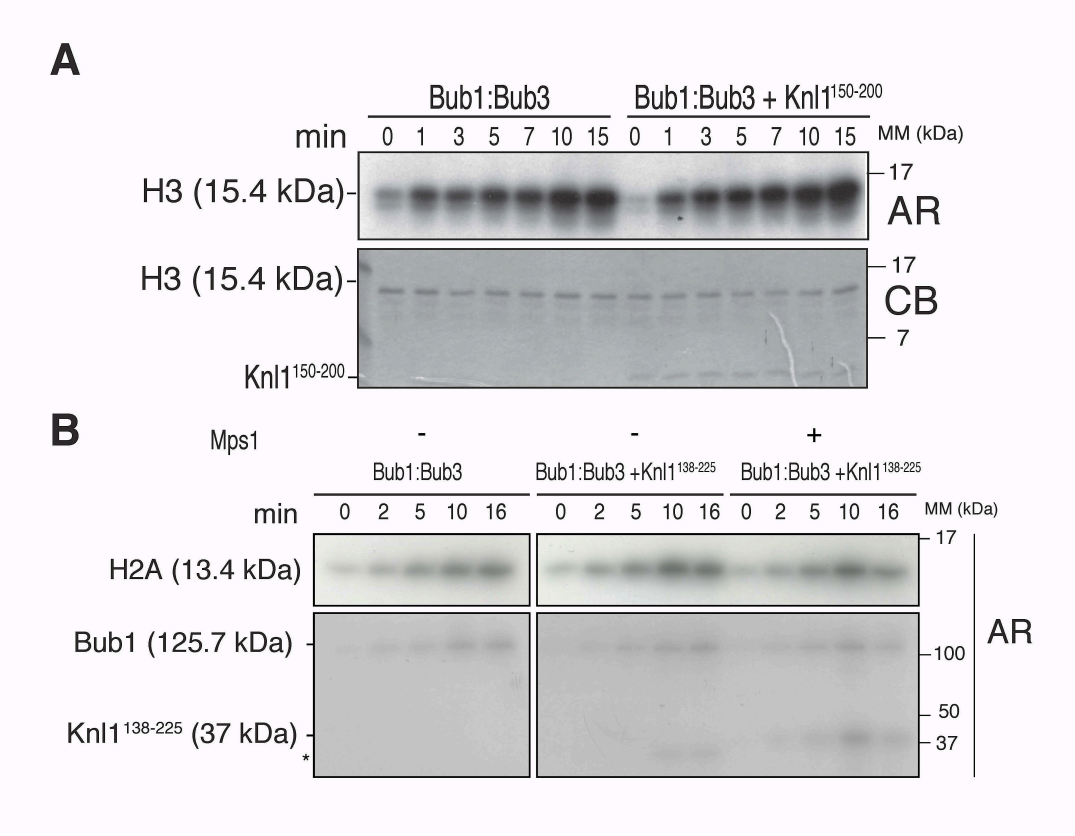

Figure 19 Knl1 binding does not regulate Bub1 kinase activity

A) Time course of H3 phosphorylation in the presence of the recombinant Bub1:Bub3 complex, in the absence (left) or in the presence (right) of Knl1$^{150–200}$. B) Time course of H2A phosphorylation in the presence of the recombinant Bub1:Bub3 complex, in the absence (left) or in the presence (right) of Knl1$^{138–225}$. Before being added to the reactions, Knl1$^{138–225}$ was used as a substrate in the absence (-) or presence (+) of recombinant Mps1 in a cold kinase reaction. Bub1 is auto-phosphorylated in all reactions. Note that Knl1$^{138-225}$ is also phosphorylated in the presence of Mps1. Asterisk indicates phosphorylation of a contaminant protein. MM, molecular mass; AR, autoradiography; CB, Coomassie brilliant blue; min, minutes.

3. Determinants of Knl1 for Bub1 recruitment

3.1 Knl1 is the kinetochore receptor of Bub1 and BubR1

Our results in Section 1 clearly indicated that the interaction of Bub1 with KI motifs is not crucial for the recruitment process. On the other hand, Knl1 has been proposed to be the kinetochore receptor for Bub1 (Kiyomitsu et al., 2007; Pagliuca et al., 2009).

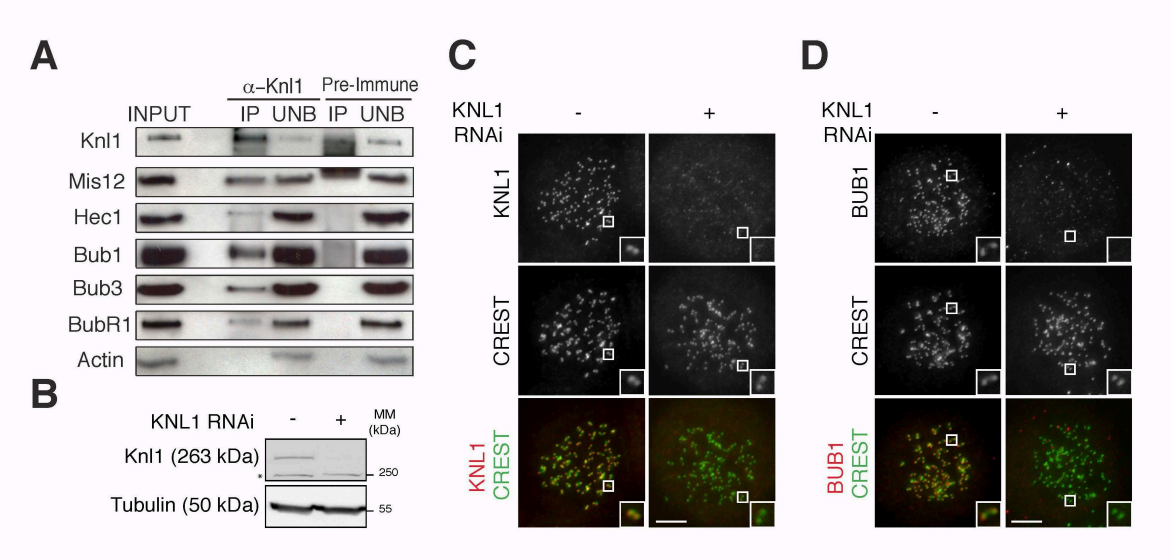

Figure 20 Bub1 recruitment is dependent on Knl1

A) Immunoprecipitation of Knl1. Extracts from nocodazole-treated HeLa cells were incubated with the (in house generated) affinity purified rabbit polyclonal anti-Knl1 antibody or pre immune serum from the same animal as a control. Co-precipitating proteins were analyzed by SDS-PAGE and subsequent Western blotting. Actin is used as a loading control. Hec1 and Mis12, two known Knl1 interactors, are present in the anti-Knl1 precipitate but not in the pre-immune serum precipitate. B) Western blotting of Flp-In T-Rex cells after 24 h depletion of Knl1 by RNAi. Tubulin is used as loading control. Asterisk indicates an unspecific band recognized by the Knl1-antibody. C-D) Immunofluorescence images of Flp-In T-REx stable cells treated as in B. CREST was used to visualize centromeres. Insets show a higher magnification of kinetochore regions (boxes). IP, immunoprecipitation; UNB, unbound; MM, molecular mass. Scale bars, 5 μm.

To corroborate this idea, we first confirmed that Knl1 and Bub1 interact. We already showed that endogenous Knl1 co-precipitated with Bub1 (Figure 10 D, see page 43). When we performed the reverse experiment and immunopurified endogenous Knl1 using a home-generated anti-Knl1 antibody from mitotic HeLa lysates, known Knl1 interactors, such as the KMN components Mis12 and Hec1, could be detected in the co-immunoprecipitate, but not

in the control one (Figure 20 A). Bub1, Bub3 and BubR1 were also present in the precipitate, supporting the idea that these proteins form a complex with Knl1. Next, we wanted to prove that Bub1 localization was dependent on Knl1. For this aim, we set up a protocol for Knl1 depletion in HeLa cells by using a combination of three siRNA oligos (see Material and Methods for details) and tested the efficiency of the depletion on the population and single cell level by using Western blotting and immunofluorescence analysis respectively. Both techniques showed that depletion of Knl1 was quite efficient (Figure 20 B and C), although some cells still retained considerable amounts of Knl1 at the kinetochore. Importantly, in Knl1-depleted cells Bub1 intensity at kinetochores dropped dramatically to ~15 % compared to the non-depleted cells (Figure 20 D), as already observed before (Kiyomitsu et al., 2007; Pagliuca et al., 2009). A similar behavior was also observed for BubR1 (data not shown), indicating that Bub1 and BubR1 localization is dependent on the presence of Knl1 at kinetochores. As Knl1 depletion does not affect the kinetochore levels of the other KMN components Mis12 and Hec1 (Kiyomitsu et al., 2007; Pagliuca et al., 2009), our results reinforce the idea that Knl1 is the receptor for Bub1 and BubR1 at the kinetochore.

Our extensive analysis on the TPR and KI interaction in section 1 rules out the possibility that Bub1 and BubR1 recruitment occurs via the interaction with KI motifs of Knl1 and suggests that their recruitment may rely on other regions of Knl1. Interestingly, all members of the Knl1 family share motifs that contain the consensus sequence [M/I/L/V]-[E/D]-[M/I/L/V]-[T/S], where Thr/Ser in position 4 is the target of the SAC kinase Mps1 (London et al., 2012; Shepperd et al., 2012; Yamagishi et al., 2012), and now generally referred to as MELT (Figure 21). Very recently, it was shown that crucial for kinetochore recruitment of Bub1 and Bub3 is their binding to the phosphorylated version of MELTs of Knl1 (London et al., 2012; Primorac et al., 2013; Shepperd et al., 2012; Yamagishi et al., 2012) (Figure 21 B). To fully understand the recruitment mechanism of Bub1 to MELT repeats of Knl1, we analyzed the MELT sequences in human Knl1 more in detail.

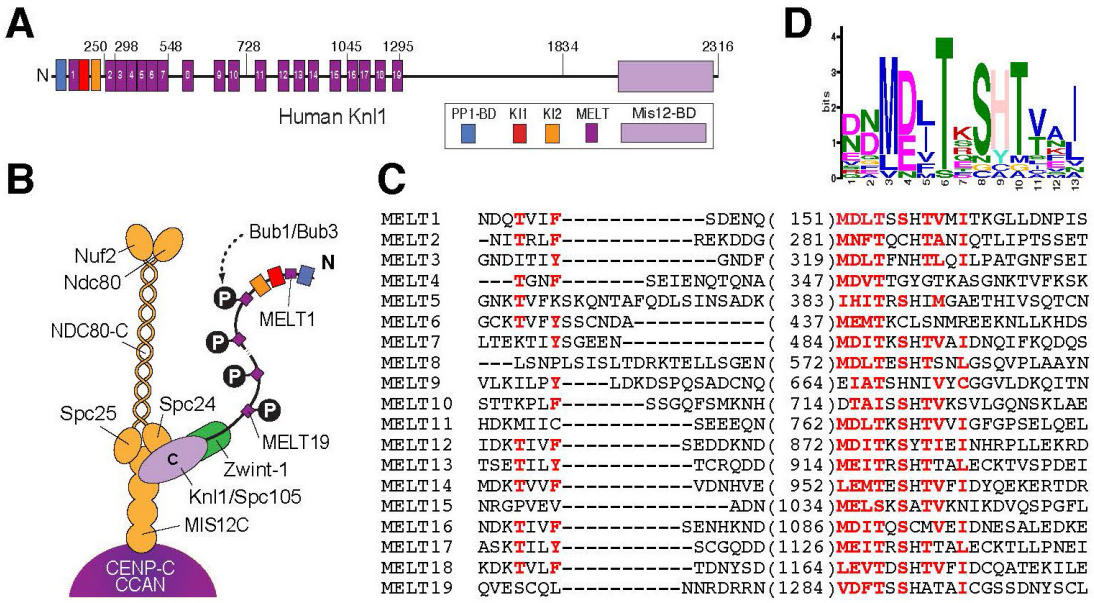

Figure 21 MELT repeats of human Knl1

A) Domain and motif organization of human Knl1. Relevant domain boundaries are indicated with residue numbers. B) Schematic of the KMN network and of the recruitment of Bub1/Bub3 to the phosphorylated (P) MELT repeats of Knl1 at the kinetochore. Mps1 kinase (not shown) is responsible for MELT phosphorylation. C) Alignment of 19 putative MELT repeats of human Knl1 showing conserved amino acids in red and bold. Numbers refer to the position of the methionine (M) in each MELT sequence. Manual scanning of the Knl1 sequence complemented an initial alignment generated with MEME suite (Bailey et al., 2009). D) Sequence logo of the MELT motif generated with MEME suite. The height of the individual letters in a stack is the probability of the letter at that position multiplied by the total information content of the stack. Numbers along the x-axis refer to the amino acid positions within the motif. Colors are based on the biochemical properties of the various amino acids: blue indicates hydrophobic, green polar, magenta acidic, red positively charged, pink histidine, orange glycine, yellow proline, turquoise tyrosine. NDC80-C, Ndc80 complex; MIS12C, Mis12-complex; N, N-terminus; BD, binding-domain.

MELT repeats are present in all organisms in a variable number (although the precise number in each species has been slightly controversial). For instance, budding and fission yeast Knl1 (Spc105 and Spc7) contain 6 and 9 MELT sequences respectively (London et al., 2012; Shepperd et al., 2012; Yamagishi et al., 2012), *C. elegans* KNL-1 8 repeats and *Drosophila melanogaster* Spc105 only two. However, *Drosophila* Spc105 contains another repeated motif whose consensus is different from the MELT (Schittenhelm et al., 2009). By using the MEME suite [Multiple EM (expectation-maximization) for Motif Elicitation] (Bailey et al., 2009) and manual scanning of human Knl1 sequence, we identified 19 MELT sequences, located, with

no obvious distribution pattern, in the first 1300 residues of Knl1 (Figure 21 A and C). Interestingly, one MELT repeat (MELT1) is preceding the KI motifs of Knl1 (Figure 21 A). The alignment of the 19 MELT repeats and the MELT consensus obtained from MEME suite (Figure 21 C and D respectively) uncovered that MELT repeats are sequences of 31-45 residues long and include several conserved residues in addition to the Met-Glu-Leu-Thr core. The functions of these conserved features are unknown. Overall, this analysis reveals that the human MELT motif, which is crucial for Bubs recruitment to Knl1, represents only a simplified consensus for a much longer and complex sequence.

3.2 Ectopic localization of Knl1 segments to centrosomes promotes recruitment of Bub1 and BubR1

Very recent work carried out in our laboratory has provided a rather detailed description of the mechanism through which Bub1/Bub3 bind to phosphorylated MELT motifs (Primorac et al., 2013). However, why there are so many MELT repeats in Knl1, and whether they are redundant or rather have unique properties is an unresolved issue. To start addressing these questions, we compared the ability of different segments of Knl1, each approximately 250 residues in length but containing a variable number of MELT sequences, to recruit Bub1 and BubR1 to an ectopic site in the cell. Previously, centrosomes have been used to target kinetochore proteins ectopically using fusions with the centrosomal kinase Plk4 (Przewloka et al., 2011). We therefore created expression constructs in which Knl1$^{1-250}$, Knl1$^{298-548}$, and Knl1$^{1045-1295}$, containing respectively MELT1 only, MELT3 to MELT7, and MELT16 to MELT19 (Figure 22 A), were fused between GFP and the centrosome-targeting domain of Plk4 (see Material and Methods for details). The GFP-Plk4 fusion was used as a control. We first opted for inducible cell lines that express the exogenous constructs at low levels, upon addition of doxycycline. However, even in the absence of doxycycline (therefore in condition of no expression), cells expressing GFP-Knl1-Plk4 constructs were very sick, whereas cells expressing the GFP-Plk4 control construct were proliferating without any evident problem.

We suspected that expression of GFP-Knl1-Plk4 constructs was very toxic and that prolonged leakage of the expression system, albeit extremely low, might account for the observed sickness of the cells. To overcome this problem, we resorted to transient expression of all the GFP-Plk4 fusions in HeLa cells. Western blot analysis of extracts of transfected HeLa cells showed that all constructs were recognized by the GFP-antibody but expressed at variable levels (Figure 22 B). Knl1$^{298-548}$ levels equaled those of the control, while Knl1$^{1-250}$ and Knl1$^{1045-1295}$ were expressed at lower levels. The reason for these differences in protein expression is unknown. To well separate centrosomes at opposite ends of the mitotic spindle and distinguish them from the chromatin region, fluorescence images were taken from transfected metaphase cells (Figure 22 C and D). All constructs, including the GFP-Plk4 control, localized efficiently to centrosomes, as shown by co-localization with the Cep135 marker. While the control construct GFP-Plk4 failed to recruit Bub1 or BubR1, all three constructs containing Knl1 segments were able to recruit Bub1 and BubR1 in variable amounts (Figure 22 C-F). Among the three tested constructs, Knl1$^{1045-1295}$ produced the most robust recruitment of Bub1 and BubR1 to centrosomes, followed by Knl1$^{298-548}$ and by Knl1$^{1-250}$ (Figure 22 E and F). At least superficially, there was no precise proportionality between the number of MELT repeats and the robustness of Bub1 and BubR1 recruitment to centrosomes. Interestingly, Knl1$^{1-250}$, with a single MELT sequence, appeared to be almost as potent as Knl1$^{298-548}$, which harbors five MELT sequences. This observation might signify that the occupancy of the single MELT repeat in Knl1$^{1-250}$ may be comparatively high relative to that of MELT motifs in the other constructs, possibly indicative of a higher binding affinity. To test this idea, we resorted to a typical non-equilibrium assay such as immunoprecipitation (IP). For this assay, we expressed GFP-tagged versions of the three Knl1 constructs and pulled down these proteins from lysates of mitotic cells with an anti-GFP antibody and, after extensive washing, probed the precipitates with antibodies against Bub1, Bub3, BubR1 and PP1γ (Figure 22 G). Indeed, GFP-Knl1$^{1-250}$ pulled down considerably larger amounts of Bub1, Bub3, BubR1 and PP1γ than

GFP-Knl1$^{298\text{-}548}$ and $^{1045\text{-}1295}$ (note that PP1γ was expected to interact exclusively with GFP-Knl1$^{1\text{-}250}$, the segment of Knl1 that contains the phosphatase binding site).

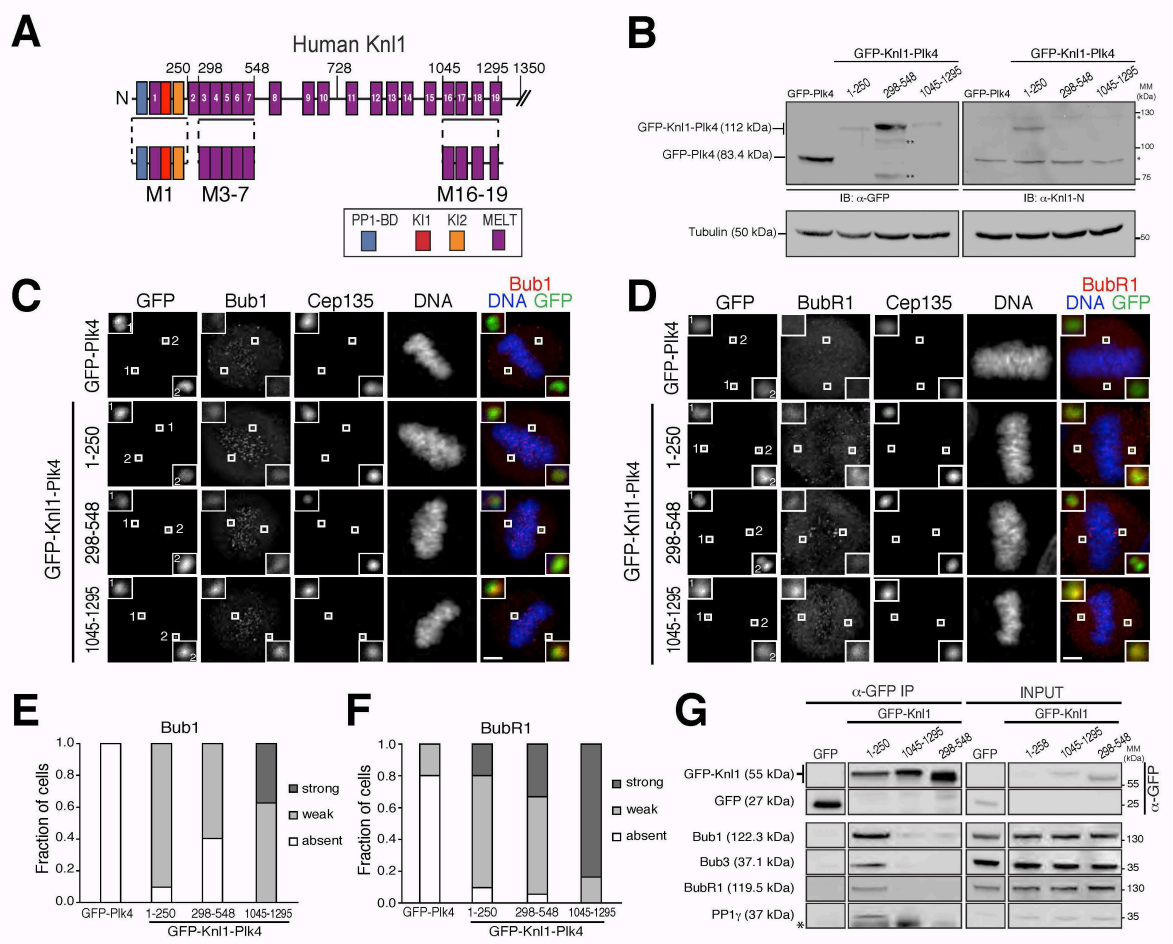

Figure 22 Ectopic localization of Knl1 segments to centrosomes promotes recruitment of Bub1 and BubR1

A) Motif organization of the first 1350 residues of human Knl1. Domain boundaries are indicated with residue numbers. B) Western blot showing the expression of GFP-Plk4 fusions in HeLa cells. Tubulin was used as loading control. Double and single asterisks indicate degradation products and unspecific bands recognized by the Knl1-N antibody, respectively. Note that the Knl1-N antibody (raised against residues 1-22 of Knl1) recognizes only GFP-Knl1$^{1\text{-}250}$-Plk4. C-D) Localization of Bub1 (C) or BubR1 (D) in representative images of HeLa cells expressing GFP-Plk4 constructs treated with MG132 for 2 hours. GFP-Plk4 is used as negative control, Cep135 staining as centrosomal marker. Insets show a higher magnification of centrosomes. E-F) Graph showing the fraction of cells in which Bub1 (C) or BubR1 (D) signals at centrosomes were strong, weak or absent in cells expressing GFP-Plk4 fusions as shown in C and D respectively. G) Western blot showing immunoprecipitates (IP) from ~6 mg mitotic lysates from Flp-In T-REx HeLa cell lines expressing the indicated N-terminally tagged GFP-Knl1 constructs. The asterisk refers to an unspecific signal. MM, molecular mass; IB, immunoblot. Scale bars, 5 μm.

Collectively, these results suggest that Knl1$^{1-250}$, Knl1$^{298-548}$, and Knl1$^{1045-1295}$ are all able to interact with Bub1 and BubR1 when targeted to centrosomes. However, while Knl1$^{298-548}$ and Knl1$^{1045-1295}$ contain multiple but relatively weak Bub1, Bub3 and BubR1 binding motifs, and dissociate readily from these proteins under conditions of non-equilibrium, Knl1$^{1-250}$ binds these proteins more tightly.

3.3 Knl1$^{1-250}$ at the kinetochore is sufficient for a robust checkpoint response

We were intrigued by the observation that Knl1$^{1-250}$, which harbors only one MELT repeat, bound considerable amounts of Bub1, Bub3 and BubR1 (Figure 22 G). We then assessed whether such amounts were sufficient to establish a checkpoint response. To test this

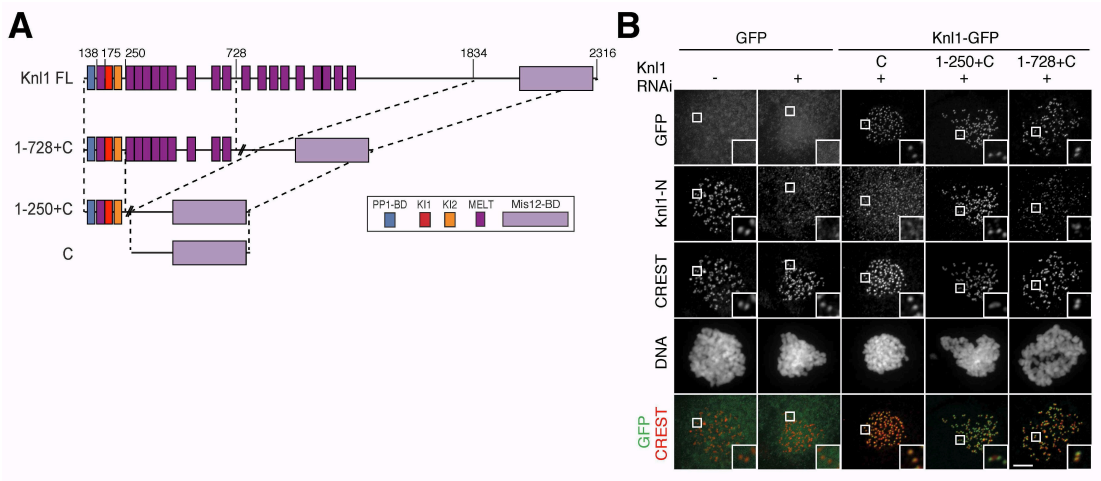

Figure 23 Design of Knl1 chimeras

A) Schematic representation of Knl1 chimeras. B) Representative images of Flp-In T-REx HeLa stable cells expressing various Knl1-GFP proteins after treatment with nocodazole for 4 hours. CREST is used to stain centromeres. Note that the Knl1-N antibody (raised against the first 22 residues of Knl1) recognizes endogenous Knl1 and Knl1-GFP chimeras, with the exception of the Knl1C-GFP, which lacks the epitope recognized by the antibody. FL, full-length; C, C-terminal domain (residues 1834-2316). Scale bar, 5 µm.

possibility, we verified if Knl1$^{1-250}$ was sufficient to sustain a SAC response when targeted to kinetochores in cells depleted of endogenous Knl1. To target Knl1$^{1-250}$ to kinetochores, we fused its coding sequence to that of the C-terminal kinetochore-targeting domain of Knl1 (residues 1834-2316) and to a C-terminal GFP (Knl1$^{1-250+C}$-GFP) (Figure 23 A). The isolated

C-terminal domain of Knl1 (Knl1^{C}-GFP) was used as a negative control. As a positive control, we used a longer fragment of Knl1 (residues 1-728), which had been previously shown to be sufficient for a robust checkpoint response (Kiyomitsu et al., 2011) (Figure 23 A). The resulting constructs were integrated at a single genomic locus in HeLa cells from which their expression was induced by addition of doxycycline (Tighe et al., 2008). The constructs (and their derivatives described later) were resistant to KNL1 siRNA depletion and were expressed

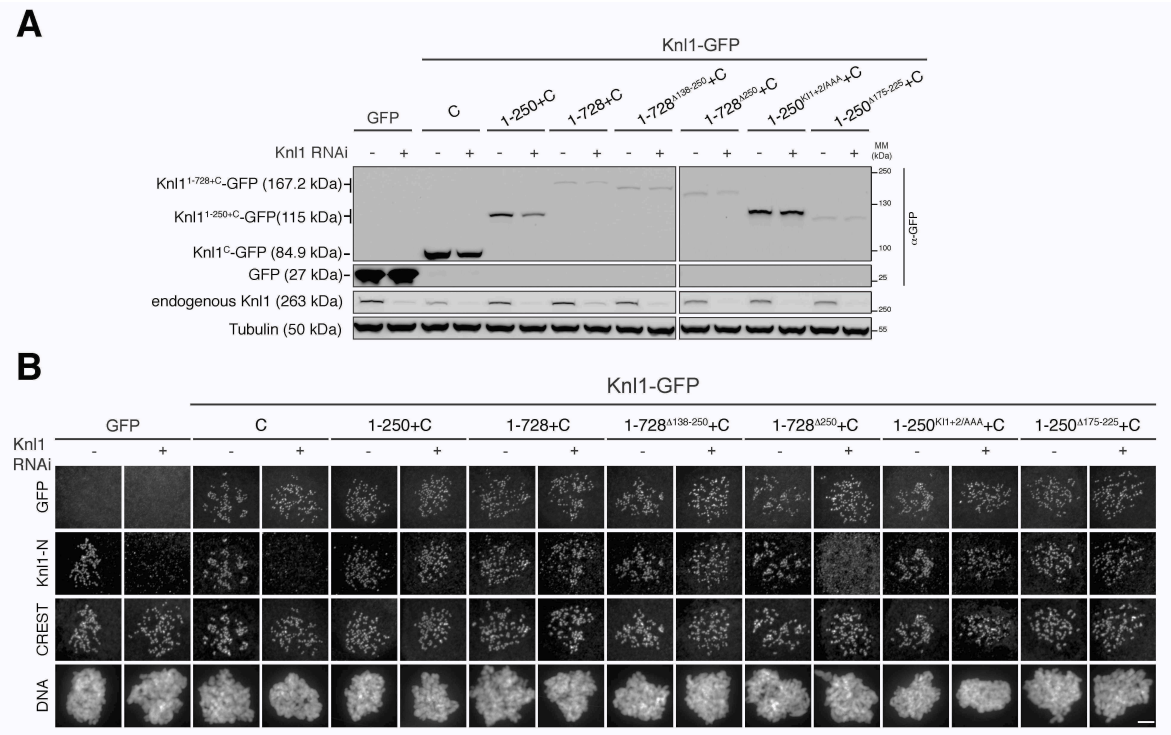

Figure 24 Expression of RNAi resistant Knl1 chimeras

A) Western blot of Flp-In T-REx stable cells expressing the indicated Knl1-GFP constructs in the presence (-) or absence (+) of endogenous Knl1. Tubulin is used as loading control. B) Representative images of Flp-In T-REx stable HeLa cells expressing GFP or Knl1-GFP chimeras treated with nocodazole for 3 hours, in the presence (-) or absence (+) of endogenous Knl1. CREST was used to stain centromeres. Note that, in the absence of endogenous Knl1, the Knl1-N antibody (raised against the first 22 residues of Knl1) recognizes all Knl1-GFP constructs, except for the one lacking the epitope (Knl11-728$^{\Delta 250+C}$-GFP). RNAi, RNA interference; MM, molecular mass. Scale bar, 5 μm.

at various levels (Figure 24 A). Immunofluorescence analysis revealed that all the constructs efficiently decorated kinetochores in the presence and absence of endogenous Knl1 (Figure 23 B and Figure 24 B), confirming previous findings indicating that the C-terminal kinetochore-targeting domain of Knl1 interacts with kinetochores regardless the presence of endogenous

Knl1 (Kiyomitsu et al., 2011). We also noticed that expression of Knl1^{C}-GFP reduced the total levels of endogenous Knl1 (Figure 24 A), probably by displacing and destabilizing Knl1 as previously suggested by Kiyomitsu and colleagues (Kiyomitsu et al., 2011).

Elimination of endogenous Knl1 by RNA interference was quite efficient, as judged by Western blotting and fluorescence microscopy (Figure 23 B and Figure 24). Nevertheless, Knl1-depleted cells were still able to mount a relatively robust checkpoint response in the presence of spindle poisons such as nocodazole or taxol (Figure 25). This phenotype is likely to reflect incomplete KNL1 depletion. Non- depleted cells arrested in mitosis for ~ 7.5 hours in the presence of 100 nM of nocodazole or 50nM of taxol. However, the checkpoint defect

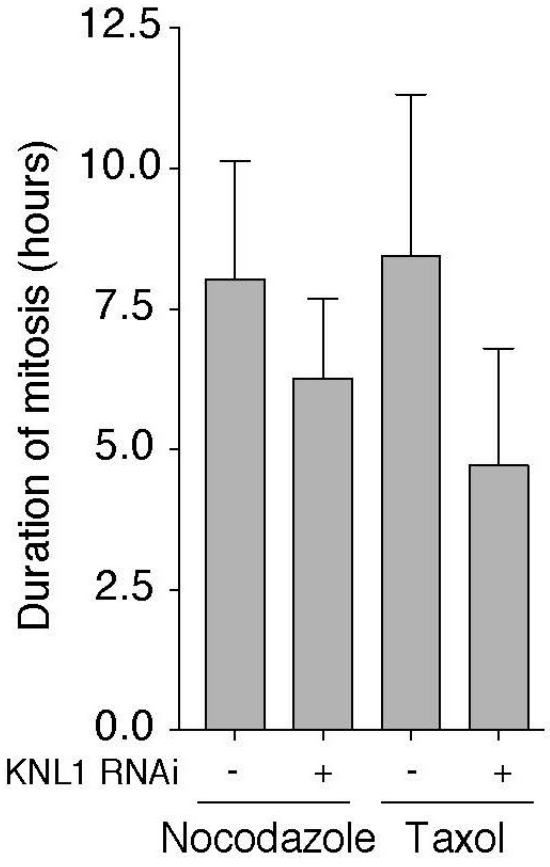

Figure 25 SAC response in Knl1 depleted cells

Graph representing the mean duration of mitosis of Flp- In T-REx stable cells in the presence of nocodazole (100nM) or taxol (50nM). Cell morphology was used to measure entry into and exit from mitosis by time-lapse microscopy (n>21 for each condition). Error bars represent SD.

displayed by cells depleted for Knl1 was slightly stronger in the presence of taxol than of nocodazole (Figure 25). To exacerbate the checkpoint defect of Knl1-depleted cells, we added a low concentration of the SAC inhibitor reversine (Santaguida et al., 2010) and therefore assessed the checkpoint response of all Knl1-GFP constructs in the presence of taxol and reversine (Figure 26 A).

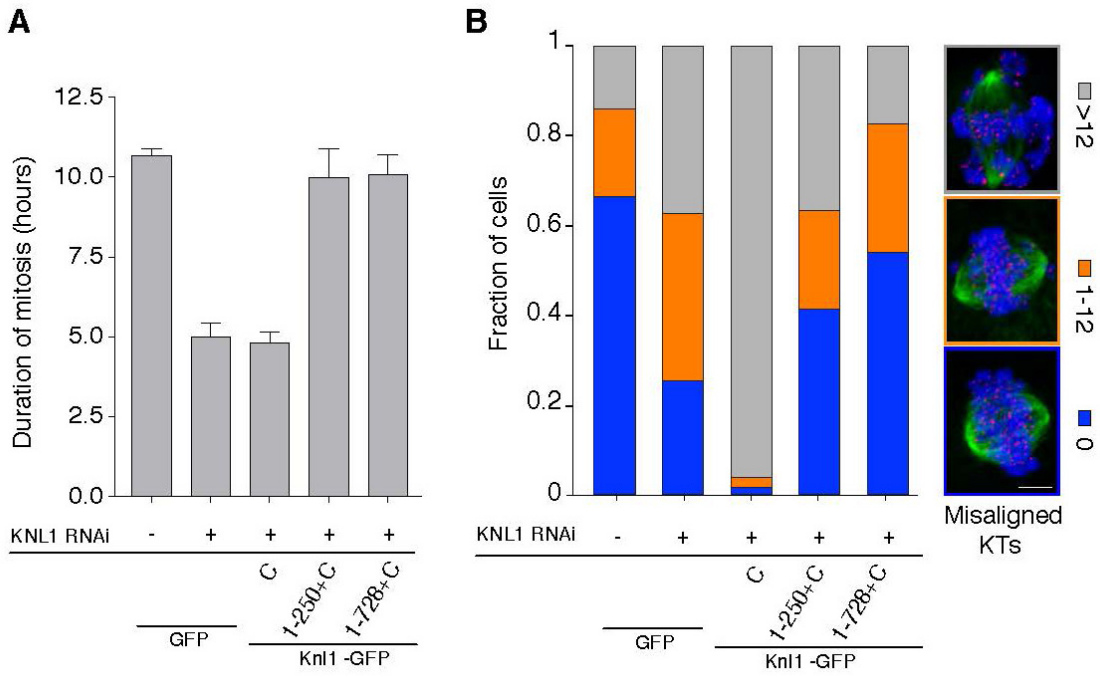

Figure 26 Knl1$^{1-250}$ is sufficient for robust SAC response when targeted to kinetochores

A) Graph representing the mean duration of mitosis of Flp- In T-REx stable cells expressing various Knl1-GFP constructs in the presence of 50 nM of taxol and 10 nM of reversine. Cell morphology was used to measure entry into and exit from mitosis by time-lapse microscopy (n>50 for each condition). Error bars represent SEM from three independent experiments. B) Quantification of chromosome alignment in Flp-In T-REx stable cells expressing the indicated Knl1-GFP constructs cells after treatment with 5 µM MG132 for 4 hours. Immunostaining shows tubulin in green, centromeres (CREST) in red and DNA in blue. The graph shows the fraction of cells (n>155 for each condition) from two independent experiments. KTs, kinetochores. Scale bar, 5 µm.

In the presence of 50 nM of taxol and 10 nM of reversine, cells expressing the C-terminal domain of Knl1 (Knl1^{C}) in the absence of endogenous Knl1 were not able to mount a checkpoint response (Figure 26 A), as observed previously (Kiyomitsu et al., 2011). Interestingly, expression of Knl1$^{1-250+C}$-GFP was sufficient to rescue the checkpoint response to levels similar to those of non-depleted and of Knl1$^{1-728+C}$-GFP expressing cells. Thus, the

first 250 residues of Knl1 contain sufficient sequence information to mount a strong checkpoint response in cells treated with spindle poisons and low concentrations of a checkpoint inhibitor.

Besides its role in checkpoint signaling, Knl1 is also important for the correct attachment of chromosomes to microtubules (Cheeseman et al., 2006; Espeut et al., 2012; Kiyomitsu et al., 2007; Pagliuca et al., 2009; Welburn et al., 2010). Consistent with this function, cells depleted for Knl1 were not able to efficiently align their chromosomes on the metaphase plate in the presence of the proteasome inhibitor MG132 (Figure 26 B). We then monitored the ability of the Knl1 constructs to complement the alignment defect caused by Knl1 depletion. Knl1^{C}-GFP construct, containing only the C-terminal kinetochore-targeting region of Knl1, dramatically exacerbated the negative effects of Knl1 depletion on chromosome alignment, as already observed (Kiyomitsu et al., 2011). On the other hand, expression of Knl1$^{1\text{-}728+C}$-GFP rescued the misalignment phenotype to levels similar to non-depleted cells. Importantly, cells expressing Knl1$^{1\text{-}250+C}$-GFP displayed a marked improvement in chromosome alignment in comparison to cells expressing only the C-terminal domain but the rescue was only partial when compared to Knl1$^{1\text{-}728+C}$-GFP.

Altogether, these results demonstrate that kinetochore localization of the first 250 residues of Knl1, which contain a single MELT repeat, can sustain the checkpoint response effectively. The same construct also supports chromosome alignment, albeit less efficiently than the Knl1$^{1\text{-}728\ +C}$ construct, which contains 10 MELT repeats.

Next, we tested whether Knl1$^{1\text{-}250+C}$-GFP was able to interact with Bub1, Bub3 and BubR1 at kinetochores. In Figure 22 G (see page 64), we showed that a soluble version of Knl1$^{1\text{-}250}$, GFP-Knl1$^{1\text{-}250}$, interacted robustly with Bub1, Bub3 and BubR1. In IP experiments, we found that the targeting of Knl1$^{1\text{-}250}$ to kinetochores by fusion to the Knl1 C-terminal domain (Knl1$^{1\text{-}250+C}$) strongly enhanced the interactions with Bub1, Bub3 and BubR1 (Figure 27 A), compared to Knl1$^{1\text{-}250}$ only, whereas no binding of Bub1, Bub3 and BubR1 could be detected

in the IP of Knl1^{C}-GFP. Kinetochore targeting of all constructs containing the C-terminal domain of Knl1 (Knl1^{C}-GFP and Knl1$^{1-250+C}$-GFP) was confirmed by concomitant IP of other KMN subunits, including Mis12, Hec1 and Zwint-1 (Figure 27 A). Next, we compared the ability of Knl1$^{1-250+C}$ and Knl1$^{1-728+C}$ constructs to pull down Bub1, Bub3, and BubR1 and the kinetochore subunit Mis12. With its 10 MELT motifs, Knl1$^{1-728+C}$ was able to pull down significantly larger amounts of Bub1, Bub3 and BubR1 compared to Knl1$^{1-250+C}$ (Figure 27 B). Similar levels of Mis12 were present in the precipitates, indicating that both proteins had reached kinetochores effectively.

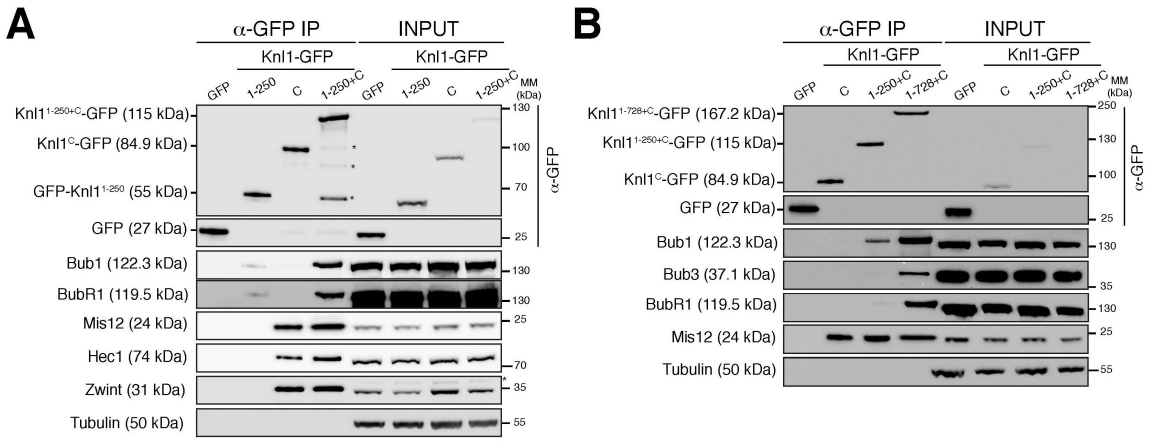

Figure 27 Kinetochore targeting enhances interactions of Knl1$^{1-250}$

Western blot of immunoprecipitates (IP) from ~5 mg (A) or ~4.2 mg (B) mitotic lysates obtained from Flp-In T-REx stable cells expressing the indicated Knl1-GFP constructs. Note that Knl1$^{1-250}$ construct used in A is N-terminally GFP-tagged, while the others carry the tag at their C-terminus. Tubulin was used as loading control. Asterisks indicate putative degradation products. MM, molecular mass.

As already shown before (Figure 20), Bub1 and BubR1 kinetochore levels drop in the absence of Knl1 (Figure 28). Consistent with its binding abilities shown in the immunoprecipitation experiment shown in Figure 27 B, Knl1$^{1-728+C}$ was also able to restore significant kinetochore levels of Bub1 and BubR1 in cells depleted for Knl1 (Figure 28). Conversely, little amounts of Bub1 and BubR1 were visible on kinetochores of cells expressing the Knl1$^{1-250+C}$ and they only slightly exceeded those rescued by Knl1^{C} (Figure 28). With a single MELT repeat, Knl1$^{1-250+C}$ is likely to bind to single Bub1 and BubR1 molecules, possibly explaining why Bub1 and BubR1 levels do not exceed the detection threshold (for Bub1) or do so only moderately (for

BubR1).

Altogether, these results indicate that MELT repeats can account for independent binding of Bub1, Bub3 and BubR1 and that the presence of a higher number of MELT correlates with more abundant binding either via IP and IF analysis. Moreover, the first 250 residues of Knl1

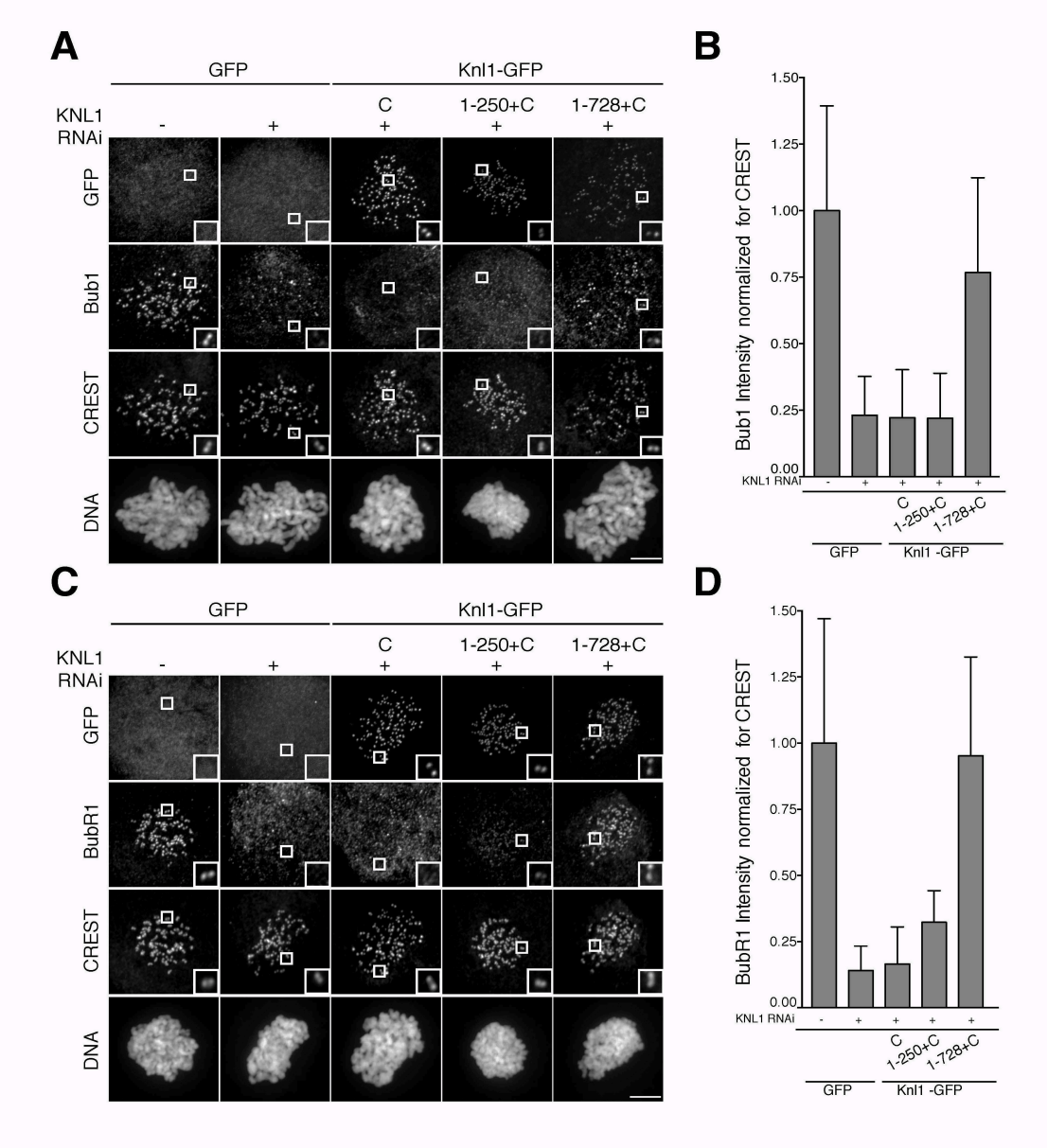

Figure 28 Rescue of Bub1 and BubR1 kinetochore levels by Knl1 chimeras

A) Representative images of Flp-In T-REx HeLa stable cells expressing the indicated Knl1-GFP proteins after treatment with nocodazole for 4 hours. CREST was used to visualize centromeres. Insets show a higher magnification of kinetochore regions (boxes). B) Quantification of Bub1 kinetochore levels normalized to the CREST kinetochore levels in cells treated as in panel A. C) Cells were treated as in panel A, but this time BubR1 instead of Bub1 is visualized. D) Quantification of BubR1 kinetochore levels normalized to the CREST kinetochore levels in cells treated as in A. The graphs in B and D show mean intensity, error bars indicate SD. Values for Bub1 (B) or BubR1 (D) in non-depleted cells are set to 1. Scale bars, 5 μm.

recruit little, almost undetectable, amounts of Bub1 and BubR1. Nevertheless, we also demonstrated that such amounts are sufficient for a robust checkpoint response, implying that a low number of Bub1 and BubR1 molecules at the kinetochore are needed for an efficient checkpoint arrest.

3.4 Molecular determinants of Bub1 and BubR1 binding to Knl1$^{1-250}$

In Figure 22 G, we showed that Bub1, Bub3, and BubR1 interact more stably with Knl1$^{1-250}$ than with Knl1$^{298-548}$ or Knl1$^{1045-1295}$. Although all these regions of Knl1 contain MELT repeats, Knl1$^{1-250}$ also contains KI1 and KI2 motifs (Figure 29 A), which interact with the TPR domain of Bub1 and BubR1 respectively (Bolanos-Garcia et al., 2011; Kiyomitsu et al., 2011; Kiyomitsu et al., 2007; Krenn et al., 2012). To test whether KI1 and KI2 contribute to the interaction of Knl1$^{1-250}$ with Bub1, BubR1 and Bub3, we created two series of deletion mutants of Knl1$^{1-250}$ as N-terminally GFP-tagged proteins in which progressively larger segments of Knl1 were removed from the N- or the C-terminus. After precipitation from lysates of mitotic cells with a GFP antibody, Western blotting was used to assess the abundance of Bub1, Bub3 and BubR1 associated with each construct (Figure 29). As already shown in Figure 22 G, Knl1$^{1-250}$ efficiently pulled down Bub1, Bub3 and BubR1. Remarkably, deletions from the C-terminus removing KI2 but leaving an intact MELT and KI1 (Knl1$^{1-188}$) not only affected the binding of BubR1 dramatically, but also caused a very strong reduction in the amounts of bound Bub1 (Figure 29 B). This result is surprising because KI2 has been shown to bind BubR1 and not Bub1 in reconstitution experiments *in vitro* (Bolanos-Garcia et al., 2011; Kiyomitsu et al., 2011; Kiyomitsu et al., 2007; Krenn et al., 2012). It suggests that binding of BubR1 through the KI2 motif might stabilize the interaction of Bub1 with the neighboring MELT1-KI1 motif. Upon additional removal of the KI1 motif (Knl1$^{1-173}$), the amounts of bound Bub1 were further reduced (Figure 29 B). All constructs contained an intact N-terminal PP1-binding site and consistently bound PP1 to similar levels.

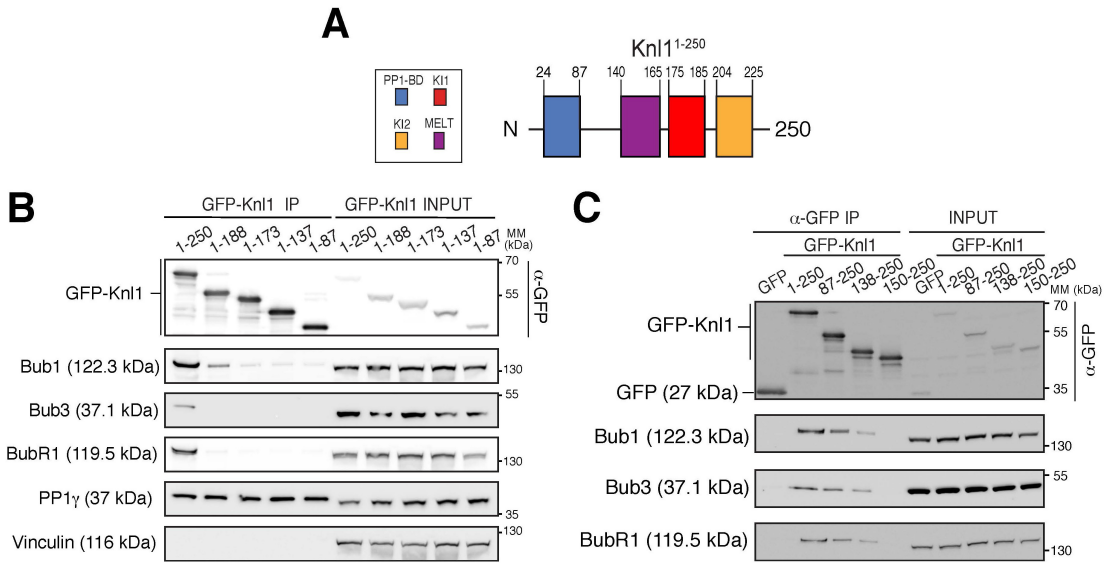

Figure 29 Molecular determinants of Bub1 and BubR1 tight binding to Knl1$^{1-250}$

A) Schematic description of the motif organization of the first 250 residues of human Knl1 (Knl1$^{1-250}$). Relevant domain boundaries are indicated with residue numbers. B-C) Western blotting of immunoprecipitates (IP) from ~3.3 mg (A) or ~3.0 mg (B) mitotic lysates from Flp-In T-REx stable cells expressing the indicated N-terminally tagged GFP-Knl1 constructs carrying C- (B) or N-terminal (C) deletions. Vinculin is used as loading control. N, N-terminus; MM, molecular mass.

Next, we tested the N-terminal deletions (Figure 29 C). Removal of the first 86 or 137 residues (Knl1$^{87-250}$ and Knl1$^{138-250}$), both of which preserve the combination of MELT1, KI1 and KI2, resulted in a relatively modest decrease in the amounts of Bub1, Bub3 and BubR1 bound to the GFP-Knl1 baits. Further deletion of 12 residues (Knl1$^{150-250}$), which affected the integrity of MELT1 but not of KI1 and KI2, resulted in the reduction of Bub1, Bub3 and BubR1 to background levels (Figure 29 C). To further confirm the contribution of MELT1, we changed its sequence from MDLT to ADLA in the context of Knl1$^{1-250}$. Consistent with our deletion studies, mutation of the MELT sequence reduced Bub1, BubR1 and Bub3 binding, albeit not completely (Figure 30 A). Collectively, these results demonstrate that both the MELT1 motif and the KI1 and KI2 motifs of Knl1$^{1-250}$ are instrumental for tight binding of Bub1, Bub3 and BubR1.

We were surprised to see that removal of the first 87 residues affected the binding of Bub1, Bub3 and BubR1 (Figure 29 C). This region of Knl1 includes the docking region for the PP1 phosphatase and the putative microtubule-binding domain (Figure 6). However, the fact that these experiments were performed with lysates from cells that had been treated with the microtubule-depolymerizing agent nocodazole argues against a contribution of the microtubule-binding domain to the association with Bub proteins in our assays. We hypothesized that the first 87 residues might affect the association with Bub1, BubR1 and Bub3 by either providing some PP1 activity that would (directly or indirectly) control these interactions or by stabilizing the conformation of the N-terminus of Knl1 (i.e. by providing a linker between the MELT-KI array and N-terminal GFP moiety). To distinguish between these two possibilities, we disrupted PP1 binding by introducing mutations in the PP1-docking sites in the context of Knl1$^{1-250}$, therefore avoiding any deletion of the N-terminus of Knl1. PP1 binding to the docking site on Knl1 is mediated by the RVSF motif (Liu et al., 2010). Consistently, mutations of the RVSF sequence into RaSa or RVdF reduced PP1 binding to Knl1$^{1-250}$ (Figure 30 B). Importantly, binding of Bub1 and BubR1 was not evidently

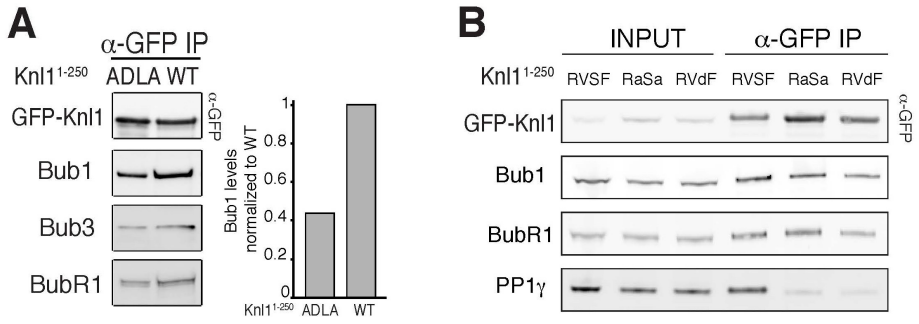

Figure 30 Effects of point mutations in GFP-Knl1$^{1-250}$

A) Immunoprecipitation (IP) of GFP-tagged Knl11-250 wild type (WT) and ADLA mutant carrying the substitutions M151A and T154A in the MELT1 sequence. On the right, a graph showing the quantification of Bub1 levels from the left panel, normalized to the corresponding GFP levels. The value of Bub1 is set to 1. B) Immunoprecipitation (IP) of GFP-tagged Knl11-250 wild type (RVSF) or mutants carrying the substitutions V59A and F61A (RaSa) or S60D (RVdF). Co-precipitating proteins were analyzed by SDS-PAGE and subsequent Western blotting. MM, molecular mass.

affected in the presence of these mutations (Figure 30 B), ruling out any contribution of PP1 binding to the interactions of Knl1$^{1-250}$ with Bub1 and BubR1. Moreover, these data suggest that the first 86 residues of Knl1 might stabilize the conformation of Knl1, possibly by preventing putative steric hindrance of the GFP moiety at the N-terminal end of Knl1.

Collectively, these results demonstrate that the MELT1 and the KI1 and KI2 motifs of Knl1$^{1-250}$, are important for tight binding of Bub1, Bub3 and BubR1. Importantly, these results also denote that the presence of MELT1 is necessary but not sufficient for a tight interaction of Bub1, Bub3 and BubR1 with the Knl1$^{1-250}$ construct, and that KI1 and KI2 strongly enhance the potency of the interaction with Bub proteins.

3.5 Robust SAC response mediated by Knl1$^{1-250}$ requires KI1 and KI2

Next we assessed whether the MELT1 and the KI constellation is required for tight binding of Bub1, BubR1 and Bub3 to the kinetochore. We therefore deleted the MELT1+KI1+KI2 region from Knl1$^{1-728+C}$ (Δ138-250), also in combination with the deletion of the first 137 residues of Knl1 (Δ250) (Figure 31 A). Both constructs were targeted to kinetochores as efficiently as their parental construct Knl1$^{1-728+C}$ (Figure 24 B, see page 66). First, we compared the amounts of Bub proteins precipitating with Knl1$^{1-728+C\ \Delta138-250}$, Knl1$^{1-728+C\ \Delta250}$, Knl1$^{1-728+C}$ and Knl1$^{1-250+C}$. Remarkably, Knl1$^{1-728+C\ \Delta138-250}$ and Knl1$^{1-728+C\ \Delta250}$, with their nine MELT repeats (only one less than the parental Knl1$^{1-728+C}$ construct), pulled down much lower amounts of Bub proteins, to levels similar to Knl1$^{1-250}$, which contains only MELT1 (Figure 31 B and C). Thus, the KI1 and KI2 motifs of Knl1 stabilize the binding of Bub1, Bub3 and BubR1 also in the context of a larger Knl1 segment containing approximately half of the MELT repeats of full-length Knl1. Next, we assessed the ability of the Knl1$^{1-728+C}$-GFP derived constructs to recruit Bub1 and BubR1 to kinetochores, after depletion of endogenous Knl1. In contrast with the IP experiment shown in Figure 31, deletions of residues 138-250 and 1-250 reduced the kinetochore recruitment of Bub1 only slightly, compared to Knl1$^{1-728+C}$

(Figure 32 A and B). In the case of BubR1, the effect of deleting the MELT1-KI array was more pronounced (Figure 32). Moreover, removal of the first 137 residues (Knl1$^{1\text{-}728+C\ \Delta 250}$) improved BubR1 kinetochore signals compared to Knl1$^{1\text{-}728+C\ \Delta 138\text{-}250}$.

Altogether, these results indicate that the MELT1 and KI array contribute to Bub1 and BubR1 binding to Knl1 in the context of larger Knl1 segments but are dispensable for Bub1 recruitment.

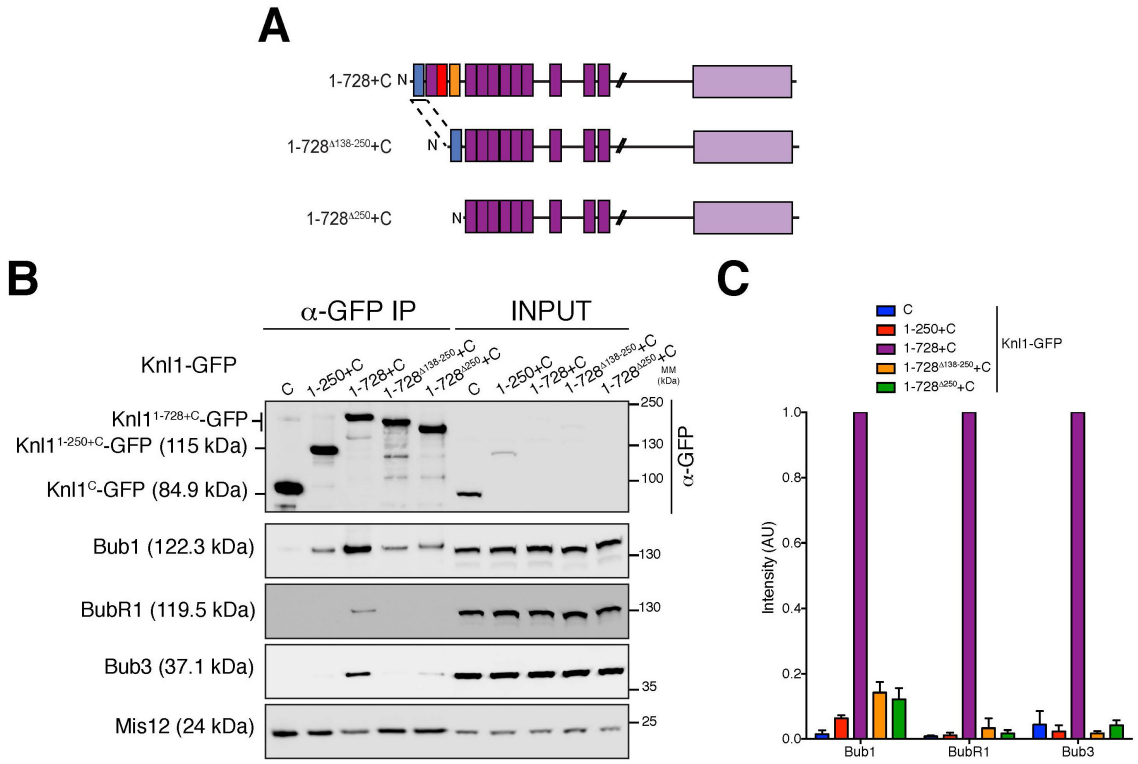

Figure 31 The MELT1 and KI constellation is required for tight Bub1 and BubR1 binding

A) Schematic representation of Knl1-GFP chimeras. Note that both deletion constructs depicted here lack MELT1 and therefore contain one MELT less than the parental construct. B) Western blot showing immunoprecipitates (IP) from ~2.4 mg mitotic lysates obtained from Flp-In T-REx stable cells expressing the indicated Knl1-GFP constructs. C) Quantification of the Western blot from C. The amounts of co-immunoprecipitating Bub1, BubR1 and Bub3 proteins were normalized to the amount of Knl1-GFP baits present in the IP. Values for the control construct Knl1$^{1\text{-}728+C}$-GFP are set to 1. The graph shows the mean intensity of two independent experiments. Error bars represent SEM. N, N-terminus, MM, molecular mass; AU, arbitrary units.

We next tested the role of KI motifs in the shorter Knl1$^{1\text{-}250+C}$ construct in the binding of Bubs to kinetochores. For this purpose, we generated Knl1$^{1\text{-}250+C}$ constructs that carried point

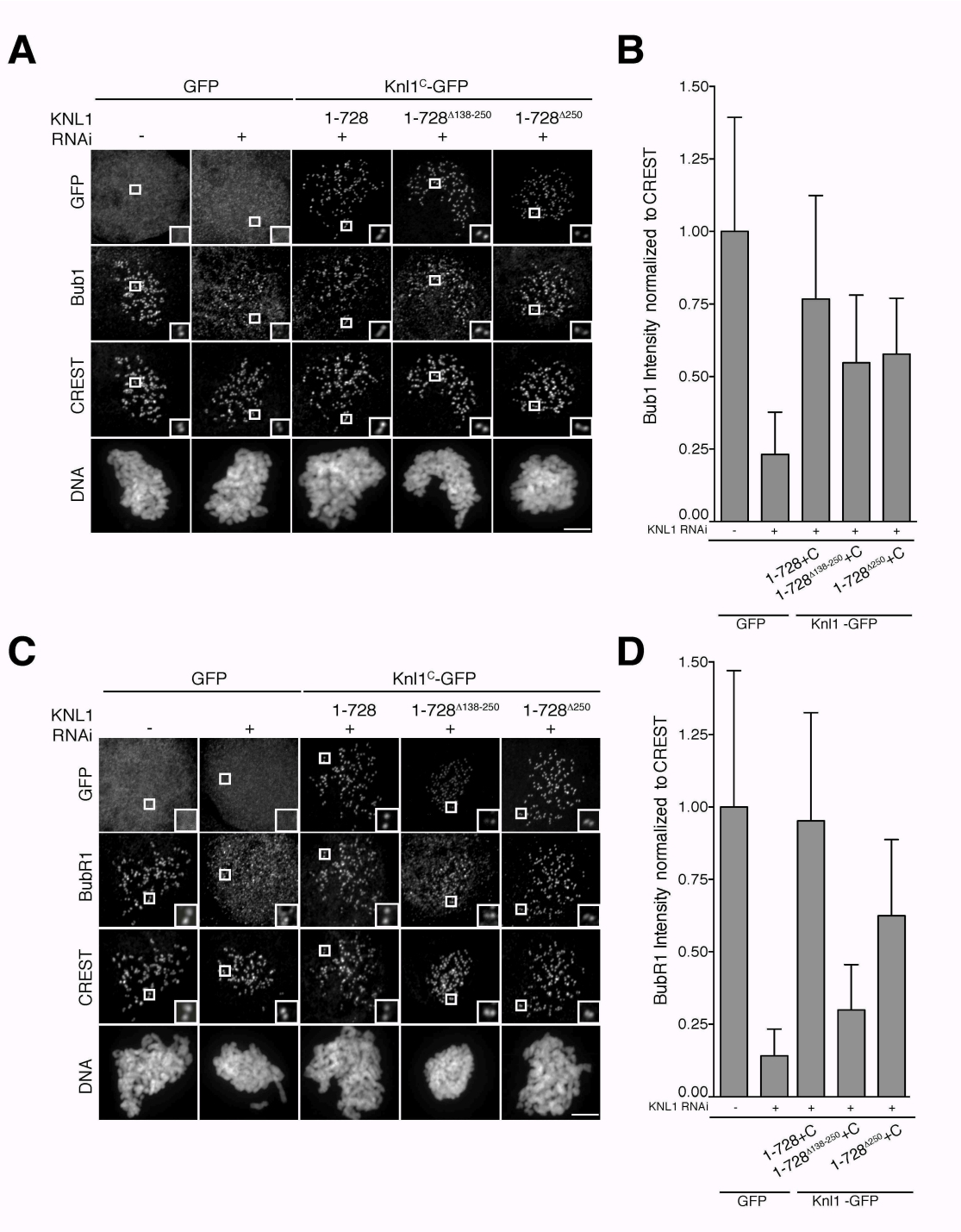

Figure 32 The MELT1 and KI motifs only marginally contribute to Bub1 and BubR1 recruitment

A) Representative images of Flp-In T-REx cells expressing various Knl1-GFP proteins after treatment with nocodazole for 4 h. CREST is used to stain centromeres. Insets show a higher magnification of kinetochore regions (boxes). B) Quantification of Bub1 kinetochore levels normalized to the CREST kinetochore levels in cells treated as in A. C) Representative images of Flp-In T-REx HeLa cells stably expressing various Knl1-GFP proteins as described in A. D) Quantification of BubR1 kinetochore levels normalized to the CREST kinetochore levels in cells treated as in C. In the graphs, the values for Bub1 (B) or BubR1 (D) intensity in non-depleted cells are set to 1. The graphs shows mean intensity, error bars indicate SD. Scale bars, 5 μm.

mutations in or a deletion of both KI1 and KI2 motifs, named KI1+2/AAA or Δ175-225 respectively (Figure 33 A). Both constructs were targeted to kinetochores as efficiently as their parental construct Knl1$^{1\text{-}250+C}$ (Figure 24 B). In IP experiments, the mutant in the KI motifs (Knl1$^{1\text{-}250\text{-}KI1+2/AAA+C}$) displayed a strongly reduced binding to Bub proteins but not to the Mis12 protein (Figure 33 B and C). A similar reduction was observed for the Knl1$^{1\text{-}250+C\ \Delta 175\text{-}225}$ deletion construct (not shown). This corroborates the view that KI motifs stabilize Bub1, Bub3 and BubR1 binding to Knl1$^{1\text{-}250+C}$.

Next, we evaluated the ability of the constructs derived from Knl1$^{1\text{-}250+C}$ and Knl1$^{1\text{-}728+C}$ to

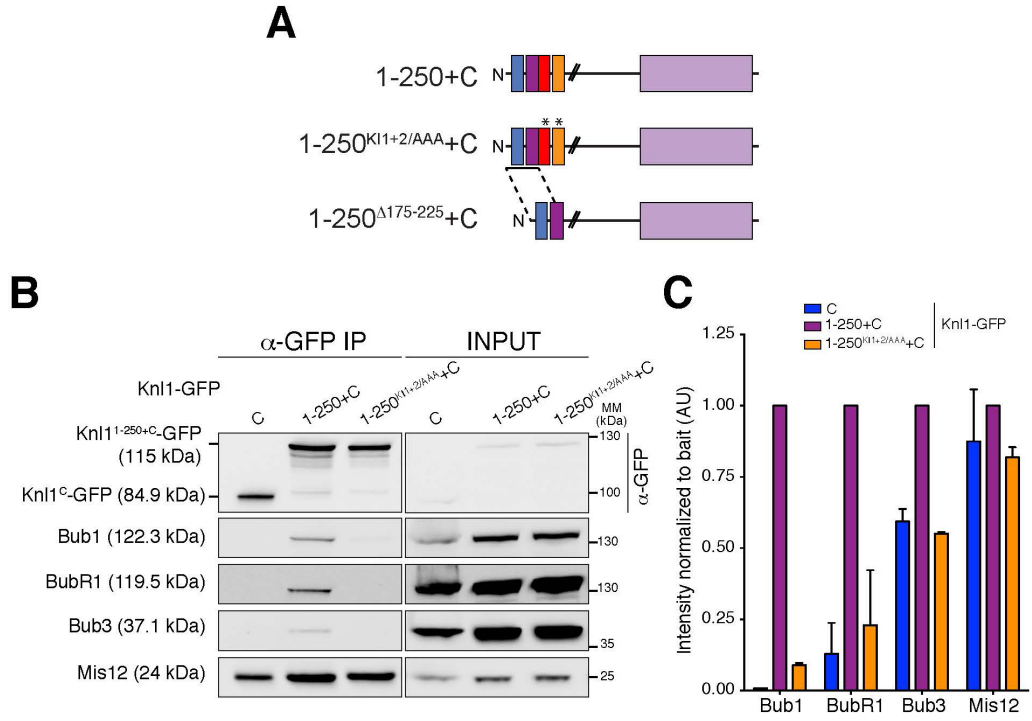

Figure 33 KI motifs contribute to Bub1 and BubR1 binding to Knl1$^{1\text{-}250+C}$-GFP

A) Schematic representation of Knl1-GFP chimeras. Asterisks refer to alanine mutations introduced in the KI motifs. Specifically, each residue in the K-I-D motif of KI1 and KI2 was mutated into alanine (indicated as KI1+2/AAA). See Figure 10 B, page 43 for the KI sequences. B) Western blot showing immunoprecipitates (IP) from ~4.2 mg mitotic lysates obtained from Flp-In T-REx stable cells expressing the indicated Knl1-GFP constructs. C) Quantification of the Western blot in B. The amounts of co-immunoprecipitating Bub1, BubR1, Bub3 and Mis12 proteins were normalized for the amount of Knl1-GFP baits present in the IP. Values for the control Knl1$^{1\text{-}250+C}$-GFP construct are set to 1. The graph shows the mean intensity of two independent experiments. Error bars represent SEM. Note that the quantification of Bub3 might suffer from the relatively low signals of Bub3.

complement the checkpoint and alignment phenotypes resulting from the depletion of Knl1 (Figure 34 and Figure 35). When we challenged the cells with 50 nM of taxol and 10 nM of reversine (same condition used in Figure 26 A, see page 68), all constructs, which bound different amounts of Bub proteins, were able to mount an equally strong checkpoint arrest (Figure 34 A). These results indicate that the strength of the SAC arrest is not proportional to the levels of Bub1 and BubR1 bound to Knl1. Moreover, in line with our previous observation, these results imply that little amount of Bub proteins is sufficient for a robust checkpoint response, at least in the mild conditions used in this assay. To assess the robustness of the SAC arrest under more stringent conditions, we repeated the experiment in the presence of higher doses of reversine (100 nM) and a lower dose of taxol (10 nM). As expected, non-depleted cells were still able to arrest (Figure 34 B), although less efficiently than non-depleted cells in milder conditions (Figure 34 A). Consistent with our previous results, Knl1$^{1\text{-}250+C}$ and Knl1$^{1\text{-}728+C}$ restored the checkpoint arrest, although the Knl1$^{1\text{-}728+C}$ seemed less proficient than Knl1$^{1\text{-}250+C}$ under these conditions (Figure 34 B). Importantly, we only obtained a partial checkpoint response in cells expressing Knl1$^{1\text{-}250\text{-}KI1+2/AAA+C}$ or Knl1$^{1\text{-}250+C\ \Delta 175\text{-}225}$ compared to Knl1$^{1\text{-}250+C}$, indicating that the presence of intact KI1 and KI2 motif affects the functional integrity of Knl1$^{1\text{-}250+C}$. On the contrary, the SAC arrest of the longer Knl1$^{1\text{-}728+C}$ was not affected by the removal of the MELT1 and KI constellation (Knl1$^{1\text{-}728+C\ \Delta 138\text{-}250}$) and moderately affected when this deletion was combined with loss of the N-terminus of Knl1 (Knl1$^{1\text{-}728+C\ \Delta 250}$).

Next, we analyzed the alignment phenotype (Figure 35). Consistent with the checkpoint analysis, the KI1 and KI2 motifs were important for chromosome alignment, as neither Knl1$^{1\text{-}250\text{-}KI1+2/AAA+C}$ nor Knl1$^{1\text{-}250+C\ \Delta 175\text{-}225}$ were able to overcome the negative effects deriving from the expression of the C-terminal region of Knl1. However, removal of the MELT1 and KI motifs (Knl1$^{1\text{-}728+C\ \Delta 138\text{-}250}$) did not affect the ability of cells to align their chromosomes, while further deletion of the first 137 residues (Knl1$^{1\text{-}728+C\ \Delta 250}$) reduced the efficiency of the

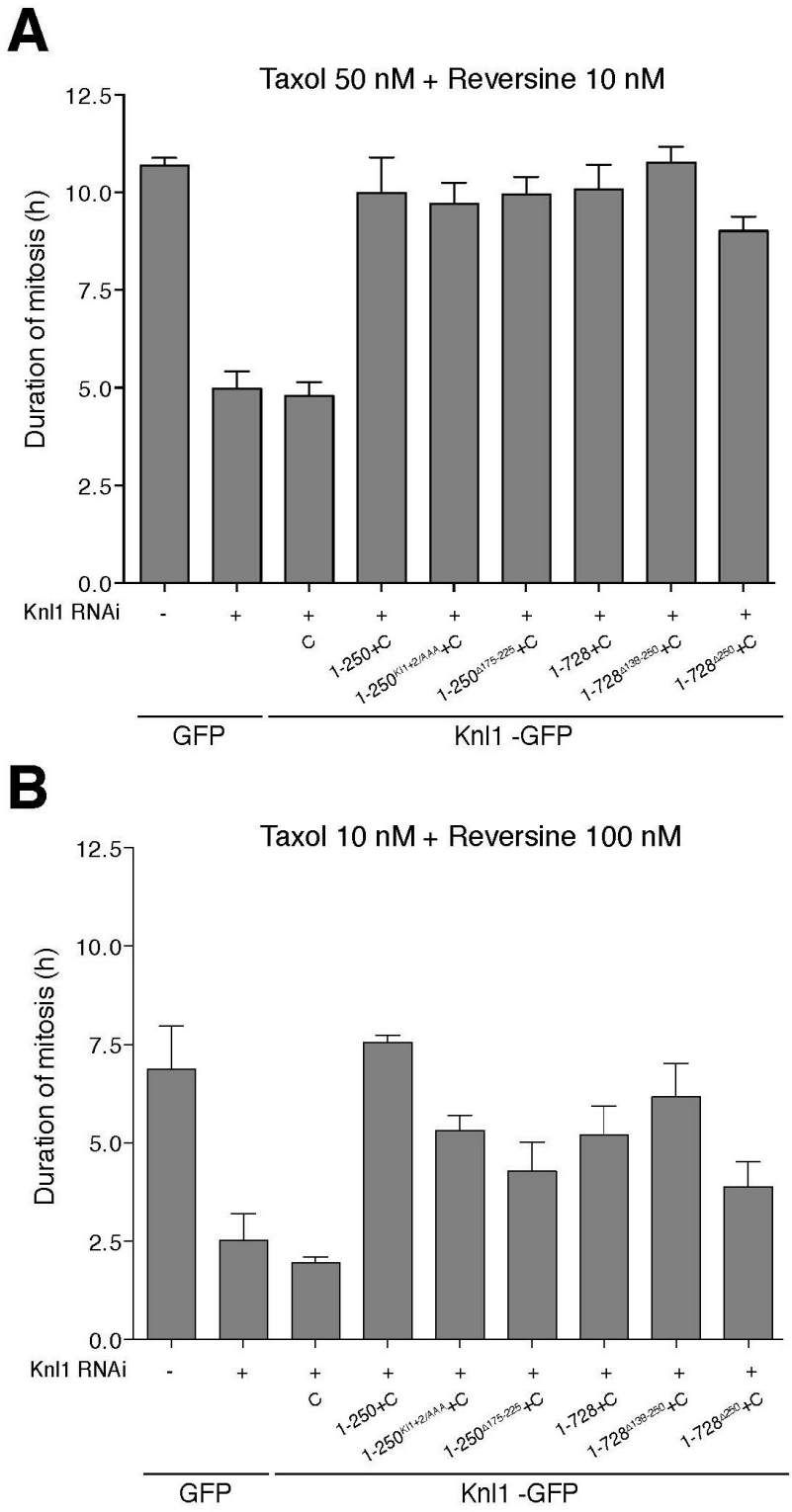

Figure 34 Checkpoint response in cells expressing Knl1-GFP chimeras

Graphs representing the mean duration of mitosis of Flp-In T-Rex HeLa stable cell lines expressing the indicated Knl1-GFP constructs in the absence of endogenous Knl1 and in the presence of 50 nM of taxol and 10 nM of reversine (A) or 10 nM of taxol and 100 nM of reversine (B). Cell morphology was used to measure entry into and exit from mitosis by time lapse microscopy using (n>53 for cell line in A, n>60 for each cell line in B). Error bars represent SEM from three (A) or two (B) independent experiments.

alignment, to levels similar to Knl1-depleted cells.

Collectively, these observations point to an important role of the KI1 and KI2 motifs in stabilizing the binding of Bub1, Bub3 and BubR1 to Knl1 and, consequently, in determining the remarkable robustness of Knl1$^{1-250}$ in the checkpoint and alignment response.

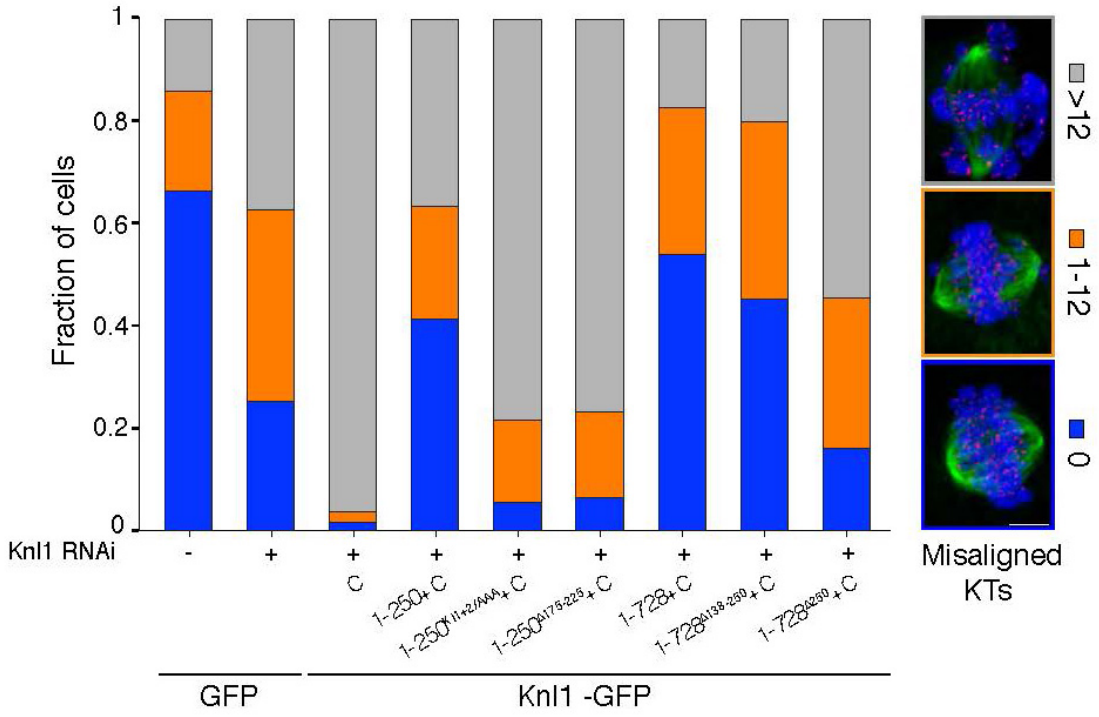

Figure 35 Alignment phenotype in cells expressing Knl1-GFP chimeras

Chromosome alignment of Flp-In T-REx stable cells expressing the indicated Knl1-GFP constructs after treatment with 5 μM MG132 for 4 hours. Immunostaining shows tubulin in green, centromeres (CREST) in red and DNA in blue. The graph shows the fraction of cells (n>155 for each condition) from two independent experiments. Scale bar, 5 μm.

3.6 MELT motifs assemble SAC complexes

As shown in Figure 22 G, the MELT1-KI1-KI2 constellation of motifs within the N-terminal region of Knl1 provides a robust site of assembly of checkpoint complexes containing Bub1, Bub3 and BubR1. To shed light on the consequences of the recruitment of these proteins to

Knl1, we precipitated GFP-Knl1$^{1-250}$ and analyzed the resulting precipitates by Western blotting to assess whether other SAC components were present. Remarkably, besides Bub1, Bub3 and BubR1, we identified in Knl1$^{1-250}$ precipitates all SAC proteins, including Mps1, Mad1, Mad2, Cdc20, and the APC/C subunit APC7 (Figure 36 A). To assess whether Bub1 was required for these interactions, we repeated the precipitation experiments from lysates of cells in which Bub1 had been depleted by RNA interference. In agreement with the prediction that Bub1 is necessary for the assembly of SAC complexes on Knl1$^{1-250}$, the levels of Bub3, BubR1, Cdc20 and Mps1 were severely affected by Bub1 depletion (Figure 36 B). These results indicate that Knl1$^{1-250}$ acts as a platform for the assembly of checkpoint complexes by initiating the recruitment of Bub1/Bub3 complexes.

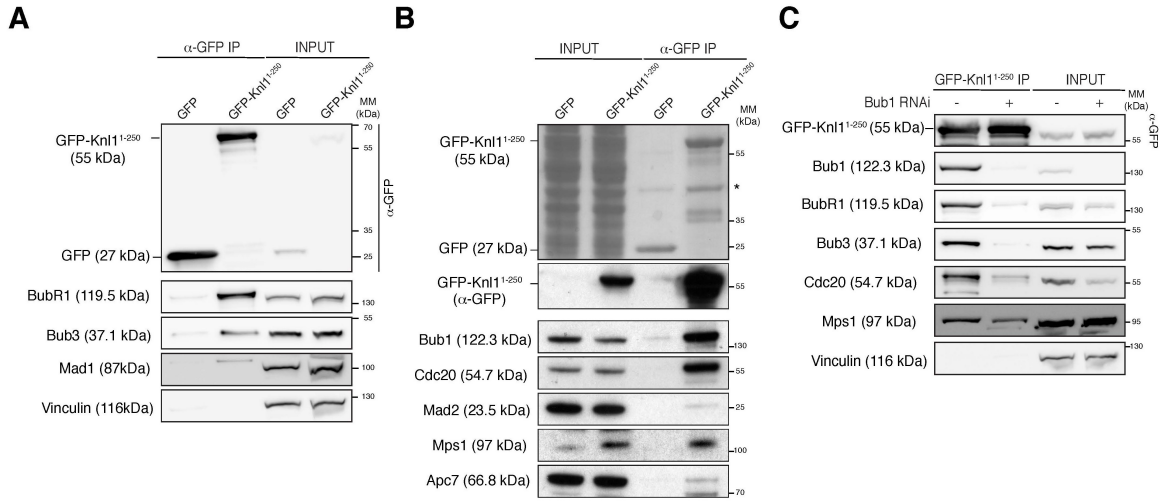

Figure 36 Knl1$^{1-250}$ is a platform for the assembly of checkpoint complexes

A-B) Western blot showing immunoprecipitates (IP) from ~10 mg (A) or ~4 mg (B) mitotic lysates obtained from Flp-In T-REx stable cells expressing GFP or GFP-Knl1$^{1-250}$. The top panel in B shows the membrane stained with Ponceau. The asterisk refers to a protein that binds non-specifically to the GFP-Trap beads during the immunoprecipitation. Vinculin was used as loading control. C) Western blot showing immunoprecipitates (IP) from ~10 mg mitotic lysates obtained from Flp-In T-REx stable cells expressing GFP-Knl11-250 after depletion of Bub1 by RNA interference and treatment with 330 nM nocodazole for 5 hours. Vinculin is used as loading control. MM, molecular mass.

4. The N-terminus of Knl1 promotes interactions within KMN complexes

While performing our co-immunoprecipitation studies on different Knl1 fragments (Figure 29, page 73) we observed that several components of the KMN such as Knl1, Hec1 and Mis12 co-precipitated with Knl1$^{1-250}$, much more efficiently than with other fragments of Knl1 (Figure 37 A). This observation suggests that Knl1$^{1-250}$ mediates interactions with KMN proteins. These interactions established by Knl1$^{1-250}$ are likely to be weaker than those with Bub1 and BubR1, as KMN components could be detected only in immunoprecipitation experiments performed with high amounts of mitotic extracts.

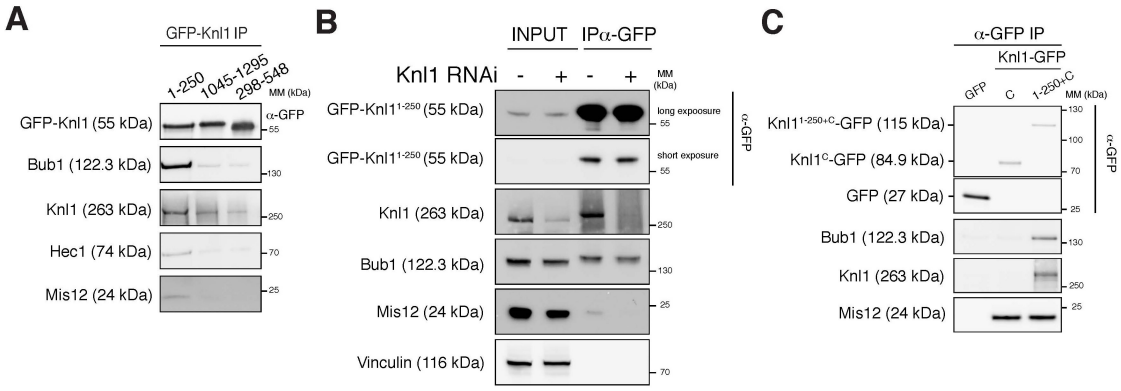

Figure 37 Knl1$^{1-250}$ promotes interactions with KMN molecules

A) Western blot showing immunoprecipitates (IP) from ~10 mg mitotic lysates obtained from Flp-In T-REx stable cells expressing GFP or GFP-Knl1$^{1-250}$. B) Western blot showing immunoprecipitates (IP) from ~10 mg mitotic lysates obtained from Flp-In T-Rex stable cells expressing GFP-Knl1$^{1-250}$ after depletion of Knl1 by RNAi and treatment with 330 nM nocodazole for 5 hours. Vinculin was used as loading control. C) Western blot showing immunoprecipitates (IP) from ~10 mg mitotic lysates obtained from Flp-In T-REx stable cells expressing the indicated constructs. MM, molecular mass.

To investigate the nature of such interactions more in detail, we repeated immunoprecipitation experiments from extracts of mitotic cells in which Knl1 had been depleted by RNA interference. Knl1 depletion was efficient and no Knl1 could be detected in the depleted IP sample (Figure 37 B. Note that GFP-Knl1$^{1-250}$ is insensitive to KNL1 RNAi). In line with the idea that Knl1$^{1-250}$ binds to Bub1/Bub3 directly, the amounts of co-precipitating Bub1 were not affected by depletion of endogenous Knl1. Conversely, the levels of Mis12 were reduced, indicating that its interaction with Knl1$^{1-250}$ is dependent on endogenous Knl1. We then asked

if Knl1$^{1-250}$ was also able to interact with KMN complexes when targeted to kinetochores (Figure 37 C). For this aim, we resorted to the cell lines expressing the Knl1 chimeras we described before (Figure 23 A). As already shown before (Figure 27 A), both Knl1$^{1-250+C}$ and Knl1^{C} constructs pulled-down Mis12, as a result of their efficient targeting to kinetochores. Interestingly, Knl1$^{1-250+C}$, but not Knl1^{C}, was able to co-precipitate endogenous Knl1 (Figure 37 C), indicating that the ability to pull down endogenous Knl1 is a unique property of the 1-250 segment of Knl1 $^{1-250}$ also at the kinetochore.

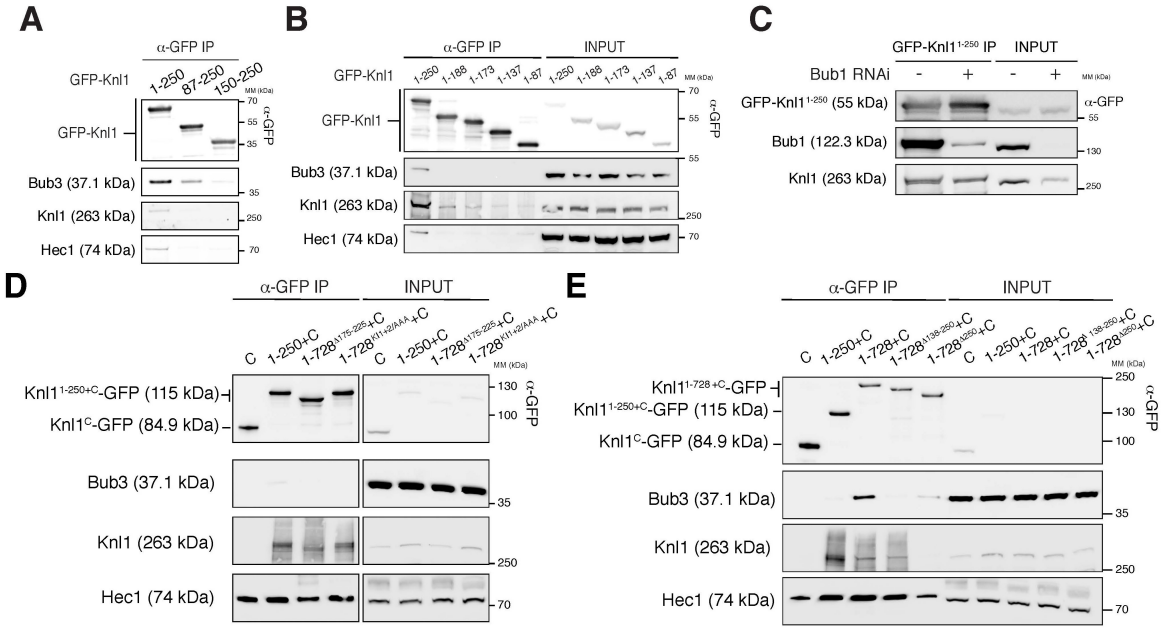

Figure 38 Determinants for the interaction with KMN molecules

Western blots showing immunoprecipitates (IP) from mitotic lysates obtained from Flp-In T-REx stable cells expressing the indicated constructs. MM, molecular mass.

Next, we tried to identify the determinants on Knl1$^{1-250}$ responsible for the interaction with KMN proteins. For this purpose, we immunoprecipitated different N- and C-terminal deletions constructs of Knl1$^{1-250}$ (already described in Figure 29, see page 73) and evaluated the co-precipitating amounts of endogenous Hec1 and Knl1 (Figure 38 A and B). Remarkably, removal of residues from both N- (Knl1$^{87-250}$, Figure 38 A) and C- terminus of Knl1$^{1-250}$ (Knl1$^{1-188}$, Figure 38 B) already caused a reduction in the amount of Hec1 and Knl1, together

with a reduction in Bub3. These studies indicate that integrity of the Knl1$^{1-250}$ is required for robust co-precipitation of KMN components.

These studies also revealed a correlation between the ability of GFP-Knl1$^{1-250}$ to pull down Bub3 and KMN components. This led us to assess the role of Bub1/Bub3 in this network of interactions. Importantly, Bub1 was not required for these interactions, as co-precipitating levels of Knl1 were unaffected in lysates from mitotic cells in which Bub1 had been efficiently depleted (Figure 38 C). Consistent with Bub1 not being required, removal or mutations of the KI motifs from Knl1$^{1-250+C}$, which were shown to reduce significantly the interactions with Bubs proteins (Figure 29 B), did not alter Knl1 levels (Figure 38 D).

To better understand the nature of these interactions, we also compared the ability of deletion constructs derived from the Knl1$^{1-728+C}$ chimeras to pull-down Knl1 and Hec1 (Figure 38 E). Deletion of the first 250 residues (Knl1$^{1-728+C\ \Delta250}$), but not of 138-250 (Knl1$^{1-728+C\ \Delta138-250}$), from Knl1$^{1-728+C}$ resulted in an evident drop in the amounts of Knl1 and Hec1, corroborating the view that the first 137 residues of Knl1 are crucial for the binding of KMN components.

Overall, our results unveil a new role of Knl1$^{1-250}$ in promoting interactions with the KMN components. They also suggest that this function requires the very N-terminus of Knl1$^{1-250}$, in a Bub1-independent fashion.

Discussion

In my doctoral work, I have addressed how Bub proteins are recruited to kinetochores and in particular to Knl1. In the course of the work, two still unpublished and partially complementary studies in human cells carried out in the laboratories of Prof. Geert J.P.L Kops and Prof. Jakob Nilsson (Vleugel et al., 2013; Zhang et al., 2013) became available to us in an effort to coordinate publication.

In the next session, I will describe the implications of my studies on the kinetochore recruitment of Bub1, BubR1 and Bub3 proteins and on SAC signaling at the kinetochore, also in the light of the abovementioned unpublished works.

The kinetochore-binding domain of Bub1 and BubR1

Previous studies have recognized both the TPR and the Bub3-binding domains as the elements that specify kinetochore localization of Bub1 and BubR1 (Elowe et al., 2010; Kiyomitsu et al., 2011; Kiyomitsu et al., 2007; Klebig et al., 2009; Malureanu et al., 2009; Taylor et al., 1998). However, the contributions of these two domains to the recruitment process have remained elusive. Our analysis has resolved this controversy supporting early models proposing that the Bub3-binding domain of Bub1 and BubR1 is necessary and sufficient for kinetochore recruitment (Taylor et al., 1998).

The TPR domains of human Bub1 and BubR1, which share a highly conserved three-dimensional structure (Bolanos-Garcia et al., 2011; Krenn et al., 2012), have been proposed to participate in the recruitment process via their interaction with the KI motifs of human Knl1 (Kiyomitsu et al., 2011; Kiyomitsu et al., 2007). Consistent with this idea, the complex of the TPR domain of Bub1 and BubR1 with KI1 and KI2 motif, respectively, can be reconstituted *in vitro* (Bolanos-Garcia et al., 2011; Krenn et al., 2012). Moreover, recent structural analysis of such complexes has unveiled that the KI-binding interface is located on the convex surface of the TPR repeats, revealing a common but unusual mode of interaction. Consistent with the

structural evidence, we have shown that, at least in the case of Bub1, the KI-binding interface is crucial for the interaction with Knl1 also in cells. The identification of such an interface within the TPR structures enabled us to specifically assess the contribution of this interaction to the recruitment process, without resorting to deletion constructs of Bub1 and BubR1. Impairment of the interaction of the TPR with the KI motif turned out to be insufficient to alter the kinetochore levels of Bub1 and BubR1. Our results strongly imply that the interaction of TPR domains with their KI motifs is not crucial for the recruitment of Bub1 and BubR1 to kinetochores. Moreover, our deletion studies rule out any contribution of the TPR domain itself, besides its interaction with KI motifs. Our analysis of the requirements for BubR1 recruitment to kinetochores is also in line with previous studies showing that BubR1(1–203) or BubR1(1–363) is unable to bind kinetochores, whereas BubR1(357-1052), lacking the TPR region, localizes normally (Elowe et al., 2010; Malureanu et al., 2009). Overall, the available evidence supports the unifying theme that the TPR regions of Bub1 and BubR1 are dispensable for kinetochore recruitment and that the residues that specify kinetochore recruitment are positioned outside this region. Similarly, the checkpoint kinase Mps1 contains a TPR domain, whose structure is very similar to those of Bub1 and BubR1 (Nijenhuis et al., 2013), despite significant sequence divergence. Importantly, Mps1 TPR domain contributes only marginally to the affinity of Mps1 for kinetochores (Nijenhuis et al., 2013), supporting the common theme that TPR domains in SAC kinases are not crucial determinants for kinetochore binding.

We have demonstrated that, at least for the case of Bub1, a minimal kinetochore-binding domain could be identified. The fragment of Bub1 encompassing residues 209-270 and including the Bub3-binding domain provides the bulk of the affinity required for kinetochore binding, likely through concomitant interactions mediated by Bub3. Recently, three independent studies have unveiled that phosphorylated MELT repeats on Knl1 are the crucial sites for Bub1 and BubR1 kinetochore recruitment in different species (London et al., 2012; Shepperd et al., 2012; Yamagishi et al., 2012). Considering this important finding, we envision

that the Bub3-binding domain of Bub1, in complex with Bub3, may recognize phosphorylated MELT repeats (Figure 39). This model is strongly supported by recent work with yeast proteins, performed in our laboratory [and currently accepted for publication (Primorac et al., 2013)]. This study describes the crystal structure of a synthetic phospho-MELT peptide in complex with Bub3 and with the Bub3-binding domain of Bub1 (the yeast equivalent of

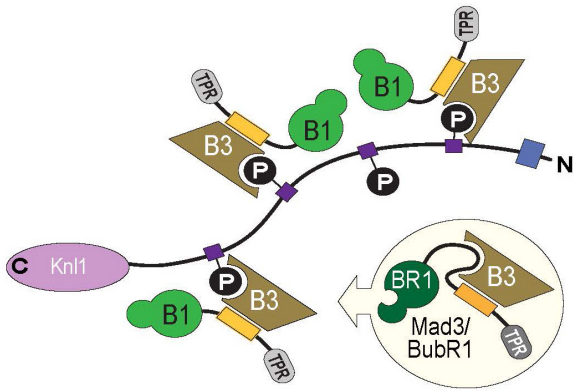

Figure 39 Recruitment of Bub1 to phosphorylated MELT repeats through the function of Bub3
Model of the putative binding of Bub1/Bub3 to phosphorylated MELT repeats of Knl1. For simplicity, only 4 MELT repeats are depicted and KI motifs have been excluded. The yellow box indicates the Bub3-binding domain. TPR, tetratricopeptide repeats; B3, Bub3; B1, Bub1; BR1, BubR1; P, phosphate, N, N-terminus. Adapted from (Primorac et al., 2013).

human Bub1$^{209-270}$) and identifies an extraordinarily well-conserved region on the side of the β-propeller of Bub3 as the phospho-MELT receptor (Primorac et al., 2013) (Figure 40 A).

Moreover, we have demonstrated that residues neighboring the Bub3-binding domain of Bub1, in particular in the N-terminal extension, are important to modulate the affinity of Bub1 for kinetochores. This is in line with Bub1 and Bub3 being reciprocally required for efficient recruitment (Logarinho et al., 2008; Meraldi et al., 2004; Sharp-Baker and Chen, 2001; Taylor et al., 1998; Vigneron et al., 2004). We speculate that Bub1 may contribute to the binding of Bub3 to phosphorylated MELT motifs. Consistent with this idea, it has been recently shown that the Bub3-binding domain of yeast Bub1 increases the affinity of Bub3 for a phosphorylated MELT peptide of ~ 10 fold (Primorac et al., 2013). It is likely that Bub1 may stabilize the phosphate of the MELT through positively charged residues located in the

N-terminal extension of the Bub3-binding domain of Bub1, as suggested by the recent structure (Figure 40 B and C, R314 and K315 of yeast Bub1) (Primorac et al., 2013).

Overall, we believe that, while residues in the *bona fide* Bub3-binding domain define the strength of the interaction with Bub3, residues located in the N-terminal extension of the Bub3-binding domain regulate the affinity of Bub3 for phosphorylated MELT motifs.

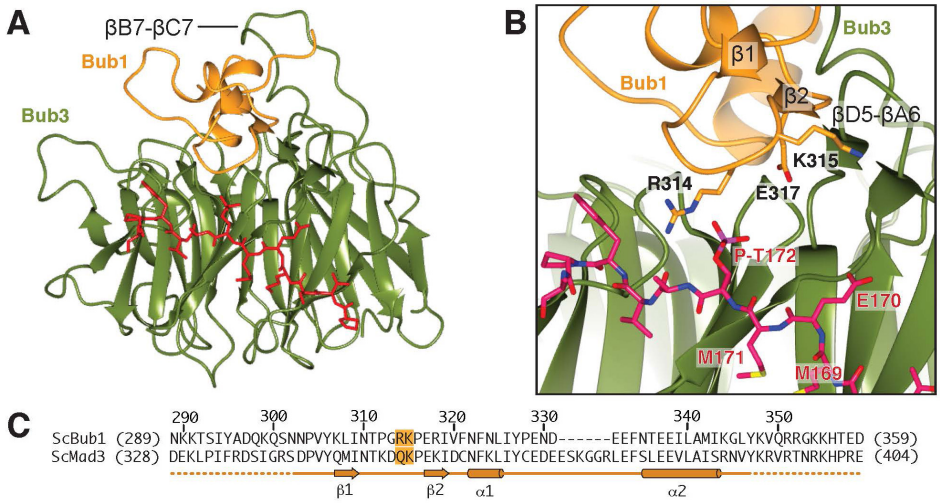

Figure 40 Structure of yeast Bub1/Bub3 in complex with phosphorylated MELT peptide

A) Structure of yeast Bub3, Bub3-binding domain of Bub1 (Bub1$^{289-359}$, including the N-terminal extension) and the phosphorylated MELT peptide (in red) of the yeast Knl1 ortholog Spc105. B) Magnification of the MELT-binding interface showing the loop of Bub1 that contains the N-terminal extension of the Bub3-binding domain. C) Alignment of the yeast Bub1$^{289-359}$ used in the structure and the equivalent sequence of BubR1/Mad3. The bona fide Bub3-binding domain of yeast Bub1 contains residues 315-356. Adapted from (Primorac et al., 2013).

Like in the case of Bub1, the Bub3-binding domain of BubR1 and its interaction with Bub3 are crucial for kinetochore localization (Elowe et al., 2010; Lara-Gonzalez et al., 2011; Malureanu et al., 2009). We suspect that the Bub3-binding domain of BubR1 may be even sufficient for localization, as indicated by our preliminary studies (not shown). As Bub3 is the bona fide MELT reader (Primorac et al., 2013) and the Bub3 moiety is the same in the BubR1/Bub3 and Bub1/Bub3 complexes, these findings allude to the possibility that the Bub3-binding domain of BubR1, in complex with Bub3, might also recognize phosphorylated MELT motifs. Our work suggests the residues in the N-terminal extension preceding the Bub3-binding domain of Bub1 and possibly BubR1 are important for the binding affinity for

kinetochores. An important implication of this model is that differences in the N-terminal extension of the Bub3-binding domains may account for differences in the affinities for phosphorylated MELT repeats. Unlike Bub1, the N-terminal extension of BubR1 contains negatively charged residues that might impair the ability of Bub3 to bind to the phosphate of the MELT sequence (See Figure 40 C for the alignment of the Bub3-binding domain of yeast Bub1 and BubR1/Mad3. Note that Asp352 of ScMad3 occupies the position of Gly313 in ScBub1). We therefore suspect that, in the BubR1/Bub3 complex, the N-terminal extension might suppress the ability of Bub3 to function as MELT reader and that binding of BubR1/Bub3 to MELT repeats at the kinetochores might require the loss of such inhibition (Figure 39). Moreover, as BubR1 localization requires Bub1 in addition to Bub3, it will be interesting to assess whether Bub1 may be important for the relief of such inhibition. In the future, additional studies are needed to confirm this hypothesis and unravel the molecular mechanisms that account for the distinct behaviors of Bub1 and BubR1 at the kinetochore.

Functions of the TPR domain of Bub1

The TPR region of Bub1 has been previously shown to be important for checkpoint function in fission yeast and human cells (Kiyomitsu et al., 2007; Klebig et al., 2009; Vanoosthuyse et al., 2004). However, it is unlikely that this reflects a requirement for the interaction of the Bub1 TPR region for KI1, as KI motifs are absent in fission yeast Spc7/Knl1. Rather, the Bub1 TPR might engage in other interactions with downstream partners of Bub1, in line with Bub1 being a scaffold at the kinetochore and with the idea that TPR domains mediate protein-protein interactions. Consistent with this view, conserved residues of the TPR of Bub1, outside the KI-binding pocket, might provide a binding site for another ligand or for an intra-molecular interaction (Krenn et al., 2012).

Bub1 interacts with BubR1 in yeast two-hybrid assays (Kiyomitsu et al., 2007), but this interaction could not be reconstituted *in vitro* with purified components (Bolanos-Garcia et al.,

2009). This interaction is in turn believed to be crucial for BubR1 recruitment to kinetochores (Fernius and Hardwick, 2007; Klebig et al., 2009; Perera et al., 2007; Sharp-Baker and Chen, 2001). Our findings indicate that the TPR domain of Bub1 is dispensable for BubR1 recruitment, arguing against the idea that Bub1 binds BubR1 via its TPR region. Additionally, our observation that a BubR1 mutant devoid of the TPR repeats decorates kinetochores effectively strongly suggests that the TPR region of BubR1 is not required for the interaction with Bub1. These data are consistent with the physical interaction between TPR-deleted versions of human Bub1 and BubR1 in yeast-two hybrid experiments (D'Arcy et al., 2010). Rather, our data imply that the determinants for this interaction are positioned outside the TPR region in both Bub1 and BubR1. Consistent with this, a conserved segment of Bub1, named conserved domain I (CDI, see Figure 6), has been implicated in BubR1 recruitment (Klebig et al., 2009) but whether it interacts directly with BubR1 is undemonstrated. Future studies are required to clarify how Bub1 and BubR1 interact with each other.

Another crucial interaction entertained by Bub1 is the one with the Mad1/Mad2 complex (Brady and Hardwick, 2000; Kim et al., 2012). Like in the case of BubR1, preliminary data rule out a contribution of the TPR domain of Bub1 in the recruitment of Mad1 to the kinetochores (not shown). Altogether, our data converge to the theme that the TPR domain of Bub1 does not mediate interactions with checkpoint proteins and that other regions of Bub1 may account for its function as a scaffold for the kinetochore recruitment of downstream components.

We have provided evidence that the TPR domain of Bub1 regulates its kinase activity, likely through residues that locate outside the KI-binding pocket of the TPR. Consistent with this role, the TPR domain is also required for the proper phosphorylation of H2A *in vivo* (data not shown) and very similar conclusions have been drawn by Ricke and colleagues (Ricke et al., 2012). Whether the TPR domain regulates an intra-molecular interaction required for full kinase activity or, rather, interacts with another factor is unclear. Structural analysis of the kinase domain of Bub1 suggested that intra-molecular conformational changes might regulate

the catalytic activity (Kang et al., 2008), supporting the former possibility. Interestingly, TPR domains have been shown before to participate in intra-molecular interactions. For example, the N-terminal TPR domain of the checkpoint protein Mps1 has been recently suggested to mediate an intra-molecular interaction with an N-terminal extension preceding the TPR itself (Nijenhuis et al., 2013). Moreover, the N-terminal TPR of protein phosphatase 5 (PP5) has been implicated in intra-molecular regulation of the catalytic activity of the C-terminal phosphatase domain (Yang et al., 2005). It is therefore likely that the N-terminal region of Bub1 influences the activity of the kinase domain at the C-terminal through intra-molecular interactions. However, whether this occurs by releasing the previously identified inhibitory mechanism (Kang et al., 2008) is currently unknown. Alternatively, the TPR domain may engage an additional factor that is required for full activity or for the inhibition of a co-purifying phosphatase. Interestingly, Bub1 and the PP1 phosphatase are both recruited to Knl1 in cells (Liu et al., 2010; Meadows et al., 2011; Rosenberg et al., 2011). It will be interesting to assess whether the TPR domain of Bub1 is indirectly regulating the kinase output by influencing the activity of PP1. Finally, *in vitro* reactions with recombinant kinases and purified components will help to clarify the role of the TPR domain in the modulation of Bub1 activity.

Bub1 is believed to be an active kinase (Kang et al., 2008). Our observation that Bub1/Bub3 complexes purified from mammalian or insect cell lysates are active in *in vitro* kinase reactions supports this idea. It has been proposed that Bub1 kinase activity is enhanced specifically on unattached chromosomes (Chen, 2004), possibly by conformational changes triggered by kinetochore binding. Our results, albeit incomplete, on the activity of Bub1/Bub3 in the presence of Knl1 fragments, which are supposed to induce and mimic kinetochore binding (Figure 19), seem to argue against this model. Future studies are required to understand if and how Bub1 kinase activity is specifically regulated at the kinetochores.

The TPR region of Bub1 has been previously shown to be important for checkpoint function (Vanoosthuyse et al., 2004; Klebig et al., 2009; Kiyomitsu et al., 2007). It is unlikely that this

reflects the role of the TPR domain in the regulation of the kinase, as the kinase activity of Bub1 might not be required for the checkpoint (Fernius and Hardwick, 2007; Klebig et al., 2009; Perera et al., 2007; Sharp-Baker and Chen, 2001). Moreover, it does not reflect the role of TPR domain as a scaffold for BubR1 and Mad1, as discussed above. Additional work is needed to elucidate the functions of the TPR domain of Bub1 in checkpoint signaling.

The role of MELT repeats in Bubs recruitment

Recent publications have suggested that phosphorylated MELT repeats of Knl1 are the crucial sites for Bub1 and BubR1 kinetochore recruitment by docking their partner Bub3 (London et al., 2012; Primorac et al., 2013; Shepperd et al., 2012; Yamagishi et al., 2012). In line with this model, we have demonstrated that: i) distinct fragments of Knl1 containing MELT repeats are able to target Bub1 and BubR1 to ectopic sites in the cells; ii) segments of Knl1 containing at least one MELT repeat associate with Bub1, Bub3 and BubR1; iii) Knl1 chimeric constructs containing several MELT repeats promote the localization of Bub1 and BubR1 to kinetochores.

Additionally, single MELT repeats act as independent docking stations for the Bub1/Bub3 complex in yeast (Primorac et al., 2013). Our finding that a fragment of Knl1 containing one MELT repeat ($Knl1^{1-250}$) binds Bub1, BubR1 and Bub3 and drives the assembly of SAC complexes suggests that this might be true also in higher organisms. However, we have shown that the $Knl1^{1-250+C}$ chimera, despite harboring one MELT repeat, did not rescue significant levels of Bub1 and BubR1 at kinetochores. As a single Bub1/Bub3 complex may be recruited to $Knl1^{1-250}$, we theorize that the signal generated by one Bub1/Bub3 molecule per Knl1 chimera might be too weak to be detected. Interestingly, when the same region of Knl1 is targeted to centrosomes, localization of Bub1 and BubR1 becomes detectable. We speculate that the Bub1 and BubR1 signals at centrosomes harboring $Knl1^{1-250}$ likely reflect larger numbers of the GFP-$Knl1^{1-250}$-Plk4 receptor on these structures relative to the number of

Knl1$^{1\text{-}250+C}$ molecules available at kinetochores. Binding of Bub proteins to MELT repeats is very sensitive to dephosphorylation (London et al., 2012). However, we exclude that discrepancies between kinetochore and centrosome recruitment reflect differences in phosphatase activity at these sites, as inhibition of phosphatase activity did not improve Bub1 and BubR1 signals at kinetochores harboring Knl1$^{1\text{-}250+C}$ molecules (data not shown). Overall, our data lend support to the model (London et al., 2012; Primorac et al., 2013; Shepperd et al., 2012; Yamagishi et al., 2012) that isolated MELT repeats may act as independent docking sites that contribute to the overall enrichment of Bub1, Bub3 and BubR1 at the kinetochore.

Whether the numerous MELT repeats present in Knl1 are equivalent in their ability to bind Bub1/Bub3 is unclear, but it is expected that sequence variation around the conserved consensus might influence the binding affinity for Bub1/Bub3. In a recent study, we have showed that synthetic peptides encompassing a single MELT repeat from *Saccharomyces cerevisiae* engage in interactions with Bub1/Bub3 with K_Ds in the sub-micromolar range (Primorac et al., 2013). Thus, we suspect that individual MELT repeats have the ability to engage in relatively tight interactions with Bub1/Bub3. This sets the expectation that multiple MELT repeats will be able to recruit multiple Bub1/Bub3 molecules. The localization studies in the presence of Knl1 chimeras presented here, albeit unsystematic, are consistent with this hypothesis, as they show that the abundance of Bub1 and BubR1 at kinetochores of Knl1-depleted cells correlates with the number of MELT modules contained in the rescue constructs. However, our finding that Knl1 fragments containing a comparable number of MELT repeats leads to unequal ectopic recruitment of Bub1 and BubR1 (Figure 22) alludes to the possibility that MELT repeats may not be equivalent in their ability to dock Bub1/Bub3 and BubR1/Bub3 complexes. Consistently, it has been reported that that Knl1 constructs harboring a low number of MELT repeats (four or six) rescue Bub1 and BubR1 signals to levels similar to the full-length Knl1 molecule (which carries 19 repeats), indicating that not all MELT repeats are actually 'functional' (Vleugel et al., 2013; Zhang et al., 2013). Whether this activity depends on the levels of phosphorylation or, rather, on differences in MELT residues

is unclear. Indeed, human MELT repeats include several conserved residues in addition to the Met-Glu-Leu-Thr consensus (see alignment of MELT repeats in Figure 21 C). We have shown that deletion of the whole MELT repeat affects the binding to Bub proteins more drastically than the ADLA mutation (Figure 29 C and Figure 30 A). We therefore speculate that residues flanking the consensus might modulate the affinity for Bub1/Bub3 binding. Consistent with this idea, the conserved TxxF motif that precedes Met-Glu-Leu-Thr consensus (see alignment of MELT repeats in Figure 21 C) has been recently reported to be required for ectopic recruitment of Bub1 and BubR1 (Vleugel et al., 2013). Understanding whether individual MELT repeats have different affinities for Bub1/Bub3 and the identification of the determinants for such differences will require a more systematic analysis of MELT-Bub1/Bub3 interactions.

According to recent reports (London et al., 2012; Shepperd et al., 2012; Yamagishi et al., 2012), binding of Bubs to the MELT repeats is phosphorylation dependent, as it relies on the phosphorylation of Thr/Ser at position 4 of the Met-Glu-Leu-Thr sequence. Our finding that mutations of the Met151 and Thr154 of MELT1 into alanine (ADLA mutant) (Figure 30) reduce the binding affinity of Bub proteins is consistent with this idea. However, we have no evidences that Thr154, either in our construct or in endogenous Knl1, is phosphorylated *in vivo* (Dephoure et al., 2008; Hegemann et al., 2011; Nousiainen et al., 2006; Yamagishi et al., 2012). Interestingly, human MELT repeats, unlike the yeast counterparts, harbor additional conserved Ser and Thr at position 6 and 8 respectively (Figure 21 B and C), suggesting that phosphorylation on residues others than Thr in position 4 might influence the binding affinity for human Bub1/Bub3.

Dephosphorylation of MELT motifs might be crucial to regulate the overall levels of Bub1 and BubR1 at the kinetochore. Human PP1 phosphatase has been implicated in MELT de-phosphorylation (London et al., 2012; Rosenberg et al., 2011; Yamagishi et al., 2012), as it docks to the RVSF motif of N-terminal Knl1 (Liu et al., 2010). Consistently, we have shown that PP1 precipitates with the N-terminus of Knl1 ($Knl1^{1-250}$) in a RVSF-dependent manner.

Importantly, its binding does not seem to be affected by the presence of Bub1, BubR1, Bub3, indicating that the PP1 recruitment to Knl1 might be Bubs-independent. Consistent with its role in MELT dephosphorylation, removal of PP1-binding site is expected to increase Bub1 and BubR1 levels due to increased phosphorylation of MELT repeats. Consistently, it has been shown recently that removal of the PP1-binding site from full-length Knl1 led to a ~ 3 fold increase in Bub1 and BubR1 kinetochore levels (Zhang et al., 2013). In contrast with this, when we deleted the PP1-binding domain from Knl1$^{1\text{-}728+C}$ no increase in Bub1 kinetochore signals was observed (and only a modest increase for BubR1). In line with our data, mutations in the PP1-docking site of KNL-1 do not affect BUB-1 targeting in *C. elegans* (Espeut et al., 2012). The reasons for these discrepancies are currently unclear.

The identification of the exact phosphorylated sites within the human MELT sequences and reconstitution of the interactions with single phosphorylated MELT repeats will help to elucidate the phospho-dependency of the binding mechanism in detail. As the number and the sequence of these modules vary extensively across species (Vleugel et al., 2013), future studies will help to clarify the species-specific differences in the mechanism of recruitment of Bub proteins.

The role of KI motifs in Bubs recruitment

We have provided evidence that a unique combination of sequence motifs allows the N-terminal region of Knl1 to establish robust interactions with Bub1, Bub3 and BubR1. This implies that in the N-terminus of Knl1, the combination of MELT repeat and KI motifs forms a higher affinity site for Bub1/Bub3 than those represented by isolated MELT repeats. The molecular basis for the special behavior of the N-terminal region of human Knl1 stems from the ability of MELT1 and the neighboring KI1 and KI2 motifs to cooperate towards the assembly of a tight complex encompassing Knl1, Bub1/Bub3, BubR1/Bub3 and other checkpoint components. As the KI1 and KI2 motifs engage the TPR regions of Bub1 and

BubR1 (Bolanos-Garcia et al., 2011; Kiyomitsu et al., 2011; Krenn et al., 2012), we speculate that this high affinity might be generated via a cooperative mechanism based on the enforced proximity of two interactions, one of the MELT repeat with Bub3-binding domain of Bub1 in complex with Bub3, and one of the KI motifs with the TPR domain of Bub1 (Figure 41).

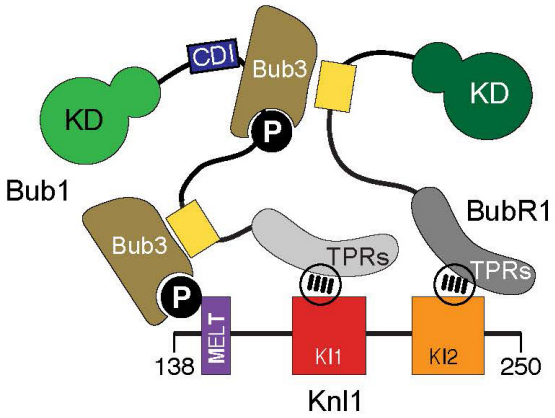

Figure 41 Mechanism of binding of Bub proteins to Knl1 N-terminus

Model of the binding of Bub1, BubR1, Bub3 to Knl1$^{138-250}$. TPRs, tetratricopeptide repeats; CDI, conserved domain 1; KD, kinase domain; P, phosphate.

This model is strongly supported by *in vitro* evidence indicating that purified Bub3/Bub1$^{1-280}$ (which includes the Bub3-binding domain and TPR) bound to a Knl1 fragment containing both MELT1 and KI1 with enhanced affinity compared to a Knl1 fragment encompassing the MELT1 only (Ivana Primorac, data not shown). We infer from these data that KI1 and KI2 motifs act as MELT enhancers by stabilizing Bub1/Bub3 binding to MELT1. Whether the KI1 and KI2 motifs can enhance the binding of Bub1/Bub3 to MELT motifs other than MELT1 in full-length Knl1 is currently unclear.

Collectively, our results provide a molecular explanation for our previous observation that mutations in the KI1-binding region of the Bub1 TPR weakened the interaction of the mutated Bub1 with kinetochore subunits in IP assays (Figure 10 D). It might seem puzzling that the same Bub1 mutants decorated kinetochores to levels that were indistinguishable from those of wild type Bub1 (Figure 12 and Figure 13). Consistently, deletion of the MELT1+KI1+KI2 array (our evidence) or deletion of KI1 (Yamagishi et al., 2012) from Knl1

did not affect substantially the recruitment of Bub1 to kinetochores. We suspect that at its steady state cellular concentration Bub1 saturates the multiple phosphorylated MELT repeats of Knl1. We speculate that for this reason, the increase in binding affinity promoted by the MELT1-KI1-KI2 combination, which likely increases the average occupancy over time of the MELT1 sequence, does not reflect in measurable differences in the overall kinetochore signal of Bub1, which reflects binding to many additional MELT repeats. Such increase in binding affinity, however, becomes evident under conditions of dilution and non-equilibrium associated with cell lysis and protein precipitation.

The robustness of the MELT1-KI1-KI2 constellation of motifs is also evident when testing the ability of the single MELT1 sequence to sustain the checkpoint after fusion of $Knl1^{1-250}$ to the kinetochore-targeting domain at the C-terminus of Knl1. In this case, the presence of KI1 and KI2 is important for a robust checkpoint response, suggesting that the occupancy of the MELT1 site influences the strength of the checkpoint signal it contributes to produce. Similarly, Vleugel and colleagues (Vleugel et al., 2013) has proven the requirement of KI1 motif for SAC function in the context of a chimeric Knl1 matching almost exactly our $Knl1^{1-250+C}$ construct.

So far, KI1 and KI2 have only been identified in vertebrate Knl1 orthologs (Bolanos-Garcia et al., 2011; Kiyomitsu et al., 2011), where they provide an anchor point for Bub1/Bub3 complexes, in addition to the Mps1-dependent MELT recruitment. Conversely, in lower organisms kinetochore recruitment of Bub1 and BubR1 is likely to rely exclusively on MELT sites. As enhancers of the function of the ubiquitous MELT motifs, the KI1 and KI2 motifs might serve as a Mps1-independent pathway that cooperates with MELT repeats to recruit Bubs to the kinetochore. However, the advantage of having both pathways in vertebrates remain unclear.

BubR1 recruitment to Knl1

Like Bub1, BubR1 recruitment has been suggested to rely on phosphorylated MELT repeats (Yamagishi et al., 2012). Our analysis of the association of BubR1 to Knl1$^{1-250}$ (Figure 29) is consistent with this idea. However, Bub1 is bound to MELT repeats and is required for BubR1 recruitment, thus raising the question whether the MELT dependency of BubR1 reflects direct binding to the MELT module or, rather, to Bub1. As already anticipated in the discussion, in the BubR1/Bub3 complex the function of Bub3 as a MELT reader might be suppressed, arguing against the former scenario. Moreover, the fact that deletion of the KI2 from Knl1 N-terminus prevents BubR1 binding but does not enhance Bub1 binding speaks against the possibility that BubR1 may compete with Bub1 for the binding to MELT repeats. Rather, these data allude to the possibility that BubR1/Bub3 may directly associate with Bub1/Bub3 pre-bound to phosphorylated MELT. This model is strongly supported by the fact that Bub1 and BubR1 interact with each other (D'Arcy et al., 2010; Kiyomitsu et al., 2007). As the Bub3-binding domain of BubR1 is required for kinetochore binding, we speculate that BubR1/Bub3 might recognize a phosphorylated site on Bub1 via its Bub3-binding domain in complex of Bub3 (Figure 41). Moreover, as Bub1 and BubR1 seem to interact in a TPR-independent manner (our evidence), this site of Bub1 might be positioned outside the TPR region (Figure 41). Additionally, as the TPR of BubR1 interacts with KI2 motif of Knl1 (Bolanos-Garcia et al., 2011; Kiyomitsu et al., 2011; Krenn et al., 2012), we propose that, at the N-terminus of Knl1, BubR1 entertains at least two interactions: one is mediated by its TPR domain with the KI2 of Knl1 and one by the Bub3-binding domain with Bub1 (Figure 41). An implication of this model is that deletion of the KI2 from the Knl1 arrangement is expected to decrease (but not prevent) the binding of BubR1, thanks to the direct interaction of BubR1 with Bub1. Our results showing that cells expressing that Knl1$^{1-250+C}$ with deletion or mutation the KI region could mount a less robust checkpoint compared to Knl1$^{1-250+C}$, is consistent with this model.

Loss of the MELT1 and KI motifs from the Knl1$^{1-728+C}$ chimeras resulted in a modest but evident decrease in the levels of BubR1 at the kinetochore, while no effect was observed for Bub1 (Figure 32), indicating that MELT1 and KI arrangement might be more relevant for the kinetochore association of BubR1 than Bub1. However the significance of this remains unclear.

We have shown that Knl1$^{1-250}$ precipitates not only with Bub1/Bub3 and BubR1, but also with Cdc20. While Bub1 is required for Mad1 and Mad2, it is likely that BubR1 may be crucial for Cdc20 association, as BubR1 interacts with Cdc20 directly (Fang, 2002; Hardwick et al., 2000; Sudakin et al., 2001). Importantly, our results indicate that the binding of BubR1 to Knl1 N-terminus and therefore to Bub1 is compatible with the ability of BubR1 to interact with Cdc20. Additional experiments are needed to assess if and how Knl1 and/or Bub1 binding

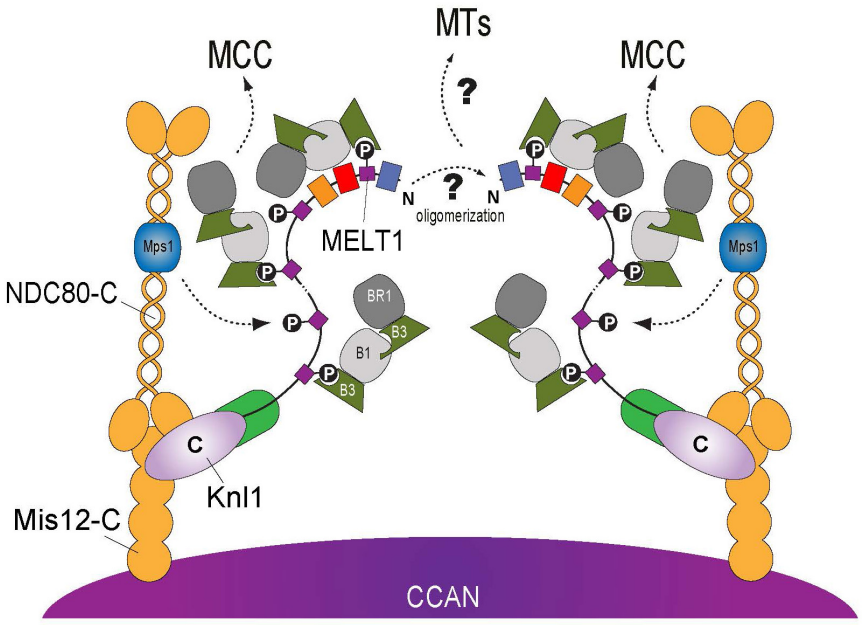

Figure 42 Overview of Bubs recruitment to the kinetochore

Schematic of Bub1, BubR1 and Bub3 recruitment to the kinetochore. Briefly, Knl1, in complex with Zwint-1 (in green), is associated with the Mis12 complex (Mis12-C) and the NDC80 complex (NDC80-C). Mps1 is recruited to NDC80 complex and phosphorylates several MELT repeats on Knl1 to recruit Bub1/Bub3 complexes (light gray). At the N-terminus of Knl1, Bub1/Bub3 recruitment is enhanced by the presence of the KI motifs. Bub1/Bub3 recruits, in turn, BubR1/Bub3 complexes (dark gray) to promote the formation of the MCC. Oligomerization of Knl1 molecules, possible mediated by the N-terminus, may position the KMN molecules in a way that maximizes binding to microtubules (MTs). For simplicity, only two KMN complexes and five MELT repeats are shown. N, N-terminus; C, C-terminus; B1, Bub1; B3, Bub3; BR1, BubR1.

affects the ability of BubR1 to interact with Cdc20 and its incorporation into the MCC (Figure 42).

Knl1 role in SAC signaling

Knl1 has emerged in recent years as a crucial platform for checkpoint signaling at the kinetochore (Foley and Kapoor, 2013; Kiyomitsu et al., 2007). Consistently, we have shown that Knl1 depletion results in a checkpoint defect. However, we were surprised to see that this checkpoint defect was only modest (in the absence of the Mps1 inhibitor reversine), as a very dramatic checkpoint failure could be observed previously upon Knl1 RNAi with a different set of siKNL1 oligos (Kiyomitsu et al., 2007). It is likely that this reflects incomplete depletion obtained by the RNAi method, as residual checkpoint phenotype has been also observed recently in two independent studies in human cells (Vleugel et al., 2013; Zhang et al., 2013) using RNAi oligos different for the ones used by us (Kiyomitsu et al., 2007). This implies that residual but undetectable levels of Knl1 are sufficient to sustain the checkpoint and, possibly, that the strong checkpoint defect observed by Kiyomitsu and colleagues might be due to putative off-target effects of Knl1 RNAi on some checkpoint proteins.

We also observed that depletion of Knl1 resulted in a compromised checkpoint response after exposure to taxol and, to a smaller extent, nocodazole, indicating that the Knl1-mediated response is exacerbated when tensionless kinetochores (in taxol), instead of unattached kinetochores (in nocodazole), are present. This behavior has been observed also in the case of inhibition of Aurora B (Ditchfield et al., 2003). Whether this phenotype reflects a partial impairment of Aurora B activity upon Knl1 depletion is unknown.

Knl1 has been proposed to participate in the SAC signaling indirectly, by providing docking sites for several SAC proteins and regulators, such as Bub1/Bub3, BubR1/Bub3 and PP1 (Kiyomitsu et al., 2011; Kiyomitsu et al., 2007; Liu et al., 2010; London et al., 2012; Meadows et al., 2011; Pagliuca et al., 2009; Rosenberg et al., 2011; Shepperd et al., 2012; Yamagishi et al.,

2012). These proteins are is in turn believed to support and modulate downstream SAC signaling events (Foley and Kapoor, 2013; Lara-Gonzalez et al., 2012). Consistently, we show that Knl1 contains SAC assembly sites around the MELT repeats and provides docking sites for Bub1/Bub3 and downstream components. Remarkably, we were able to precipitate Knl1$^{1-250}$ not only with Bub1/Bub3 and BubR1, but also with other checkpoint components, including Mad1, Mad2, and Cdc20. The exact order of recruitment of these components is not certain, but Bub1/Bub3 is likely to be the recruited as first, as Bub1 is recruited to kinetochores in very early prophase, while BubR1 becomes visible there only later (Jablonski et al., 1998; Johnson et al., 2004). Consistently, we have demonstrated that at least some of these interactions with Knl1 N-terminus are dependent on Bub1. It is likely that Bub1 binding is required for Mad1, Mad2 and BubR1, which in turn may be crucial for Cdc20 association. Overall, our analysis corroborates the view that the role of Knl1 in the checkpoint function is indirect, promoting the association of Bub1/Bub3 to favor downstream events.

Interestingly, we observed a shortening of the mitotic arrest when we deleted the N-terminal 137 residues of Knl1, which includes the microtubule-binding domain and PP1-docking site. It is unlikely that this phenotype is due to loss of PP1 activity, as mutations of the PP1-docking site have been shown to delay mitotic exit (Espeut et al., 2012; Meadows et al., 2011; Rosenberg et al., 2011), consistent with PP1's role as silencer of the checkpoint (Foley and Kapoor, 2013). Similarly, the microtubule-binding domain has been implicated in SAC extinction in *C. elegans*, rather then SAC activation (Espeut et al., 2012). Rather, it indicates that the first 137 residues of Knl1 might be important for the regulation of the recruitment of other checkpoint proteins. The fact that it contains an Aurora B phosphorylation site (Liu et al., 2010) makes Aurora B a likely candidate. Whether Knl1 contains low affinity sites for Aurora B or other checkpoint proteins, other than Bub1/Bub3 or BubR1/Bub3, is unknown. The identification of such sites, together with the current knowledge of the function of MELT repeats, will allow the creation of separation of function mutants that could be used eventually to discriminate between indirect and direct roles of Knl1 in SAC signaling.

The existence, in all eukaryotes, of multiple repeated and independent modules in Knl1 may provide a molecular explanation for the robustness of the checkpoint response. However, our studies indicate that the function of Knl1 to mount a SAC response is independent from its protein length and from the number of recruitment modules, as cells expressing a Knl1 chimera containing one MELT repeat establish a checkpoint response as strong as cells expressing a longer Knl1 construct including 10 MELT motifs. Moreover, our data indicate that one MELT repeat is sufficient to generate a checkpoint response, indicating that low levels of Bub1/Bub3 at the kinetochore are sufficient for the checkpoint. This is consistent with recent similar studies in human cells (Vleugel et al., 2013; Zhang et al., 2013) and with the previous observation that *D. melanogaster* larvae expressing N-terminal and C-terminal fusion of Knl1/Spc105, where only two MELT repeats are present, are completely viable (Schittenhelm et al., 2009). Moreover, this is also consistent with previous finding that cells depleted for Bub1 but with low residual levels were able to mount a robust checkpoint (Johnson et al., 2004; Meraldi and Sorger, 2005). As anticipated before, we speculate that one MELT repeat binds one molecule of Bub1/Bub3 and one molecule of BubR1/Bub3 and Cdc20 that amplifies the checkpoint signaling, possibly via a cytosolic loop. Therefore, the SAC robustness, rather than arising from the MELT module itself, might arise from the signaling cascade downstream to Bub1/Bub3, but additional work is needed to understand how this can be achieved.

The existence of multiple and independent MELT repeats in Knl1 raises the question whether MELT repeats might suffer from some position effect within Knl1 molecule. Indeed, co-localization of the checkpoint proteins, together with their relative positions, within the kinetochore structure is crucial for SAC signaling, as suggested recently (Maldonado and Kapoor, 2011). For instance, BubR1:Cdc20 and Mad2:Cdc20 complexes need to come in close contact in order to be efficiently incorporated in the MCC. Whether distinct BubR1/Bub3 complexes docked onto different MELT repeats are equipotent in reaching

Mad2:Cdc20 is currently unknown. Moreover, recruitment of PP1γ to kinetochore-bound Knl1 is required for checkpoint silencing and for the removal of checkpoint proteins from the kinetochore (Funabiki and Wynne, 2013; London et al., 2012; Rosenberg et al., 2011; Wu et al., 2009). Therefore, all these interactions are likely to be controlled by PP1 activity, indicating that the relative positions of SAC complexes and PP1 might be crucial for efficient silencing. Comparative analysis of MELT repeats in equivalent positions within Knl1 sequence will help to clarify these questions about checkpoint regulation.

Role of Knl1 in chromosome alignment

Beside its regulatory function, Knl1 has also been implicated in kinetochore-microtubule attachments (Cheeseman et al., 2006; Espeut et al., 2012). Consistent with this role, we have shown that cells depleted for Knl1 exhibit defects in chromosome congression to the metaphase plate, as also observed previously (Kiyomitsu et al., 2007). Remarkably, expression of the C-terminal domain of Knl1 exacerbated the alignment defect of Knl1-depleted cells. This might reflect the displacement of residual levels of Knl1, as previously suggested (Kiyomitsu et al., 2011). However, we observed that most of the cells exhibited major misalignment defects and no clear metaphase could be observed due probably to hyper-stabilization of kinetochore-microtubules attachments. This phenotype is unlikely due to high levels of phosphatase activity, such as PP1 and PP2A, because the regions of Knl1 that recruit PP1 and PP2A locate outside the C-terminal region (N-terminal of Knl1 and MELT/BubR1, respectively) (Espeut et al., 2012; Kruse et al., 2013; Liu et al., 2010; Meadows et al., 2011; Rosenberg et al., 2011; Suijkerbuijk et al., 2012b; Xu et al., 2013). Rather, this phenotype might be due to reduced Aurora B activity. Indeed, Bub1 has been suggested to promote Aurora B activity by promoting CPC enrichment at the centromere via H2A phosphorylation (Fernius and Hardwick, 2007; Kawashima et al., 2010; Perera et al., 2007; Wang et al., 2011; Yamagishi et al., 2010). Importantly, fusion of N-terminal regions to the C-terminal domain of

Knl1 could suppress this phenotype. As each of the N-terminal fusions used contains MELT modules, the amounts of Bub1 recruited to Knl1 might be crucial for Aurora B activity in the destabilization of erroneous kinetochore-microtubule attachments. Additionally, we exclude that the suppression of the misalignment phenotype of Knl1^{C} cells is due to the function of the microtubule-binding domain of Knl1 or PP1-docking sites, as the Knl1$^{1\text{-}728+C\ \Delta 250}$ lacking both motifs was still able to suppress the dominant behavior resulting from expression of the C-terminus of Knl1.

The observation that kinetochore levels of the KMN proteins, especially the Ndc80 complex, are not strongly affected by the absence of Knl1 (Kiyomitsu et al., 2007; Pagliuca et al., 2009) raises the question whether the alignment phenotype observed in Knl1 depleted cells reflects indirect contributions from the checkpoint proteins that are recruited to it, rather than defects in the microtubule-binding activity of the KMN network. Indeed, Bub1 and BubR1 have also been implicated in the regulation of kinetochore microtubule interactions (Ditchfield et al., 2003; Johnson et al., 2004; Lampson and Kapoor, 2005; Meraldi and Sorger, 2005; Suijkerbuijk et al., 2012a; Windecker et al., 2009), in addition to their role in the SAC. Consistently, our complementation experiments with Knl1 chimeras recruiting different amounts of Bub1 and BubR1 indicate that the efficiency of the alignment rescue correlates with the number of MELT modules and the amounts of Bub1/Bub3/BubR1 in an additive fashion. In particular, one MELT module does not seem to be sufficient to sustain robust alignment, despite being very efficient in mounting a SAC response, indicating that the alignment efficiency is very sensitive to the amounts of kinetochore-bound Bubs. The provided evidences therefore reinforce the view that the role of Knl1 in the regulation of kinetochore-microtubule attachments is likely to be indirect, possibly via the recruitment of Bub1/Bub3 and BubR1/Bub3 complexes. However, how Bub1/Bub3 and BubR1/Bub3 can promote the formation of kinetochore/microtubule attachments remain elusive.

In addition to its indirect role, we cannot exclude that Knl1 might also contribute directly to the efficiency of kinetochore-microtubule interactions. As the deletion of the first 137 residues

of Knl1 decreased moderately the efficiency of the rescue, the microtubule-binding domain might be one direct contribution, although it has been shown not to play a significant role in the formation of load-bearing attachments (Espeut et al., 2012). Our complementation experiments, albeit unsystematic, also indicate that the length of Knl1 might be important. As this region of Knl1 might be important for KMN oligomerization (see next paragraph), this may reflect the need for a certain length or flexibility of Knl1 and/or some structural and architectural arrangements of the KMN complexes at the microtubule-binding site. Overall, our results support the idea that Knl1 promotes the efficiency of chromosome alignment both directly and indirectly. In the future, separation of function mutants of Knl1 could be used to further investigate its contributions to kinetochore-microtubule interactions.

Oligomerization of KMN complexes

The KMN complex is composed of 3 different sub-complexes: the Knl1 complex, the Ndc80 complex and the Mis12 complex (Cheeseman et al., 2004; De Wulf et al., 2003; Desai et al., 2003; Liu et al., 2005; Nekrasov et al., 2003; Obuse et al., 2004; Pinsky et al., 2003; Przewloka et al., 2007; Westermann et al., 2003). *In vitro* reconstitution studies and fluorescence methods have suggested that these sub-complexes are present with a 1:1:1 stoichiometry per KMN complex (Cheeseman et al., 2006; Johnston et al., 2010; Petrovic et al., 2010). Moreover, studies of copy number of kinetochore proteins of DT40 chicken cells have estimated ~ 8 KMN molecules per microtubule, for a total number of ~30 KMN complexes per single kinetochore in these cells (Johnston et al., 2010). However, the architecture of the KMN complexes at each microtubule-binding site is unknown.

Here, we have demonstrated that the N-terminus of Knl1 mediates interactions with KMN components, indicating the existence of some level of oligomerization of KMN molecules. So far, this seems a unique feature of the N-terminus of Knl1 as other Knl1 fragments could not precipitate KMN components efficiently, but we cannot exclude that additional regions of

Knl1 may also promote the oligomerization of KMN complexes via similar or distinct mechanisms. Interestingly, oligomerization of Ndc80 complexes, along the microtubule protofilament, has been reported before (Alushin et al., 2010). However, it is very unlikely that the oligomerization that we observed is a result of the microtubule-dependent oligomeric state of Ndc80 complexes, as our experiments were preformed from lysates of cells that had been treated with high doses of the microtubule-depolymerizing drug nocodazole.

We have also demonstrated that within the N-terminus of Knl1, the first 137 residues are crucial for the oligomerization state. As this region is already quite dense of motifs, it is unlikely that this requirement reflects the presence of unidentified functional features. Rather, it suggests that the microtubule-binding domain and/or the PP1 docking site of Knl1 are important. The fact that our interaction studies were carried out with lysates from cells treated with the microtubule- depolymerizing agent nocodazole seems to speak against a role of the microtubule-binding domain, although we cannot exclude that this domain may have functions other than binding to microtubules. Future studies are needed to assess whether the presence or activity of PP1 may regulate the oligomerization of Knl1.

Our data rule out the possibility that oligomerization of KMN complexes is mediated by the Bub proteins and their binding to MELT and KI motifs. Moreover, this oligomerization is not dependent on the activity of the SAC kinases Mps1 and Aurora B (not shown), reinforcing the idea that checkpoint signaling might not be relevant for the oligomerization of KMN complexes. Rather, this may reflect a structural feature of the kinetochore architecture.

As Knl1 is the most enriched KMN component in our oligomerization studies, it is tempting to speculate that oligomerization of KMN complexes might be achieved through oligomerization of Knl1 molecules. Indeed, a large oligomeric state has been observed before for recombinant *C. elegans* Knl1 (Espeut et al., 2012). We suspect that the N-terminus of Knl1 may establish some intra or inter-molecular interactions with another segment of Knl1 (Figure 42). However, these putative interactions could not be reconstituted *in vitro* with fragments of Knl1 encompassing its N- and C-terminus (Jenny Keller and Ivan Primorac, personal

communication), arguing against this possibility. However, the affinity of such interactions might be very low and therefore difficult to be observed in reconstitution experiments. Moreover, we cannot exclude that the N-terminus of Knl1 may entertain interactions with residues that map outside the C-terminal domain of Knl1. Future experiments are needed to understand the molecular mechanism of the oligomeric state of KMN complexes and its relevance for the architecture of KMN complexes at kinetochore sites.

In conclusion, we have taken major steps in unraveling the intricate mechanism of recruitment of Bub1, BubR1 and Bub3 checkpoint proteins to kinetochore structures. We hope this analysis will pave the way for a deeper understanding of the molecular mechanisms through which the spindle assembly checkpoint prevents genetic instability.

Material and Methods

Plasmids for mammalian expression

All plasmids (except the one used in Figure 9 D) were derived from the pcDNA5/FRT/TO vector (Invitrogen). The control plasmid for GFP expression was created by amplifying the GFP sequence from pEGFP-C1 (Clontech) and cloning it into the pcDNA5/FRT/TO vector (Invitrogen) previously modified to carry an internal ribosomal entry site (IRES) sequence, to obtain the pcDNA5/FRT/TO GFP-IRES vector. This vector was then used for subsequent cloning steps. To create all N-terminally-tagged GFP fusions, KNL1 fragments were amplified by PCR from a full-length human KNL1 cDNA (isoform 2), a gift from M. Yanagida (University of Kyoto, Kyoto, Japan) and sub-cloned in frame with the GFP tag. To generate PLK4 fusions, the sequence encoding for the centrosome localization domain of human Plk4 (Plk4 CLD, residues 475-970) was amplified by PCR from human PLK4, a gift from Monica Bettencourt-Dias (Instituto Gulbenkian de Ciência, Oeiras, Portugal), and cloned into pCDNA5/FRT/TO-GFP-IRES. KNL1 fragments were then cloned between the GFP and PLK4 CLD sequences. To generate C-terminally tagged KNL1-GFP constructs, the DNA sequence encoding residues 1834-2316 of Knl1 was amplified by PCR and inserted before the GFP sequence using restriction free cloning (Bond and Naus, 2012). Sequences encoding N-terminal KNL1 fragments were then added to those encoding $KNL1^{C}$ in sequential steps with the same protocol. Mutations and deletions within the KNL1-GFP constructs were generated by standard site-directed mutagenesis or by a mutagenesis protocol adapted from (Liu and Naismith, 2008). KNL1 constructs were made siRNA-resistant by changing the sequence targeted by HSS183683 to 'CACCCAATGTCACACTGCGAACATTCAG', by HSS125942 to 'TCTATTGTGGAGGTGTTCTAGACAA' and by HSS125943 to 'CCCACTGGAAGAGTGGTCAAACAAT'. To create all N-terminal GFP-BUB1 plasmids, BUB1 sequences were obtained by PCR amplification from a pEGFP-C1 vector containing

RNAi resistant BUB1 (a kind gift of M. Yanagida, University of Kyoto, Kyoto, Japan) and subcloned into the pcDNA5/FRT/TO GFP-IRES vector. To create all N-terminal GFP-fusions, BUBR1 sequences were amplified by PCR and cloned in frame with GFP tag in the pcDNA5/FRT/TO GFP-IRES vector. To create the BUB1(Δ189)-GFP fusion used in Figure 9 D, BUB1 sequence was cloned into pEGFP-N1 (Clontech) using BglII/XmaI restrictions sites. Site-directed mutagenesis was performed with the QuickChange Mutagenesis kit (Agilent Technologies) to generate single and multiple mutants in the BUB1 and BUBR1 constructs. pcDNA5/FRT/TO-based plasmids were used for both transient transfections and for the creation of Flp-In T-REx stable inducible cell lines. All plasmids were verified by DNA sequencing.

Cell culture, transfections and stable cell lines

HeLa cells were grown in DMEM (PAN Biotech) supplemented with 10 % FBS (Clontech), penicillin and streptomycin (GIBCO) and 2 mM L-glutamine (PAN Biotech). For transient transfection experiments, HeLa cells were transfected with X-tremeGENE transfection agent (Roche) at 3:1 ratio with plasmid DNA, according to the manufacturer's instructions. Cells were analyzed 36-68 hours post-transfection.

To generate stable cell lines, the Flp-In T-REx system (Invitrogen) was used. It allows the generation of stable mammalian cell lines exhibiting tetracycline-inducible expression of a gene of interest from a unique genomic location. Briefly, this system is based on a Flp-In T-REx host cell line carrying a unique Flp Recombination Target site (FRT, the site for Flp recombinase) together with a Zeocin resistance gene. This host cells line has been engineered to carry a Tet repressor cassette (linked to a Blasticidin resistance) that drives constitutive expression of the Tet repressor protein. Flp-In T-Rex host cell line are resistant to Zeocin and Blasticin. The gene of interest (GOI) is cloned in the pcDNA5FRT-TO plasmid containing a FRT site and a Hygromycin resistance gene. To generate the corresponding stable Flp-In T-

Rex cell line, the pCDNA5FRT-TO plasmid containing your GOI is co-transfected with the pOG44 vector coding for the Flp recombinase. The Flp recombinase mediates homologous recombination between the two FRT sites so that the GOI is integrated into the genome at the unique FRT site. By integration of the GOI Zeocin resistance is lost and Hygromycin resistance is gained. Cells that integrate the GOI become therefore sensitive to Zeocin but resistant to Hygromycin and Blasticidin and can be selected with Hygromic and Blastidicin containing medium. The constitutively expressed Tet repressor binds to a Tet operator in the promoter of your GOI, leading to repression of transcription. Expression of the GOI can then be induced by addition Tetracycline or its analogue Doxycycline to the culturing medium. Tetracycline binds the Tet repressor and prevents its binding to the promoter, hence allowing transcription of your GOI. Flp-In T-REx HeLa host cells were a gift from S.S. Taylor (University of Manchester, Manchester, England, UK). Flp-In T-REx host cell lines were maintained in DMEM with 10 % tetracycline-free FBS (Clontech) supplemented with 50 μg/ml Zeocin (Invitrogen). Flp-In T-REx HeLa expression cell lines were generated as described previously (Screpanti et al., 2011). N-terminally and C-terminally tagged KNL1 constructs were expressed by addition of 0.2 μg/ml and 1 μg/ml doxycycline (Sigma) for 24 hours, respectively. Expression of BUB1 and BUBR1 constructs was induced with 0.5 μg/ml of doxycycline for 24 hours. Unless differently specified, nocodazole (Sigma-Aldrich) and MG132 (Calbiochem) were used at concentration of 3.3 μM or 10 μM, respectively. Thymidine (2mM) and taxol were obtained from Sigma-Aldrich, reversine form Cayman.

Synchronization protocols and RNAi

siKNL1 (Invitrogen; HSS183683 5'-CACCCAGUGUCAUACAGCCAAUAUU-3'; HSS125942 5'-UCUACUGUGGUGGAGUUCUUGAUAA-3'; HSS125943 5'-CCCUCUGGAGGAAUGGUCUAAUAAU-3') and siBUB1 (Dharmacon; 5'-GGUUGCCAACACAAGUUCU 3') duplexes were transfected with Lipofectamine 2000

(Invitrogen) at 60 nM and 50 nM, respectively, for 1 day according to manufacturer's instructions. In the experiments shown in Figure 12 and Figure 16, after 5 h from transfection of siRNA duplexes, cells were synchronized with a double thymidine arrest (DTA). Briefly, cells were washed with PBS, treated with thymidine for 16 h and then released into fresh medium. 3 h after the release, siRNA duplexes were transfected again. After 5 h from the transfection, cells were treated with thymidine for 16hr and released in fresh medium.

Immunoprecipitation and Western Blot

To generate mitotic populations for immunoprecipitation experiments, cells were treated with 330nM nocodazole for 16 hours. Mitotic cells were then harvested by shake off and lysed in lysis buffer [150 mM KCl, 75 mM Hepes, pH 7.5, 1.5 mM EGTA, 1.5 mM $MgCl_2$, 10 % glycerol, and 0.075 % NP-40 supplemented with protease inhibitor cocktail (Serva) and PhosSTOP phosphatase inhibitors (Roche)]. Extracts were pre-cleared with a mixture of protein A–Sepharose (CL-4B; GE Healthcare) and protein G–Sepharose (rec-Protein G-Sepharose 4B; Invitrogen) for 1 hour at 4 °C. Subsequently, extracts were incubated with GFP-Traps (ChromoTek; 3 µl/mg of extract) for 2–4 hours at 4 °C. Immunoprecipitates were washed with lysis buffer and resuspended in sample buffer, boiled and analyzed by SDS-PAGE and Western blotting using 4-12 % gradient gels (NuPAGE® Bis-Tris Gels Life technologies). The following antibodies were used: anti-GFP (in house made rabbit polyclonal antibody; 1:1,000-4,000), anti-Hec1 (human Ndc80; mouse clone 9G3.23; Gene- Tex, Inc.; 1:1,000), anti-Mis12 (in house made mouse monoclonal antibody; clone QA21-74-4-3; 1:1500 or clone Q015, 1:5), anti-Knl1 (in house made rabbit polyclonal antibody; 1:1000), anti-Bub1 (rabbit polyclonal; Abcam; 1:5000), anti-BubR1 (mouse monoclonal; BD; 1:1000), anti-Bub3 (mouse monoclonal; BD; 1:1000), anti-PP1γ (goat polyclonal, Santa Cruz, 1:500), anti-Vinculin (mouse monoclonal; clone hVIN-1; Sigma-Aldrich; 1:1000), anti-Mps1 (mouse monoclonal; UPSTATE/Millipore; 1:1000), anti-Mad1 (in house made mouse monoclonal; clone BB3-8;

1:100), anti-Mad2 (rabbit polyclonal; Bethyl; 1:200), anti-Zwint-1 (in house made rabbit polyclonal SI0507; 1:1200), anti-Tubulin (mouse monoclonal; Sigma; 1:6000), anti-Cdc20 (rabbit polyclonal; Santa Cruz; 1:500), anti-APC7 (in house made rabbit polyclonal; 1:1000), anti–Actin (mouse monoclonal antibody AC-40, Sigma-Aldrich, working dilution 1:1000), anti-Phospho-S10-H3 (rabbit polyclonal 06-570, Millipore, working dilution 1:1000). Secondary antibodies were anti–mouse (Amersham), anti–rabbit (Amersham), anti-goat (Santa Cruz) affinity-purified with horseradish peroxidase conjugate (working dilution of 1:10000). After incubation with ECL Western blotting system (GE Healthcare), images (except those in Figure 10 D, Figure 12 B, Figure 13 A-E and Figure 20 A) were acquired with ChemiBIS 3.2 (DNR Bio-Imaging Systems) in 16-bit TIFF format. After adjusting the levels with Image J software, images were cropped and converted to 8-bit. Unmodified 16-bit TIFF images were used for quantification with Image J software. Blots in Figure 15 B and Figure 18 A were incubated with anti-Mouse and anti-Rabbit IRDye 680LT or IRDye 800CW secondary antibodies from LI-COR (working dilution 1:10000) and scanned with LI-COR Odyssey 3.0. All measurements were graphed with Excel (Microsoft) and GraphPad Prism version 6.0 for Mac OS X (GraphPad Software, San Diego California USA).

Live cell imaging

Cells were plated on a 24-well μ-Plate (Ibidi®). Drugs were diluted in CO_2 Independent Medium (Gibco®) and added to the cells 1 hour before filming. Cells were imaged every 45 to 60 min in a heated chamber (37°C) on an Zeiss IX-81 Axiovert microscope equipped with a 40X objective and a CCD camera (Cool Snap ES, Roper Scientific Photometrics), and controlled by MetaMorph 7.7.7.4 software (Visitron Systems), or on a 3i Marianas™ system (Intelligent Imaging Innovations Inc.) equipped with Axio Observer Z1 microscope (Zeiss), Plan-Apochromat 63x/1.4NA Objective (Zeiss), Orca Flash 4.0 sCMOS Camera (Hamamatsu) and controlled by Slidebook Software 5.5 (Intelligent Imaging Innovations Inc).

For cells expressing the Knl1-GFP proteins, only cells in which kinetochores were visible were considered for the analysis.

Immunofluorescence

HeLa or Flp-In T-REx HeLa cells were grown on coverslips pre-coated with poly-D-Lysine (Millipore, 15 μg/ml) or Poly-L-Lysine (Sigma) respectively. For the experiments with Plk4 fusions, cells were fixed with methanol for 10 min and then rehydrated with PBS. For all other experiments, cells were arrested in prometaphase by the addition of nocodazole and fixed using paraformaldehyde 4 %. Cells were stained for GFP (GFP-Booster, Chromotek 1:300), Bub1 (mouse, ab54893, 1:400), BubR1 (mouse, ab4637, 1:400), Knl1 N-terminus (rabbit, in house generated, 1:1000), CREST/anti-centromere antibodies (Antibodies, Inc., 1:150), Tubulin (mouse, Sigma T9026 1:8000), Cep135 (rabbit, 1:3000, a kind gift from A. Bird, Max Planck Institute for Molecular Physiology, Dortmund, Germany) diluted in 2 % BSA-PBS for 2 h. Goat anti–human and chicken anti–rabbit Alexa Fluor 647 (Invitrogen), and goat anti–rabbit and anti–mouse RRX (Jackson ImmunoResearch Laboratories, Inc.) were used as secondary antibodies. DNA was stained with 0.5 μg/ml DAPI (Serva) and coverslips were mounted with Mowiol mounting media (Calbiochem). Images in Figure 8-16 were acquired using a confocal microscope TCS SP2 (Leica) equipped with a 63× NA 1.4 objective lens using the LCS 3D software (Leica). Images in Figure 11 were acquired as Z-sections at 0.2442 μm and converted into maximal intensity projections using ImageJ Software. All other images were acquired at room temperature using a spinning disk confocal device on the 3i Marianas™ system (Intelligent Imaging Innovations Inc.) equipped with an Axio Observer Z1 microscope (Zeiss), a CSU-X1 confocal scanner unit (Yokogawa Electric Corporation), Plan-Apochromat 63x or 100x/1.4NA objectives and Orca Flash 4.0 sCMOS Camera (Hamamatsu). Images were acquired as z sections at 0.27 μm with Slidebook Software 5.5 (Intelligent Imaging Innovations Inc). Images were converted into maximal intensity

projections, exported and converted into 8-bit. Quantification of kinetochore signals was performed on unmodified 16-bit z-series images using Imaris 7.3.4 32-bit software (Bitplane). After background subtraction, all signals were normalized to CREST. At least 180 kinetochores were analyzed per condition. Measurements were exported in Excel (Microsoft) and graphed with GraphPad Prism.

In vitro kinase assays

Recombinant His-Bub1:Bub3 wild type and kinase-dead kinases were expressed and purified from Sf9 insect cells infected with recombinant baculoviruses as previously described (Santaguida et al., 2010). Briefly, the complex was isolated on Ni–nitrilotriacetic acid beads and further purified by size exclusion chromatography. Kinase assays were performed in 30 µl reaction volume as described previously (Santaguida et al., 2010). Briefly, reaction mixes contained 50 µM ATP, 1 mM DTT, Phosphatase Inhibitors Cocktail (Sigma-Aldrich), 10 µCi γ-[^{32}P]ATP and 10µM of H2A or 1ug H3 (Sigma-Aldrich) as substrate, diluted in Bub1 kinase buffer (50 mM Tris-HCl pH 7.6, 150 mM NaCl, 10 mM $MgCl_2$ and 1 mM EDTA). His-Bub1:Bub3 kinases were used at concentration of 50 nM. The full-length H2A of *Xenopus laevis* (a kind gift of Fabrizio Villa, European Institute of Oncology, Milan, Italy) has been expressed in *E.coli* and purified under denaturing conditions and refolded following and modifying the original protocol described in (Luger et al., 1997). 2OH-BNPP1 inhibitor (a kind gift of K. Shokat) was used at a final concentration of 5 µM. Knl1$^{150-250}$ or GST-Knl1$^{138-225}$-His6 fragments purified from *E. coli* lysates (gifts from X. Li and I. Primorac, respectively) were used at the final concentration of 1.8 µM or 1uM, respectively. For the assay shown in Figure 19 B, pre-phosphorylation was performed in 36 ul reactions, containing 5 uM GST-Knl1$^{138-225}$-His6 and 5 ng of recombinant GST-Mps1 kinase (TTK, Life technologies) diluted in kinase buffer (12.5 mM Tris, pH 7.5, 35 mM KCl, 10 mM $MgCl_2$, 0.5 mM EGTA 0.5 mM, 0.005% Triton X-100, 2.5 mM DTE, 500 uM ATP) and incubated at 30 C for 3 h. 5ul volume

of the pre-phopshorylation mix was then added to reactions containing 2.5 uM H2A and 25 nM His-Bub1:Bub3 diluted in Bub1 kinase buffer. For immunoprecipitation followed by kinase assay, Flp-In T-Rex cells were lysed in lysis Buffer [150 mM KCl, 75 mM Hepes pH 7.5, 1.5 mM MgCl2, 10% Glycerol, 0.075 % NP-40, supplemented with protease inhibitors cocktail (Protease Inhibitor Cocktail Set III, Calbiochem) and PhosSTOP phosphatase inhibitors (Roche)]. After immunoprecipitation, beads were washed with Bub1 kinase buffer and incubated with kinase reactions for 1 h at 30°C. Reactions were quenched with SDS loading buffer. Proteins were resolved on a SDS-PAGE and incorporation of 32P was visualized by autoradiography.

Acknowledgements

I would like to acknowledge Andrea and my supervisors Simona and Susanne for their support. Thanks to all the people that contributed to the project: Xiaozheng Li, Annemarie Wehenkel, Stefano Santaguida, Ivana Primorac, Katharina Overlack, Stefano Maffini, Jasmin Nelles, Susan von Gerwen, Claudia Breit and Tanja Bange. I am especially very grateful to Stefano Maffini, Anna De Antoni, Stefano Santaguida and Sebastiano Pasqualato for sharing reagents, for helpful discussions and their support with experiments. Thanks to Amanda Oldani, Sara Barozzi and the Imaging facility at the IEO, and Slava Ziegler, Georg Holtermann and Ingrid Vetter at MPI, for microscopy support. Thanks to all current and previous members of the Musacchio laboratory for providing reagents, for stimulating discussions and for the nice working atmosphere. Thanks to the Boehringer Ingelheim Fonds and IMPRS (International Max Planck Research School) for financial support. I am also grateful to Prof. Geert Kops and Prof. Jakob Nilsson for communicating results prior to publication.

Thanks everyone.

References

Abrieu, A., L. Magnaghi-Jaulin, J.A. Kahana, M. Peter, A. Castro, S. Vigneron, T. Lorca, D.W. Cleveland, and J.C. Labbe. 2001. Mps1 is a kinetochore-associated kinase essential for the vertebrate mitotic checkpoint. *Cell*. 106:83-93.

Akiyoshi, B., C.R. Nelson, J.A. Ranish, and S. Biggins. 2009. Analysis of Ipl1-mediated phosphorylation of the Ndc80 kinetochore protein in Saccharomyces cerevisiae. *Genetics*. 183:1591-1595.

Alushin, G.M., V.H. Ramey, S. Pasqualato, D.A. Ball, N. Grigorieff, A. Musacchio, and E. Nogales. 2010. The Ndc80 kinetochore complex forms oligomeric arrays along microtubules. *Nature*. 467:805-810.

Asbury, C.L., D.R. Gestaut, A.F. Powers, A.D. Franck, and T.N. Davis. 2006. The Dam1 kinetochore complex harnesses microtubule dynamics to produce force and movement. *Proceedings of the National Academy of Sciences of the United States of America*. 103:9873-9878.

Bailey, T.L., M. Boden, F.A. Buske, M. Frith, C.E. Grant, L. Clementi, J. Ren, W.W. Li, and W.S. Noble. 2009. MEME SUITE: tools for motif discovery and searching. *Nucleic acids research*. 37:W202-208.

Bharadwaj, R., W. Qi, and H. Yu. 2004. Identification of two novel components of the human NDC80 kinetochore complex. *The Journal of biological chemistry*. 279:13076-13085.

Bock, L.J., C. Pagliuca, N. Kobayashi, R.A. Grove, Y. Oku, K. Shrestha, C. Alfieri, C. Golfieri, A. Oldani, M. Dal Maschio, R. Bermejo, T.R. Hazbun, T.U. Tanaka, and P. De Wulf. 2012. Cnn1 inhibits the interactions between the KMN complexes of the yeast kinetochore. *Nature cell biology*. 14:614-624.

Boens, S., K. Szeker, A. Van Eynde, and M. Bollen. 2013. Interactor-guided dephosphorylation by protein phosphatase-1. *Methods Mol Biol*. 1053:271-281.

Bolanos-Garcia, V.M., and T.L. Blundell. 2011. BUB1 and BUBR1: multifaceted kinases of the cell cycle. *Trends in biochemical sciences*. 36:141-150.

Bolanos-Garcia, V.M., T. Kiyomitsu, S. D'Arcy, D.Y. Chirgadze, J.G. Grossmann, D. Matak-Vinkovic, A.R. Venkitaraman, M. Yanagida, C.V. Robinson, and T.L. Blundell. 2009. The crystal structure of the N-terminal region of BUB1 provides insight into the mechanism of BUB1 recruitment to kinetochores. *Structure*. 17:105-116.

Bolanos-Garcia, V.M., T. Lischetti, D. Matak-Vinkovic, E. Cota, P.J. Simpson, D.Y. Chirgadze, D.R. Spring, C.V. Robinson, J. Nilsson, and T.L. Blundell. 2011. Structure of a Blinkin-BUBR1 complex reveals an interaction crucial for kinetochore-mitotic checkpoint regulation via an unanticipated binding Site. *Structure*. 19:1691-1700.

Bond, S.R., and C.C. Naus. 2012. RF-Cloning.org: an online tool for the design of restriction-free cloning projects. *Nucleic acids research*. 40:W209-213.

Boyarchuk, Y., A. Salic, M. Dasso, and A. Arnaoutov. 2007. Bub1 is essential for assembly of the functional inner centromere. *The Journal of cell biology*. 176:919-928.

Brady, D.M., and K.G. Hardwick. 2000. Complex formation between Mad1p, Bub1p and Bub3p is crucial for spindle checkpoint function. *Curr Biol*. 10:675-678.

Burton, J.L., and M.J. Solomon. 2007. Mad3p, a pseudosubstrate inhibitor of APCCdc20 in the spindle assembly checkpoint. *Genes & development*. 21:655-667.

Cai, S., C.B. O'Connell, A. Khodjakov, and C.E. Walczak. 2009. Chromosome congression in the absence of kinetochore fibres. *Nature cell biology*. 11:832-838.

Carmena, M., M. Wheelock, H. Funabiki, and W.C. Earnshaw. 2012. The chromosomal passenger complex (CPC): from easy rider to the godfather of mitosis. *Nature reviews. Molecular cell biology*. 13:789-803.

Carroll, C.W., K.J. Milks, and A.F. Straight. 2010. Dual recognition of CENP-A nucleosomes is required for centromere assembly. *The Journal of cell biology*. 189:1143-1155.

Ceulemans, H., V. Vulsteke, M. De Maeyer, K. Tatchell, W. Stalmans, and M. Bollen. 2002. Binding of the concave surface of the Sds22 superhelix to the alpha 4/alpha 5/alpha 6-triangle of protein phosphatase-1. *The Journal of biological chemistry*. 277:47331-47337.

Chan, G.K., S.A. Jablonski, V. Sudakin, J.C. Hittle, and T.J. Yen. 1999. Human BUBR1 is a mitotic checkpoint kinase that monitors CENP-E functions at kinetochores and binds the cyclosome/APC. *The Journal of cell biology*. 146:941-954.

Chan, Y.W., A.A. Jeyaprakash, E.A. Nigg, and A. Santamaria. 2012. Aurora B controls kinetochore-microtubule attachments by inhibiting Ska complex-KMN network interaction. *The Journal of cell biology*. 196:563-571.

Chao, W.C., K. Kulkarni, Z. Zhang, E.H. Kong, and D. Barford. 2012. Structure of the mitotic checkpoint complex. *Nature*. 484:208-213.

Cheeseman, I.M., J.S. Chappie, E.M. Wilson-Kubalek, and A. Desai. 2006. The conserved KMN network constitutes the core microtubule-binding site of the kinetochore. *Cell*. 127:983-997.

Cheeseman, I.M., and A. Desai. 2008. Molecular architecture of the kinetochore-microtubule interface. *Nature reviews. Molecular cell biology*. 9:33-46.

Cheeseman, I.M., S. Niessen, S. Anderson, F. Hyndman, J.R. Yates, 3rd, K. Oegema, and A. Desai. 2004. A conserved protein network controls assembly of the outer kinetochore and its ability to sustain tension. *Genes & development*. 18:2255-2268.

Chen, R.H. 2002. BubR1 is essential for kinetochore localization of other spindle checkpoint proteins and its phosphorylation requires Mad1. *The Journal of cell biology*. 158:487-496.

Chen, R.H. 2004. Phosphorylation and activation of Bub1 on unattached chromosomes facilitate the spindle checkpoint. *The EMBO journal*. 23:3113-3121.

Choi, E., H. Choe, J. Min, J.Y. Choi, J. Kim, and H. Lee. 2009. BubR1 acetylation at prometaphase is required for modulating APC/C activity and timing of mitosis. *The EMBO journal*. 28:2077-2089.

Ciferri, C., J. De Luca, S. Monzani, K.J. Ferrari, D. Ristic, C. Wyman, H. Stark, J. Kilmartin, E.D. Salmon, and A. Musacchio. 2005. Architecture of the human ndc80-hec1 complex, a critical constituent of the outer kinetochore. *The Journal of biological chemistry*. 280:29088-29095.

Ciferri, C., S. Pasqualato, E. Screpanti, G. Varetti, S. Santaguida, G. Dos Reis, A. Maiolica, J. Polka, J.G. De Luca, P. De Wulf, M. Salek, J. Rappsilber, C.A. Moores, E.D. Salmon, and A. Musacchio. 2008. Implications for kinetochore-microtubule attachment from the structure of an engineered Ndc80 complex. *Cell*. 133:427-439.

D'Andrea, L.D., and L. Regan. 2003. TPR proteins: the versatile helix. *Trends in biochemical sciences*. 28:655-662.

D'Arcy, S., O.R. Davies, T.L. Blundell, and V.M. Bolanos-Garcia. 2010. Defining the molecular basis of BubR1 kinetochore interactions and APC/C-CDC20 inhibition. *The Journal of biological chemistry*. 285:14764-14776.

Davenport, J., L.D. Harris, and R. Goorha. 2006. Spindle checkpoint function requires Mad2-dependent Cdc20 binding to the Mad3 homology domain of BubR1. *Experimental cell research*. 312:1831-1842.

De Antoni, A., C.G. Pearson, D. Cimini, J.C. Canman, V. Sala, L. Nezi, M. Mapelli, L. Sironi, M. Faretta, E.D. Salmon, and A. Musacchio. 2005. The Mad1/Mad2 complex as a template for Mad2 activation in the spindle assembly checkpoint. *Curr Biol*. 15:214-225.

De Wulf, P., A.D. McAinsh, and P.K. Sorger. 2003. Hierarchical assembly of the budding yeast kinetochore from multiple subcomplexes. *Genes & development*. 17:2902-2921.

DeLuca, J.G., W.E. Gall, C. Ciferri, D. Cimini, A. Musacchio, and E.D. Salmon. 2006. Kinetochore microtubule dynamics and attachment stability are regulated by Hec1. *Cell*. 127:969-982.

Dephoure, N., C. Zhou, J. Villen, S.A. Beausoleil, C.E. Bakalarski, S.J. Elledge, and S.P. Gygi. 2008. A quantitative atlas of mitotic phosphorylation. *Proceedings of the National Academy of Sciences of the United States of America*. 105:10762-10767.

Desai, A., S. Rybina, T. Muller-Reichert, A. Shevchenko, A. Shevchenko, A. Hyman, and K. Oegema. 2003. KNL-1 directs assembly of the microtubule-binding interface of the kinetochore in C. elegans. *Genes & development*. 17:2421-2435.

Ditchfield, C., V.L. Johnson, A. Tighe, R. Ellston, C. Haworth, T. Johnson, A. Mortlock, N. Keen, and S.S. Taylor. 2003. Aurora B couples chromosome alignment with anaphase by targeting BubR1, Mad2, and Cenp-E to kinetochores. *The Journal of cell biology*. 161:267-280.

Dong, Y., K.J. Vanden Beldt, X. Meng, A. Khodjakov, and B.F. McEwen. 2007. The outer plate in vertebrate kinetochores is a flexible network with multiple microtubule interactions. *Nature cell biology*. 9:516-522.

Elowe, S. 2011. Bub1 and BubR1: at the interface between chromosome attachment and the spindle checkpoint. *Molecular and cellular biology*. 31:3085-3093.

Elowe, S., K. Dulla, A. Uldschmid, X. Li, Z. Dou, and E.A. Nigg. 2010. Uncoupling of the spindle-checkpoint and chromosome-congression functions of BubR1. *Journal of cell science*. 123:84-94.

Emanuele, M.J., W. Lan, M. Jwa, S.A. Miller, C.S. Chan, and P.T. Stukenberg. 2008. Aurora B kinase and protein phosphatase 1 have opposing roles in modulating kinetochore assembly. *The Journal of cell biology*. 181:241-254.

Espeut, J., D.K. Cheerambathur, L. Krenning, K. Oegema, and A. Desai. 2012. Microtubule binding by KNL-1 contributes to spindle checkpoint silencing at the kinetochore. *The Journal of cell biology*. 196:469-482.

Fang, G. 2002. Checkpoint protein BubR1 acts synergistically with Mad2 to inhibit anaphase-promoting complex. *Molecular biology of the cell*. 13:755-766.

Fava, L.L., M. Kaulich, E.A. Nigg, and A. Santamaria. 2011. Probing the in vivo function of Mad1:C-Mad2 in the spindle assembly checkpoint. *The EMBO journal*. 30:3322-3336.

Fernius, J., and K.G. Hardwick. 2007. Bub1 kinase targets Sgo1 to ensure efficient chromosome biorientation in budding yeast mitosis. *PLoS genetics*. 3:e213.

Flemming, W. 1882. Zellsubstanz, Kern, und Zelltheilung. *F.C.W. Vogel, Leipzig*.

Foley, E.A., and T.M. Kapoor. 2013. Microtubule attachment and spindle assembly checkpoint signalling at the kinetochore. *Nature reviews. Molecular cell biology*. 14:25-37.

Francisco, L., W. Wang, and C.S. Chan. 1994. Type 1 protein phosphatase acts in opposition to IpL1 protein kinase in regulating yeast chromosome segregation. *Molecular and cellular biology*. 14:4731-4740.

Funabiki, H., and D.J. Wynne. 2013. Making an effective switch at the kinetochore by phosphorylation and dephosphorylation. *Chromosoma*. 122:135-158.

Gascoigne, K.E., K. Takeuchi, A. Suzuki, T. Hori, T. Fukagawa, and I.M. Cheeseman. 2011. Induced ectopic kinetochore assembly bypasses the requirement for CENP-A nucleosomes. *Cell*. 145:410-422.

Gassmann, R., A.J. Holland, D. Varma, X. Wan, F. Civril, D.W. Cleveland, K. Oegema, E.D. Salmon, and A. Desai. 2010. Removal of Spindly from microtubule-attached kinetochores controls spindle checkpoint silencing in human cells. *Genes & development*. 24:957-971.

Gillett, E.S., C.W. Espelin, and P.K. Sorger. 2004. Spindle checkpoint proteins and chromosome-microtubule attachment in budding yeast. *The Journal of cell biology*. 164:535-546.

Gordon, D.J., B. Resio, and D. Pellman. 2012. Causes and consequences of aneuploidy in cancer. *Nature reviews. Genetics*. 13:189-203.

Grishchuk, E.L., A.K. Efremov, V.A. Volkov, I.S. Spiridonov, N. Gudimchuk, S. Westermann, D. Drubin, G. Barnes, J.R. McIntosh, and F.I. Ataullakhanov. 2008. The Dam1 ring binds microtubules strongly enough to be a processive as well as energy-efficient coupler for chromosome motion. *Proceedings of the National Academy of Sciences of the United States of America*. 105:15423-15428.

Grove, T.Z., A.L. Cortajarena, and L. Regan. 2008. Ligand binding by repeat proteins: natural and designed. *Current Opinion in Structural Biology*. 18:507-515.

Han, J.S., A.J. Holland, D. Fachinetti, A. Kulukian, B. Cetin, and D.W. Cleveland. 2013. Catalytic Assembly of the Mitotic Checkpoint Inhibitor BubR1-Cdc20 by a Mad2-Induced Functional Switch in Cdc20. *Molecular cell*. 51:92-104.

Hardwick, K.G., R.C. Johnston, D.L. Smith, and A.W. Murray. 2000. MAD3 encodes a novel component of the spindle checkpoint which interacts with Bub3p, Cdc20p, and Mad2p. *The Journal of cell biology*. 148:871-882.

Harris, L., J. Davenport, G. Neale, and R. Goorha. 2005. The mitotic checkpoint gene BubR1 has two distinct functions in mitosis. *Experimental cell research*. 308:85-100.

Hegemann, B., J.R. Hutchins, O. Hudecz, M. Novatchkova, J. Rameseder, M.M. Sykora, S. Liu, M. Mazanek, P. Lenart, J.K. Heriche, I. Poser, N. Kraut, A.A. Hyman, M.B. Yaffe, K. Mechtler, and J.M. Peters. 2011. Systematic phosphorylation analysis of human mitotic protein complexes. *Science signaling*. 4:rs12.

Hendrickx, A., M. Beullens, H. Ceulemans, T. Den Abt, A. Van Eynde, E. Nicolaescu, B. Lesage, and M. Bollen. 2009. Docking motif-guided mapping of the interactome of protein phosphatase-1. *Chemistry & biology*. 16:365-371.

Heroes, E., B. Lesage, J. Gornemann, M. Beullens, L. Van Meervelt, and M. Bollen. 2013. The PP1 binding code: a molecular-lego strategy that governs specificity. *The FEBS journal*. 280:584-595.

Hewitt, L., A. Tighe, S. Santaguida, A.M. White, C.D. Jones, A. Musacchio, S. Green, and S.S. Taylor. 2010. Sustained Mps1 activity is required in mitosis to recruit O-Mad2 to the Mad1-C-Mad2 core complex. *The Journal of cell biology*. 190:25-34.

Hori, T., M. Amano, A. Suzuki, C.B. Backer, J.P. Welburn, Y. Dong, B.F. McEwen, W.H. Shang, E. Suzuki, K. Okawa, I.M. Cheeseman, and T. Fukagawa. 2008. CCAN makes multiple contacts with centromeric DNA to provide distinct pathways to the outer kinetochore. *Cell*. 135:1039-1052.

Hori, T., W.H. Shang, K. Takeuchi, and T. Fukagawa. 2013. The CCAN recruits CENP-A to the centromere and forms the structural core for kinetochore assembly. *The Journal of cell biology*. 200:45-60.

Hornung, P., M. Maier, G.M. Alushin, G.C. Lander, E. Nogales, and S. Westermann. 2011. Molecular architecture and connectivity of the budding yeast Mtw1 kinetochore complex. *Journal of molecular biology*. 405:548-559.

Howell, B.J., B.F. McEwen, J.C. Canman, D.B. Hoffman, E.M. Farrar, C.L. Rieder, and E.D. Salmon. 2001. Cytoplasmic dynein/dynactin drives kinetochore protein transport to the spindle poles and has a role in mitotic spindle checkpoint inactivation. *The Journal of cell biology*. 155:1159-1172.

Howell, B.J., B. Moree, E.M. Farrar, S. Stewart, G. Fang, and E.D. Salmon. 2004. Spindle checkpoint protein dynamics at kinetochores in living cells. *Curr Biol*. 14:953-964.

Hoyt, M.A. 2001. A new view of the spindle checkpoint. *The Journal of cell biology*. 154:909-911.

Hsu, J.Y., Z.W. Sun, X. Li, M. Reuben, K. Tatchell, D.K. Bishop, J.M. Grushcow, C.J. Brame, J.A. Caldwell, D.F. Hunt, R. Lin, M.M. Smith, and C.D. Allis. 2000. Mitotic phosphorylation of histone H3 is governed by Ipl1/aurora kinase and Glc7/PP1 phosphatase in budding yeast and nematodes. *Cell*. 102:279-291.

Hsu, K.S., and T. Toda. 2011. Ndc80 internal loop interacts with Dis1/TOG to ensure proper kinetochore-spindle attachment in fission yeast. *Curr Biol*. 21:214-220.

Hua, S., Z. Wang, K. Jiang, Y. Huang, T. Ward, L. Zhao, Z. Dou, and X. Yao. 2011. CENP-U cooperates with Hec1 to orchestrate kinetochore-microtubule attachment. *The Journal of biological chemistry*. 286:1627-1638.

Hwang, L.H., L.F. Lau, D.L. Smith, C.A. Mistrot, K.G. Hardwick, E.S. Hwang, A. Amon, and A.W. Murray. 1998. Budding yeast Cdc20: a target of the spindle checkpoint. *Science*. 279:1041-1044.

Ito, D., Y. Saito, and T. Matsumoto. 2012. Centromere-tethered Mps1 pombe homolog (Mph1) kinase is a sufficient marker for recruitment of the spindle checkpoint protein Bub1, but not Mad1. *Proceedings of the National Academy of Sciences of the United States of America*. 109:209-214.

Izawa, D., and J. Pines. 2012. Mad2 and the APC/C compete for the same site on Cdc20 to ensure proper chromosome segregation. *The Journal of cell biology*. 199:27-37.

Jablonski, S.A., G.K. Chan, C.A. Cooke, W.C. Earnshaw, and T.J. Yen. 1998. The hBUB1 and hBUBR1 kinases sequentially assemble onto kinetochores during prophase with hBUBR1 concentrating at the kinetochore plates in mitosis. *Chromosoma*. 107:386-396.

Jeyaprakash, A.A., A. Santamaria, U. Jayachandran, Y.W. Chan, C. Benda, E.A. Nigg, and E. Conti. 2012. Structural and functional organization of the Ska complex, a key component of the kinetochore-microtubule interface. *Molecular cell*. 46:274-286.

Johnson, V.L., M.I. Scott, S.V. Holt, D. Hussein, and S.S. Taylor. 2004. Bub1 is required for kinetochore localization of BubR1, Cenp-E, Cenp-F and Mad2, and chromosome congression. *Journal of cell science*. 117:1577-1589.

Johnston, K., A. Joglekar, T. Hori, A. Suzuki, T. Fukagawa, and E.D. Salmon. 2010. Vertebrate kinetochore protein architecture: protein copy number. *The Journal of cell biology*. 189:937-943.

Kang, J., M. Yang, B. Li, W. Qi, C. Zhang, K.M. Shokat, D.R. Tomchick, M. Machius, and H. Yu. 2008. Structure and substrate recruitment of the human spindle checkpoint kinase Bub1. *Molecular cell*. 32:394-405.

Kasuboski, J.M., J.R. Bader, P.S. Vaughan, S.B. Tauhata, M. Winding, M.A. Morrissey, M.V. Joyce, W. Boggess, L. Vos, G.K. Chan, E.H. Hinchcliffe, and K.T. Vaughan. 2011. Zwint-1 is a novel Aurora B substrate required for the assembly of a dynein-binding platform on kinetochores. *Molecular biology of the cell*. 22:3318-3330.

Kawashima, S.A., Y. Yamagishi, T. Honda, K. Ishiguro, and Y. Watanabe. 2010. Phosphorylation of H2A by Bub1 prevents chromosomal instability through localizing shugoshin. *Science*. 327:172-177.

Kelly, A.E., C. Ghenoiu, J.Z. Xue, C. Zierhut, H. Kimura, and H. Funabiki. 2010. Survivin reads phosphorylated histone H3 threonine 3 to activate the mitotic kinase Aurora B. *Science*. 330:235-239.

Kerres, A., V. Jakopec, and U. Fleig. 2007. The conserved Spc7 protein is required for spindle integrity and links kinetochore complexes in fission yeast. *Molecular biology of the cell*. 18:2441-2454.

Kim, S., H. Sun, D.R. Tomchick, H. Yu, and X. Luo. 2012. Structure of human Mad1 C-terminal domain reveals its involvement in kinetochore targeting. *Proceedings of the National Academy of Sciences of the United States of America*. 109:6549-6554.

Kim, Y., A.J. Holland, W. Lan, and D.W. Cleveland. 2010. Aurora kinases and protein phosphatase 1 mediate chromosome congression through regulation of CENP-E. *Cell*. 142:444-455.

King, E.M., N. Rachidi, N. Morrice, K.G. Hardwick, and M.J. Stark. 2007. Ipl1p-dependent phosphorylation of Mad3p is required for the spindle checkpoint response to lack of tension at kinetochores. *Genes & development*. 21:1163-1168.

Kiyomitsu, T., O. Iwasaki, C. Obuse, and M. Yanagida. 2010. Inner centromere formation requires hMis14, a trident kinetochore protein that specifically recruits HP1 to human chromosomes. *The Journal of cell biology*. 188:791-807.

Kiyomitsu, T., H. Murakami, and M. Yanagida. 2011. Protein interaction domain mapping of human kinetochore protein Blinkin reveals a consensus motif for binding of spindle assembly checkpoint proteins Bub1 and BubR1. *Molecular and cellular biology*. 31:998-1011.

Kiyomitsu, T., C. Obuse, and M. Yanagida. 2007. Human Blinkin/AF15q14 is required for chromosome alignment and the mitotic checkpoint through direct interaction with Bub1 and BubR1. *Developmental cell*. 13:663-676.

Klebig, C., D. Korinth, and P. Meraldi. 2009. Bub1 regulates chromosome segregation in a kinetochore-independent manner. *The Journal of cell biology*. 185:841-858.

Kline-Smith, S.L., S. Sandall, and A. Desai. 2005. Kinetochore-spindle microtubule interactions during mitosis. *Current opinion in cell biology*. 17:35-46.

Kolodner, R.D., D.W. Cleveland, and C.D. Putnam. 2011. Cancer. Aneuploidy drives a mutator phenotype in cancer. *Science*. 333:942-943.

Kops, G.J., Y. Kim, B.A. Weaver, Y. Mao, I. McLeod, J.R. Yates, 3rd, M. Tagaya, and D.W. Cleveland. 2005. ZW10 links mitotic checkpoint signaling to the structural kinetochore. *The Journal of cell biology*. 169:49-60.

Krenn, V., A. Wehenkel, X. Li, S. Santaguida, and A. Musacchio. 2012. Structural analysis reveals features of the spindle checkpoint kinase Bub1-kinetochore subunit Knl1 interaction. *The Journal of cell biology*. 196:451-467.

Kruse, T., G. Zhang, M.S. Larsen, T. Lischetti, W. Streicher, T. Kragh Nielsen, S.P. Bjorn, and J. Nilsson. 2013. Direct binding between BubR1 and B56-PP2A phosphatase complexes regulate mitotic progression. *Journal of cell science*. 126:1086-1092.

Kulukian, A., J.S. Han, and D.W. Cleveland. 2009. Unattached kinetochores catalyze production of an anaphase inhibitor that requires a Mad2 template to prime Cdc20 for BubR1 binding. *Developmental cell*. 16:105-117.

Lampson, M.A., and T.M. Kapoor. 2005. The human mitotic checkpoint protein BubR1 regulates chromosome-spindle attachments. *Nature cell biology*. 7:93-98.

Lara-Gonzalez, P., M.I. Scott, M. Diez, O. Sen, and S.S. Taylor. 2011. BubR1 blocks substrate recruitment to the APC/C in a KEN-box-dependent manner. *Journal of cell science*. 124:4332-4345.

Lara-Gonzalez, P., F.G. Westhorpe, and S.S. Taylor. 2012. The spindle assembly checkpoint. *Curr Biol*. 22:R966-980.

Larsen, N.A., J. Al-Bassam, R.R. Wei, and S.C. Harrison. 2007. Structural analysis of Bub3 interactions in the mitotic spindle checkpoint. *Proceedings of the National Academy of Sciences of the United States of America*. 104:1201-1206.

Larsen, N.A., and S.C. Harrison. 2004. Crystal structure of the spindle assembly checkpoint protein Bub3. *Journal of molecular biology*. 344:885-892.

Lesage, B., M. Beullens, L. Pedelini, M.A. Garcia-Gimeno, E. Waelkens, P. Sanz, and M. Bollen. 2007. A complex of catalytically inactive protein phosphatase-1 sandwiched between Sds22 and inhibitor-3. *Biochemistry*. 46:8909-8919.

Li, R., and A.W. Murray. 1991. Feedback control of mitosis in budding yeast. *Cell*. 66:519-531.

Liu, D., M. Vleugel, C.B. Backer, T. Hori, T. Fukagawa, I.M. Cheeseman, and M.A. Lampson. 2010. Regulated targeting of protein phosphatase 1 to the outer kinetochore by KNL1 opposes Aurora B kinase. *The Journal of cell biology*. 188:809-820.

Liu, H., and J.H. Naismith. 2008. An efficient one-step site-directed deletion, insertion, single and multiple-site plasmid mutagenesis protocol. *BMC biotechnology*. 8:91.

Liu, S.T., J.B. Rattner, S.A. Jablonski, and T.J. Yen. 2006. Mapping the assembly pathways that specify formation of the trilaminar kinetochore plates in human cells. *The Journal of cell biology*. 175:41-53.

Liu, X., I. McLeod, S. Anderson, J.R. Yates, 3rd, and X. He. 2005. Molecular analysis of kinetochore architecture in fission yeast. *The EMBO journal*. 24:2919-2930.

Logarinho, E., T. Resende, C. Torres, and H. Bousbaa. 2008. The human spindle assembly checkpoint protein Bub3 is required for the establishment of efficient kinetochore-microtubule attachments. *Molecular biology of the cell*. 19:1798-1813.

London, N., S. Ceto, J.A. Ranish, and S. Biggins. 2012. Phosphoregulation of Spc105 by Mps1 and PP1 regulates Bub1 localization to kinetochores. *Curr Biol*. 22:900-906.

Luger, K., T.J. Rechsteiner, A.J. Flaus, M.M. Waye, and T.J. Richmond. 1997. Characterization of nucleosome core particles containing histone proteins made in bacteria. *Journal of molecular biology*. 272:301-311.

Luo, X., G. Fang, M. Coldiron, Y. Lin, H. Yu, M.W. Kirschner, and G. Wagner. 2000. Structure of the Mad2 spindle assembly checkpoint protein and its interaction with Cdc20. *Nature structural biology*. 7:224-229.

Luo, X., Z. Tang, J. Rizo, and H. Yu. 2002. The Mad2 spindle checkpoint protein undergoes similar major conformational changes upon binding to either Mad1 or Cdc20. *Molecular cell*. 9:59-71.

Luo, X., Z. Tang, G. Xia, K. Wassmann, T. Matsumoto, J. Rizo, and H. Yu. 2004. The Mad2 spindle checkpoint protein has two distinct natively folded states. *Nature structural & molecular biology*. 11:338-345.

Maciejowski, J., K.A. George, M.E. Terret, C. Zhang, K.M. Shokat, and P.V. Jallepalli. 2010. Mps1 directs the assembly of Cdc20 inhibitory complexes during interphase and mitosis to control M phase timing and spindle checkpoint signaling. *The Journal of cell biology*. 190:89-100.

Magidson, V., C.B. O'Connell, J. Loncarek, R. Paul, A. Mogilner, and A. Khodjakov. 2011. The spatial arrangement of chromosomes during prometaphase facilitates spindle assembly. *Cell*. 146:555-567.

Maldonado, M., and T.M. Kapoor. 2011. Constitutive Mad1 targeting to kinetochores uncouples checkpoint signalling from chromosome biorientation. *Nature cell biology*. 13:475-482.

Malureanu, L.A., K.B. Jeganathan, M. Hamada, L. Wasilewski, J. Davenport, and J.M. van Deursen. 2009. BubR1 N terminus acts as a soluble inhibitor of cyclin B degradation by APC/C(Cdc20) in interphase. *Developmental cell*. 16:118-131.

Mapelli, M., F.V. Filipp, G. Rancati, L. Massimiliano, L. Nezi, G. Stier, R.S. Hagan, S. Confalonieri, S. Piatti, M. Sattler, and A. Musacchio. 2006. Determinants of conformational dimerization of Mad2 and its inhibition by p31comet. *The EMBO journal*. 25:1273-1284.

Mapelli, M., L. Massimiliano, S. Santaguida, and A. Musacchio. 2007. The Mad2 conformational dimer: structure and implications for the spindle assembly checkpoint. *Cell*. 131:730-743.

Martin-Lluesma, S., V.M. Stucke, and E.A. Nigg. 2002. Role of Hec1 in spindle checkpoint signaling and kinetochore recruitment of Mad1/Mad2. *Science*. 297:2267-2270.

Maskell, D.P., X.W. Hu, and M.R. Singleton. 2010. Molecular architecture and assembly of the yeast kinetochore MIND complex. *The Journal of cell biology*. 190:823-834.

McAinsh, A.D., P. Meraldi, V.M. Draviam, A. Toso, and P.K. Sorger. 2006. The human kinetochore proteins Nnf1R and Mcm21R are required for accurate chromosome segregation. *The EMBO journal*. 25:4033-4049.

Meadows, J.C., L.A. Shepperd, V. Vanoosthuyse, T.C. Lancaster, A.M. Sochaj, G.J. Buttrick, K.G. Hardwick, and J.B. Millar. 2011. Spindle checkpoint silencing requires association of PP1 to both Spc7 and kinesin-8 motors. *Developmental cell*. 20:739-750.

Meraldi, P., V.M. Draviam, and P.K. Sorger. 2004. Timing and checkpoints in the regulation of mitotic progression. *Developmental cell*. 7:45-60.

Meraldi, P., and P.K. Sorger. 2005. A dual role for Bub1 in the spindle checkpoint and chromosome congression. *The EMBO journal*. 24:1621-1633.

Miller, S.A., M.L. Johnson, and P.T. Stukenberg. 2008. Kinetochore attachments require an interaction between unstructured tails on microtubules and Ndc80(Hec1). *Curr Biol*. 18:1785-1791.

Miranda, J.J., P. De Wulf, P.K. Sorger, and S.C. Harrison. 2005. The yeast DASH complex forms closed rings on microtubules. *Nature structural & molecular biology*. 12:138-143.

Morrow, C.J., A. Tighe, V.L. Johnson, M.I. Scott, C. Ditchfield, and S.S. Taylor. 2005. Bub1 and aurora B cooperate to maintain BubR1-mediated inhibition of APC/CCdc20. *Journal of cell science*. 118:3639-3652.

Musacchio, A., and E.D. Salmon. 2007. The spindle-assembly checkpoint in space and time. *Nature reviews. Molecular cell biology*. 8:379-393.

Neer, E.J., C.J. Schmidt, R. Nambudripad, and T.F. Smith. 1994. The ancient regulatory-protein family of WD-repeat proteins. *Nature*. 371:297-300.

Nekrasov, V.S., M.A. Smith, S. Peak-Chew, and J.V. Kilmartin. 2003. Interactions between centromere complexes in Saccharomyces cerevisiae. *Molecular biology of the cell*. 14:4931-4946.

Nijenhuis, W., E. von Castelmur, D. Littler, V. De Marco, E. Tromer, M. Vleugel, M.H. van Osch, B. Snel, A. Perrakis, and G.J. Kops. 2013. A TPR domain-containing N-terminal module of MPS1 is required for its kinetochore localization by Aurora B. *The Journal of cell biology*. 201:217-231.

Nishino, T., F. Rago, T. Hori, K. Tomii, I.M. Cheeseman, and T. Fukagawa. 2013. CENP-T provides a structural platform for outer kinetochore assembly. *The EMBO journal*. 32:424-436.

Nousiainen, M., H.H. Sillje, G. Sauer, E.A. Nigg, and R. Korner. 2006. Phosphoproteome analysis of the human mitotic spindle. *Proceedings of the National Academy of Sciences of the United States of America*. 103:5391-5396.

Obuse, C., O. Iwasaki, T. Kiyomitsu, G. Goshima, Y. Toyoda, and M. Yanagida. 2004. A conserved Mis12 centromere complex is linked to heterochromatic HP1 and outer kinetochore protein Zwint-1. *Nature cell biology*. 6:1135-1141.

Pagliuca, C., V.M. Draviam, E. Marco, P.K. Sorger, and P. De Wulf. 2009. Roles for the conserved spc105p/kre28p complex in kinetochore-microtubule binding and the spindle assembly checkpoint. *PLoS ONE*. 4:e7640.

Perera, D., V. Tilston, J.A. Hopwood, M. Barchi, R.P. Boot-Handford, and S.S. Taylor. 2007. Bub1 maintains centromeric cohesion by activation of the spindle checkpoint. *Developmental cell*. 13:566-579.

Perpelescu, M., and T. Fukagawa. 2011. The ABCs of CENPs. *Chromosoma*. 120:425-446.

Petrovic, A., S. Pasqualato, P. Dube, V. Krenn, S. Santaguida, D. Cittaro, S. Monzani, L. Massimiliano, J. Keller, A. Tarricone, A. Maiolica, H. Stark, and A. Musacchio. 2010.

The MIS12 complex is a protein interaction hub for outer kinetochore assembly. *The Journal of cell biology*. 190:835-852.

Pinsky, B.A., C.V. Kotwaliwale, S.Y. Tatsutani, C.A. Breed, and S. Biggins. 2006. Glc7/protein phosphatase 1 regulatory subunits can oppose the Ipl1/aurora protein kinase by redistributing Glc7. *Molecular and cellular biology*. 26:2648-2660.

Pinsky, B.A., C.R. Nelson, and S. Biggins. 2009. Protein phosphatase 1 regulates exit from the spindle checkpoint in budding yeast. *Curr Biol.* 19:1182-1187.

Pinsky, B.A., S.Y. Tatsutani, K.A. Collins, and S. Biggins. 2003. An Mtw1 complex promotes kinetochore biorientation that is monitored by the Ipl1/Aurora protein kinase. *Developmental cell*. 5:735-745.

Posch, M., G.A. Khoudoli, S. Swift, E.M. King, J.G. Deluca, and J.R. Swedlow. 2010. Sds22 regulates aurora B activity and microtubule-kinetochore interactions at mitosis. *The Journal of cell biology*. 191:61-74.

Primorac, I., J. Weir, E. Chrioli, F. Gross, I. Hoffmann, S. Van Grewen, A. Cilberto, and A. Musacchio. 2013. Bub3 reads phosphorylated MELT repeats to promote spindle assembly checkpoint signaling. *eLife*. under revision.

Przewloka, M.R., Z. Venkei, V.M. Bolanos-Garcia, J. Debski, M. Dadlez, and D.M. Glover. 2011. CENP-C is a structural platform for kinetochore assembly. *Curr Biol.* 21:399-405.

Ricke, R.M., K.B. Jeganathan, L. Malureanu, A.M. Harrison, and J.M. van Deursen. 2012. Bub1 kinase activity drives error correction and mitotic checkpoint control but not tumor suppression. *The Journal of cell biology*. 199:931-949.

Rieder, C.L., R.W. Cole, A. Khodjakov, and G. Sluder. 1995. The checkpoint delaying anaphase in response to chromosome monoorientation is mediated by an inhibitory signal produced by unattached kinetochores. *The Journal of cell biology*. 130:941-948.

Rischitor, P.E., K.M. May, and K.G. Hardwick. 2007. Bub1 is a fission yeast kinetochore scaffold protein, and is sufficient to recruit other spindle checkpoint proteins to ectopic sites on chromosomes. *PLoS ONE*. 2:e1342.

Roberts, B.T., K.A. Farr, and M.A. Hoyt. 1994. The Saccharomyces cerevisiae checkpoint gene BUB1 encodes a novel protein kinase. *Molecular and cellular biology*. 14:8282-8291.

Rosenberg, J.S., F.R. Cross, and H. Funabiki. 2011. KNL1/Spc105 recruits PP1 to silence the spindle assembly checkpoint. *Curr Biol.* 21:942-947.

Santaguida, S., and A. Musacchio. 2009. The life and miracles of kinetochores. *The EMBO journal*. 28:2511-2531.

Santaguida, S., A. Tighe, A.M. D'Alise, S.S. Taylor, and A. Musacchio. 2010. Dissecting the role of MPS1 in chromosome biorientation and the spindle checkpoint through the small molecule inhibitor reversine. *The Journal of cell biology*. 190:73-87.

Saurin, A.T., M.S. van der Waal, R.H. Medema, S.M. Lens, and G.J. Kops. 2011. Aurora B potentiates Mps1 activation to ensure rapid checkpoint establishment at the onset of mitosis. *Nature communications*. 2:316.

Scheufler, C., A. Brinker, G. Bourenkov, S. Pegoraro, L. Moroder, H. Bartunik, F.U. Hartl, and I. Moarefi. 2000. Structure of TPR domain-peptide complexes: critical elements in the assembly of the Hsp70-Hsp90 multichaperone machine. *Cell.* 101:199-210.

Schittenhelm, R.B., R. Chaleckis, and C.F. Lehner. 2009. Intrakinetochore localization and essential functional domains of Drosophila Spc105. *The EMBO journal.* 28:2374-2386.

Schmidt, J.C., H. Arthanari, A. Boeszoermenyi, N.M. Dashkevich, E.M. Wilson-Kubalek, N. Monnier, M. Markus, M. Oberer, R.A. Milligan, M. Bathe, G. Wagner, E.L. Grishchuk, and I.M. Cheeseman. 2012. The kinetochore-bound Ska1 complex tracks depolymerizing microtubules and binds to curved protofilaments. *Developmental cell.* 23:968-980.

Screpanti, E., A. De Antoni, G.M. Alushin, A. Petrovic, T. Melis, E. Nogales, and A. Musacchio. 2011. Direct binding of Cenp-C to the Mis12 complex joins the inner and outer kinetochore. *Curr Biol.* 21:391-398.

Shah, J.V., E. Botvinick, Z. Bonday, F. Furnari, M. Berns, and D.W. Cleveland. 2004. Dynamics of centromere and kinetochore proteins; implications for checkpoint signaling and silencing. *Curr Biol.* 14:942-952.

Sharp-Baker, H., and R.H. Chen. 2001. Spindle checkpoint protein Bub1 is required for kinetochore localization of Mad1, Mad2, Bub3, and CENP-E, independently of its kinase activity. *The Journal of cell biology.* 153:1239-1250.

Shepperd, L.A., J.C. Meadows, A.M. Sochaj, T.C. Lancaster, J. Zou, G.J. Buttrick, J. Rappsilber, K.G. Hardwick, and J.B. Millar. 2012. Phosphodependent recruitment of Bub1 and Bub3 to Spc7/KNL1 by Mph1 kinase maintains the spindle checkpoint. *Curr Biol.* 22:891-899.

Simonetta, M., R. Manzoni, R. Mosca, M. Mapelli, L. Massimiliano, M. Vink, B. Novak, A. Musacchio, and A. Ciliberto. 2009. The influence of catalysis on mad2 activation dynamics. *PLoS biology.* 7:e10.

Sliedrecht, T., C. Zhang, K.M. Shokat, and G.J. Kops. 2010. Chemical genetic inhibition of Mps1 in stable human cell lines reveals novel aspects of Mps1 function in mitosis. *PLoS ONE.* 5:e10251.

Stone, E.M., H. Yamano, N. Kinoshita, and M. Yanagida. 1993. Mitotic regulation of protein phosphatases by the fission yeast sds22 protein. *Curr Biol.* 3:13-26.

Storchova, Z., J.S. Becker, N. Talarek, S. Kogelsberger, and D. Pellman. 2011. Bub1, Sgo1, and Mps1 mediate a distinct pathway for chromosome biorientation in budding yeast. *Molecular biology of the cell.* 22:1473-1485.

Stucke, V.M., C. Baumann, and E.A. Nigg. 2004. Kinetochore localization and microtubule interaction of the human spindle checkpoint kinase Mps1. *Chromosoma.* 113:1-15.

Stucke, V.M., H.H. Sillje, L. Arnaud, and E.A. Nigg. 2002. Human Mps1 kinase is required for the spindle assembly checkpoint but not for centrosome duplication. *The EMBO journal.* 21:1723-1732.

Sudakin, V., G.K. Chan, and T.J. Yen. 2001. Checkpoint inhibition of the APC/C in HeLa cells is mediated by a complex of BUBR1, BUB3, CDC20, and MAD2. *The Journal of cell biology*. 154:925-936.

Suijkerbuijk, S.J., T.J. van Dam, G.E. Karagoz, E. von Castelmur, N.C. Hubner, A.M. Duarte, M. Vleugel, A. Perrakis, S.G. Rudiger, B. Snel, and G.J. Kops. 2012a. The vertebrate mitotic checkpoint protein BUBR1 is an unusual pseudokinase. *Developmental cell*. 22:1321-1329.

Suijkerbuijk, S.J., M. Vleugel, A. Teixeira, and G.J. Kops. 2012b. Integration of kinase and phosphatase activities by BUBR1 ensures formation of stable kinetochore-microtubule attachments. *Developmental cell*. 23:745-755.

Takeuchi, K., and T. Fukagawa. 2012. Molecular architecture of vertebrate kinetochores. *Experimental cell research*. 318:1367-1374.

Tang, Z., R. Bharadwaj, B. Li, and H. Yu. 2001. Mad2-Independent inhibition of APCCdc20 by the mitotic checkpoint protein BubR1. *Developmental cell*. 1:227-237.

Tang, Z., H. Shu, D. Oncel, S. Chen, and H. Yu. 2004. Phosphorylation of Cdc20 by Bub1 provides a catalytic mechanism for APC/C inhibition by the spindle checkpoint. *Molecular cell*. 16:387-397.

Taylor, S.S., E. Ha, and F. McKeon. 1998. The human homologue of Bub3 is required for kinetochore localization of Bub1 and a Mad3/Bub1-related protein kinase. *The Journal of cell biology*. 142:1-11.

Taylor, S.S., and F. McKeon. 1997. Kinetochore localization of murine Bub1 is required for normal mitotic timing and checkpoint response to spindle damage. *Cell*. 89:727-735.

Teichner, A., E. Eytan, D. Sitry-Shevah, S. Miniowitz-Shemtov, E. Dumin, J. Gromis, and A. Hershko. 2011. p31comet Promotes disassembly of the mitotic checkpoint complex in an ATP-dependent process. *Proceedings of the National Academy of Sciences of the United States of America*. 108:3187-3192.

Tighe, A., O. Staples, and S. Taylor. 2008. Mps1 kinase activity restrains anaphase during an unperturbed mitosis and targets Mad2 to kinetochores. *The Journal of cell biology*. 181:893-901.

Tipton, A.R., K. Wang, L. Link, J.J. Bellizzi, H. Huang, T. Yen, and S.T. Liu. 2011. BUBR1 and closed MAD2 (C-MAD2) interact directly to assemble a functional mitotic checkpoint complex. *The Journal of biological chemistry*. 286:21173-21179.

Tooley, J.G., S.A. Miller, and P.T. Stukenberg. 2011. The Ndc80 complex uses a tripartite attachment point to couple microtubule depolymerization to chromosome movement. *Molecular biology of the cell*. 22:1217-1226.

van der Waal, M.S., A.T. Saurin, M.J. Vromans, M. Vleugel, C. Wurzenberger, D.W. Gerlich, R.H. Medema, G.J. Kops, and S.M. Lens. 2012. Mps1 promotes rapid centromere accumulation of Aurora B. *EMBO reports*. 13:847-854.

Vanoosthuyse, V., and K.G. Hardwick. 2009. A novel protein phosphatase 1-dependent spindle checkpoint silencing mechanism. *Curr Biol*. 19:1176-1181.

Vanoosthuyse, V., R. Valsdottir, J.P. Javerzat, and K.G. Hardwick. 2004. Kinetochore targeting of fission yeast Mad and Bub proteins is essential for spindle checkpoint function but not for all chromosome segregation roles of Bub1p. *Molecular and cellular biology*. 24:9786-9801.

Varetti, G., C. Guida, S. Santaguida, E. Chiroli, and A. Musacchio. 2011. Homeostatic control of mitotic arrest. *Molecular cell*. 44:710-720.

Varma, D., S. Chandrasekaran, L.J. Sundin, K.T. Reidy, X. Wan, D.A. Chasse, K.R. Nevis, J.G. DeLuca, E.D. Salmon, and J.G. Cook. 2012. Recruitment of the human Cdt1 replication licensing protein by the loop domain of Hec1 is required for stable kinetochore-microtubule attachment. *Nature cell biology*. 14:593-603.

Vigneron, S., S. Prieto, C. Bernis, J.C. Labbe, A. Castro, and T. Lorca. 2004. Kinetochore localization of spindle checkpoint proteins: who controls whom? *Molecular biology of the cell*. 15:4584-4596.

Vleugel, M., E. Hoogendoorn, B. Snel, and G.J. Kops. 2012. Evolution and function of the mitotic checkpoint. *Developmental cell*. 23:239-250.

Vleugel, M., E. Tromer, M. Omerzu, V. Groenewold, W. Nijenhuis, B. Snel, and G.J.P.L. Kops. 2013. Progressive accuracy of chromosome segregation by arrayed generic BUB recruitment modules in the kinetochore scaffold KNL1. *The Journal of cell biology*. under revision.

Wang, F., J. Dai, J.R. Daum, E. Niedzialkowska, B. Banerjee, P.T. Stukenberg, G.J. Gorbsky, and J.M. Higgins. 2010. Histone H3 Thr-3 phosphorylation by Haspin positions Aurora B at centromeres in mitosis. *Science*. 330:231-235.

Wang, F., N.P. Ulyanova, M.S. van der Waal, D. Patnaik, S.M. Lens, and J.M. Higgins. 2011. A positive feedback loop involving Haspin and Aurora B promotes CPC accumulation at centromeres in mitosis. *Curr Biol*. 21:1061-1069.

Wang, H.W., S. Long, C. Ciferri, S. Westermann, D. Drubin, G. Barnes, and E. Nogales. 2008. Architecture and flexibility of the yeast Ndc80 kinetochore complex. *Journal of molecular biology*. 383:894-903.

Wang, X., J.R. Babu, J.M. Harden, S.A. Jablonski, M.H. Gazi, W.L. Lingle, P.C. de Groen, T.J. Yen, and J.M. van Deursen. 2001. The mitotic checkpoint protein hBUB3 and the mRNA export factor hRAE1 interact with GLE2p-binding sequence (GLEBS)-containing proteins. *The Journal of biological chemistry*. 276:26559-26567.

Weaver, B.A., and D.W. Cleveland. 2006. Does aneuploidy cause cancer? *Current opinion in cell biology*. 18:658-667.

Wei, R.R., J. Al-Bassam, and S.C. Harrison. 2007. The Ndc80/HEC1 complex is a contact point for kinetochore-microtubule attachment. *Nature structural & molecular biology*. 14:54-59.

Wei, R.R., P.K. Sorger, and S.C. Harrison. 2005. Molecular organization of the Ndc80 complex, an essential kinetochore component. *Proceedings of the National Academy of Sciences of the United States of America*. 102:5363-5367.

Welburn, J.P., and I.M. Cheeseman. 2008. Toward a molecular structure of the eukaryotic kinetochore. *Developmental cell*. 15:645-655.

Welburn, J.P., E.L. Grishchuk, C.B. Backer, E.M. Wilson-Kubalek, J.R. Yates, 3rd, and I.M. Cheeseman. 2009. The human kinetochore Ska1 complex facilitates microtubule depolymerization-coupled motility. *Developmental cell*. 16:374-385.

Welburn, J.P., M. Vleugel, D. Liu, J.R. Yates, 3rd, M.A. Lampson, T. Fukagawa, and I.M. Cheeseman. 2010. Aurora B phosphorylates spatially distinct targets to differentially regulate the kinetochore-microtubule interface. *Molecular cell*. 38:383-392.

Westermann, S., A. Avila-Sakar, H.W. Wang, H. Niederstrasser, J. Wong, D.G. Drubin, E. Nogales, and G. Barnes. 2005. Formation of a dynamic kinetochore- microtubule interface through assembly of the Dam1 ring complex. *Molecular cell*. 17:277-290.

Westermann, S., I.M. Cheeseman, S. Anderson, J.R. Yates, 3rd, D.G. Drubin, and G. Barnes. 2003. Architecture of the budding yeast kinetochore reveals a conserved molecular core. *The Journal of cell biology*. 163:215-222.

Westermann, S., D.G. Drubin, and G. Barnes. 2007. Structures and functions of yeast kinetochore complexes. *Annual review of biochemistry*. 76:563-591.

Westermann, S., and A. Schleiffer. 2013. Family matters: structural and functional conservation of centromere-associated proteins from yeast to humans. *Trends in cell biology*. 23:260-269.

Westermann, S., H.W. Wang, A. Avila-Sakar, D.G. Drubin, E. Nogales, and G. Barnes. 2006. The Dam1 kinetochore ring complex moves processively on depolymerizing microtubule ends. *Nature*. 440:565-569.

Windecker, H., M. Langegger, S. Heinrich, and S. Hauf. 2009. Bub1 and Bub3 promote the conversion from monopolar to bipolar chromosome attachment independently of shugoshin. *EMBO reports*. 10:1022-1028.

Wu, H., Z. Lan, W. Li, S. Wu, J. Weinstein, K.M. Sakamoto, and W. Dai. 2000. p55CDC/hCDC20 is associated with BUBR1 and may be a downstream target of the spindle checkpoint kinase. *Oncogene*. 19:4557-4562.

Wu, J.Q., J.Y. Guo, W. Tang, C.S. Yang, C.D. Freel, C. Chen, A.C. Nairn, and S. Kornbluth. 2009. PP1-mediated dephosphorylation of phosphoproteins at mitotic exit is controlled by inhibitor-1 and PP1 phosphorylation. *Nature cell biology*. 11:644-651.

Xu, P., E.A. Raetz, M. Kitagawa, D.M. Virshup, and S.H. Lee. 2013. BUBR1 recruits PP2A via the B56 family of targeting subunits to promote chromosome congression. *Biology open*. 2:479-486.

Yamagishi, Y., T. Honda, Y. Tanno, and Y. Watanabe. 2010. Two histone marks establish the inner centromere and chromosome bi-orientation. *Science*. 330:239-243.

Yamagishi, Y., C.H. Yang, Y. Tanno, and Y. Watanabe. 2012. MPS1/Mph1 phosphorylates the kinetochore protein KNL1/Spc7 to recruit SAC components. *Nature cell biology*. 14:746-752.

Yang, J., S.M. Roe, M.J. Cliff, M.A. Williams, J.E. Ladbury, P.T. Cohen, and D. Barford. 2005. Molecular basis for TPR domain-mediated regulation of protein phosphatase 5. *The EMBO journal*. 24:1-10.

Yang, M., B. Li, D.R. Tomchick, M. Machius, J. Rizo, H. Yu, and X. Luo. 2007. p31comet blocks Mad2 activation through structural mimicry. *Cell*. 131:744-755.

Zeytuni, N., and R. Zarivach. 2012. Structural and functional discussion of the tetra-trico-peptide repeat, a protein interaction module. *Structure*. 20:397-405.

Zhang, G., T. Lischetti, and J. Nilsson. 2013. Multiple functional binding sites for Bub1 and BubR1 on KNL1 regulated by PP1 and Mps1. *The EMBO journal*. submitted.